**A Study of Accuracy of Bathymetric Data for Acoustic Propagation Modelling**

*Patrícia dos Santos Pinheiro*[!] **patpin@americaonline.com** *Jorge J. C. Palma*[!]**,**
(1) LAGEMAR – Depto. de Geologia, IGEO/UFF

**Abstract**

Sea-bottom topography is an important parameter in studies on marine acoustics since the sea floor acts as a reflection and scattering boundary in underwater sound propagation. This effect varies with scale of relief. Back scattering coefficient is frequency independent for large-scale bottom roughness and frequency dependent for small bottom irregularities as compared to signal wavelength.

It follows that parameterization of bottom topography influence on marine acoustics depends strongly on the quality of bathymetric database provided for modeling underwater sound propagation.

As part of a Brazilian Navy project for environmental characterization of South Atlantic, for acoustic purposes a methodology was developed for the construction of a well-constrained quality comprehensive bathymetric database. It is based on crossover error analysis and minimization of a rather heterogeneous data set of ~ 1,475,000 points covering a prototype study area along the southeastern Brazilian continental margin.

Results obtained until the present show that the system is efficient in relation to irregular distribution of the cruise surveys. Further work will be a zoning of the according to coverage density, data accuracy, and resolution based on spectral analysis.

# Amazon Shelf Break Carbonate Reefs

*Alberto Figueiredo Jr, Lagemar-Universidade Federal Fluminense, Brazil,alberto@igeo.uff.br*
*Guisela Santiago Grossmann., Lagemar-Universidade Federal Fluminense, Brazil, guisela@igeo.uff.b*

**Abstract**

Paper describes occurrence of carbonate reef like features on shelf break of Amazon continental shelf. Morphological, seismic and environmental data are used in support to this interpretation.

**Introduction**

The Amazon River is the largest river in world with a water discharge ranging between 80,000 to 250,000 $m^3/s$ (Oltman, 1968; Muller-Karger *et al.* 1988) while exceptionally can reach up to 354,793 $m^3/s$ (Figueiredo, 1993). This water discharge annually transports 1.2 x $10^9$ tons of sediment to continental shelf (Meade *et al.* 1985) where approximately 90 % is silt and clay size sediments (Gibbs, 1967; Meade, 1985). About half of the sediment accumulates on the shelf with maximum depositional rates between 40 - 50 m (Kuehl *et al.* 1986) creating a feature mapped in early researches as the Amazon subaqueous delta (Figueiredo *et al.* 1972, Martins *et al.* 1972).

Despite being predominately dominated by muddier sediments, siliciclastic relict sands, rich in carbonates occurs as a rim to the subaqueous delta (Zembruscki *et al.* 1970; Barreto *et al.* 1975). The carbonatic sediment is composed by algae and briozoans debris and also by ooids. Accordingly to Milliman and Barreto (1975) the ooids lying in water depths between 80 and 200 m and range in age from 17 and 20 thousand years and were formed when sea-level was low and water clear. Despite many publications on the Amazon margin no one have deal with carbonate reefs so far.

This paper describes occurrence of carbonate reefs along the north portion of the Brazilian shelf break based on seismic data and bottom samples (Figure 1).

**The Data Set**

The data set comprises digital seismic data acquired with *Parasound* echosounder system during cooperative scientific program between Fluminense Federal University and Bremen University on board of R/V Meteor, during cruise 34, leg 4 in 1996 (Fisher *et al.*, 1996). During AmasSeds research program between Brazilian and American universities also some 3.5 kHz profiles detected the carbonate features (Costa, 1997; Costa and Figueiredo, 1998).

In order to obtain better resolution, digital data from *Parasound* System were processed using University of Bremen's Sesuit software, version 1998.

During Meteor cruise 34-4, a piston core (GeoB 3920-2) was also collected 1,800-m land ward of the reef and measurements of P wave velocity, gama density, magnetic susceptibility and color reflectance were performed.

**Results**

Investigation of nutrients content in the water column during AmasSeds project have shown that oceanic water is the dominant source of ammonium and an important source of phosphate to the algal blooms on the outer shelf (DeMaster and Pope, 1996). Nutrients are carried from open ocean to the shelf break due to advection of subsurface waters in a estuarine like situation. As for the algae, these nutrients are also important to development and sustainability of reef building biota.

Reefs were first noticed on 3.5 kHz AmasSdes records and lately on Parasound data (Fig. 2). As seem on seismic lines, carbonate reefs are highly reflective and non-transparent to seismic waves. They occurs as an elongated feature in the shelf break between 80 to 125-m water depth, offshore Cape Cassiporé in Amapá where shelf narrows to 150-km wide. Reef can be 200 to 3,000-m wide with topographic expression from 3 to 6-m on the inner side and 15 to 37-m on the outer side, however, total carbonate thickness was not possible to be measured. Top of the reef can be flat or undulating and a common characteristic is that the reef acts as a barrier for sediment going to deep-sea. Based on seismic profiles from Araújo (1994), Costa and Figueiredo Jr. (1998) and this paper, reefs are composed of several isolated bodies with lateral continuity inferred to be at least 50 km. Coordinates of portion of the reef, accordingly to Meteor data set is $4^o$ 27.43' N and $50^o$ 0,86' W at 128 m water depth.

Besides appropriated environmental conditions and morphological characteristics, other data supporting the reef interpretation, are the ooids collected by Milliman and Barreto (1975) and more recently the Meteor core with abundant beach rock fragments. Beach rocks and ooids are good indication of carbonate rich environment.

Carbonate reef in a muddier shelf break environment is very attractive for oil industry since it is the place where slope reflectors are anchored and the shelf reflectors end. The intention of this paper is to highlight the occurrence of these reefs in order to provoke further research development in the area.

**Conclusion**

Morphological, seismic and environmental characteristics of the feature under investigation points out to a carbonate reef.

**References**


Araújo, T.C.M., 1994, Seismostratigraphic interpretation of the Amazon continental margin in view of sea-level changes and subsidence of the sea floor. Doctoral dissertation, University of Kiel, Germany, 119pp.

Costa, E.A., 1997, Caracterização de ecofácies e processos sedimentares da plataforma continental amazônica: MSc. Thesis, Fluminense Federal University, 138pp.

Costa, E.A. and Figueiredo Jr., A.G., 1998, Echo-character and sedimentary processes on the Amazon continental shelf. Academia Brasileira de Ciências, Anais, 70 (2), 187-200.

DeMaster, D.J. and Pope, R.H., 1996, Nutrient dynamics in Amazon shelf waters: results from AmasSeds. Continental Shelf Research, 16 (3), 263-289.

Barreto, H.T., Milliman, J.D., Amaral, C.A.B. and Francisconi, O., 1975, Upper continental margin sedimentation off Brazil: northern Brazil. Contributions to Sedimentology, 4, 11-43.

Figueiredo Jr., A.G., 1993, Modelo de sedimentação atual da plataforma amazônica, Thesis for full professor selective process, Dept. of Geology, Fluminense Federal University, 42pp.

Figueiredo Jr., A.G. and Nittrouer, C.A., 1995, New insights to high-resolution stratigraphy on the Amazon continental shelf. Marine Geology, 125, 393-399.

Fisher, G., Arz, H., Baschek, B., Bassek, D., Costa, E.A., Dierssen, H., Deeken, A. Diekamp, V., Eichner, C., Engelbrecht, I., Enneking, K., Figueiredo, A.G.Jr., Flechsenhaar, K., Frederichs, T., Freesemann, A., Garternicht, U., Herz, M.v., Hübscher, C., Karwath, B., Kasten, S., Kinkel, H., Kölling, M., Miesner, I., Ratmeyer, V., Schlünz, B., Schneidr, R., Schmieder, F., Ruhland, G. and Zabel, M., 1996, Report and preliminary results of Meteor-cruise M 34/4, Recife-Bridgetown, 19.3-15.4.1996. Report no. 80 Berichte, Fachbereich Geowissenschaften, Universität Bremen, Germany, 105p.

Gibbs, R.J., 1967, The geochemistry of the Amazon River system: Part I. The factors that control the salinity and the composition and concentration of the suspended solids. Geological Society of America Bulletim, 78, 1203-1232.

Kuehl, S.A., DeMaster, D.J. and Nittrouer, C.A., Nature of sediment accumulation on the Amazon continental shelf. Continental Shelf Research, 6, 209-225.

Mead, R.H., 1985, Suspended sediment in the Amazon River and its tributaries in Brazil during 1982-84. U.S. Geological Survey, Open-file Report, 85-492.

Mead, R.H., Dunne, T., Richey, J.E., Santos, U.M. and Salati, E., 1985, Storage and remobilization of suspended sediment in the lower Amazon river of Brazil. Science, 228, 488-490.

Milliman, J.D. and Barreto, H.T., 1975, Relict magnesian clacite oolite and subsidence of the Amazon shelf. Sedimentology, 22, 137-145.

Muller-Karger, F.E., McClain, C.R. and Richardson, P.L., 1968, The dispersal of the Amazon's water. Nature, 333, 56-69.

Oltman, R.E., 1968, Reconnaissance investigations of the discharge and water quality of the Amazon River. U.S. Geological Survey Circular, 552, 16pp.

Zembruscki, S.G., Gorini, M.A., Palma, J.J.C. e Costa, M.P.A., 1970, XL Comissão oceanográfica, Operação Geomar I. Costa norte/nordeste/geologia marinha. Boletim DHN, DG-32-I, 70pp.


**Acknowledgments**


Alberto G. Figueiredo Jr. is sponsored in his research by the Brazilian National Research Council (CNPq) and Guisela S. Grossmann by the Brazilian National Petroleum Agency (ANP). We thank to Dr. Gerold Wefer and Gerard Fisher of Univ. Bremen, for our participation on Meteor cruises and collection of data of our interest.

**Amazon Shelf Break Carbonates Reefs**

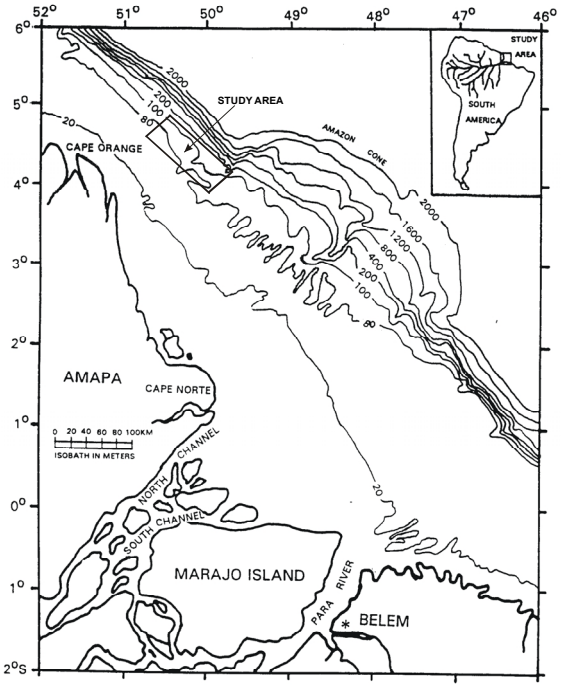


Figura 1 – Study area located in the shelf break were continental shelf is narrow.

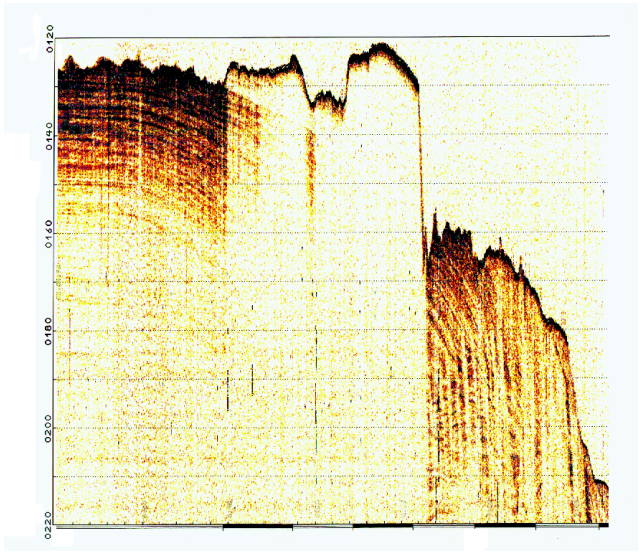


Figure 2 – Shelf carbonate reef as seem on Parasound System.

# Arcabouço estratigráfico da Bacia de Bransfield (Península Antárctica) sob o enfoque da Estratigrafia de Seqüências

*Carlos Maurício C. de Almeida, SCHLUMBERGER;*
*Hélio J. P. Severiano Ribeiro, LENEP/UENF.*

**Abstract**

The Bransfield Basin (BB) is a back-arc basin situated at the northern tip of the Antarctic Peninsula and presents a complicated tectonic history involving compressive, extensional and strike-slip processes. From reflection seismic data acquired by PETROBRÁS and Marinha do Brasil in the austral summers of 1987/88 was elaborated a stratigraphic framework based in seismic stratigraphic interpretations (Sequence Stratigraphy) in the Central Bransfield Subbasin. In this seismic stratigraphic interpretation were identified three seismic sequences (SS1, SS2 and SS3 from the top to the base) limited by three unconformities (D1, D2 and D3). The SS3 sequence is formed by strong layered reflections (parallel/subparallel) below continental shelf and reflections parallels with low continuity below slope/continental rise. In general, SS1 appear as a faulted and folded sedimentary wedge that is filling several grabens. SS2 was divided in three system tracts: a Lowstand System Tract (LST), a Transgressive System Tract (TST) and a Highstand System Tract (HST). Inside SS2 there is a conspicuous downlap surface (DLS). The LST is composed by mounds (fans) below slope/continental rise and its reflections shows a hummocky configuration changing to parallel/subparallel offshore. TST appear as a wedge with reflections showing parallel/subparallel configuration onlapping and downlapping D2. HST shows a progradational reflections (oblique-tangential) with intermediate/ weak continuity. The reflections of TST and HST terminate updip in erosional truncation. SS1 shows progradational clinoforms (sigmoidal-oblique) in which occur a lateral and vertical change in its seismic facies and presents a distinct topset and foreset beds. These seismic sequences were correlated with seismic stratigraphic interpretations performed in BB and neighborhood as well compared with the "Vail's Curve" and a oxygen isotope curve, suggesting a good correlation. These correlations together with the derived drill information of the DSDP/ODP programs induce the following sequences deposition ages: SS3 (older than 11 Ma), SS2 (11 – 5 Ma) and SS1 (5 Ma-Present).

**Introdução**

Nos verões austrais de 1987 e 1988 o foram efetuados dois levantamentos geofísicos marinhos na margem norte da Península Antártica, vinculados ao Programa Antártico Brasileiro - PROANTAR (Figura 1). Tais levantamentos concentraram-se no Estreito de Bransfield, sendo utilizado o Navio Oceanográfico Almirante Câmara da MARINHA DO BRASIL.

Os dados sísmicos foram obtidos com um cabo do tipo *streamer*, 72 canais, e registrados num sismógrafo DFS-V. A fonte sísmica foram 8 *air guns*, totalizando um volume de 540 $in^3$ à uma pressão operacional de 4.500 psi. Estas linhas sísmicas foram preliminarmente interpretados por Gamboôa & Maldonado (1990).

O objetivo deste trabalho foi a reinterpretação destas mesmas linhas sísmica sob o enfoque da Estratigrafia de Seqüências *stricto sensu*, partindo da identificação dos principais limites de seqüências (**discordâncias**), as quais subdividiram o pacote sedimentar da Bacia de Bransfield em 3 seqüências sísmicas.

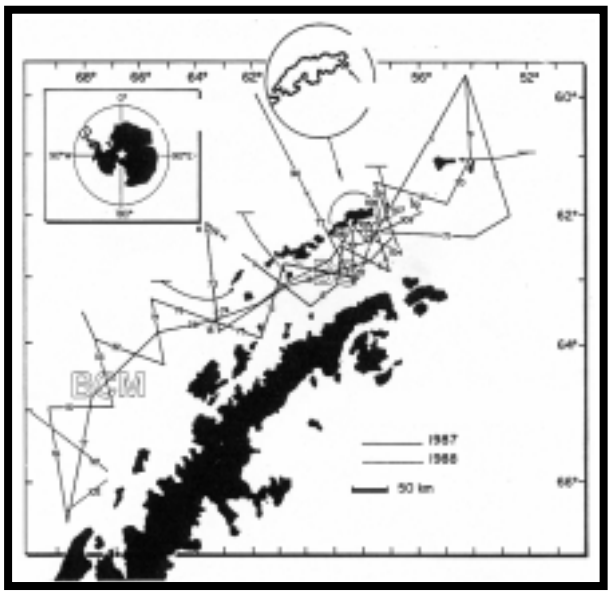


Figura 1 – Localização das seções sísmicas de reflexão. BS = Estreito de Bransfield; BCM = Margem continental de Bellingshausen (modif. Gamboôa & Maldonado, 1990).

**Sismo-estratigrafia e estratigrafia de seqüências**

A Figura 2 apresenta a interpretação de uma seção sísmica *dip* (SA500010), que melhor sintetizou as unidades sísmicas identificadas na área.

A fácies sísmica do embasamento continental não é visualizada face à baixa razão sinal/ruído ou encoberto por múltiplas. O embasamento oceânico apresenta configuração caótica, com o topo marcado por hipérboles de difração, que constitui a discordância **D3**.

A seqüência **SS3** sobrejaz **D3**, compondo-se por reflexões de média/alta continuidade e configuração paralela/subparalela, sugerindo estratos contínuos, de ambiente amplo e uniforme. As reflexões fortes são interpretadas como intercalação de folhelhos/siltitos com arenitos. Esta fácies sísmica deve consistir num ambiente marinho nerítico. **SS3** apresenta um suave mergulho bacia adentro e, igual ao embasamento, está com dobras/falhas, relacionadas à subducção na Fossa Shetland do Sul e ao movimento da Cordilheira Scotia do Sul. No talude/sopé continental os refletores de **SS3** têm baixa/média continuidade e configuração paralela a subparalela, com geometria de preenchimento frente de talude, constituindo,

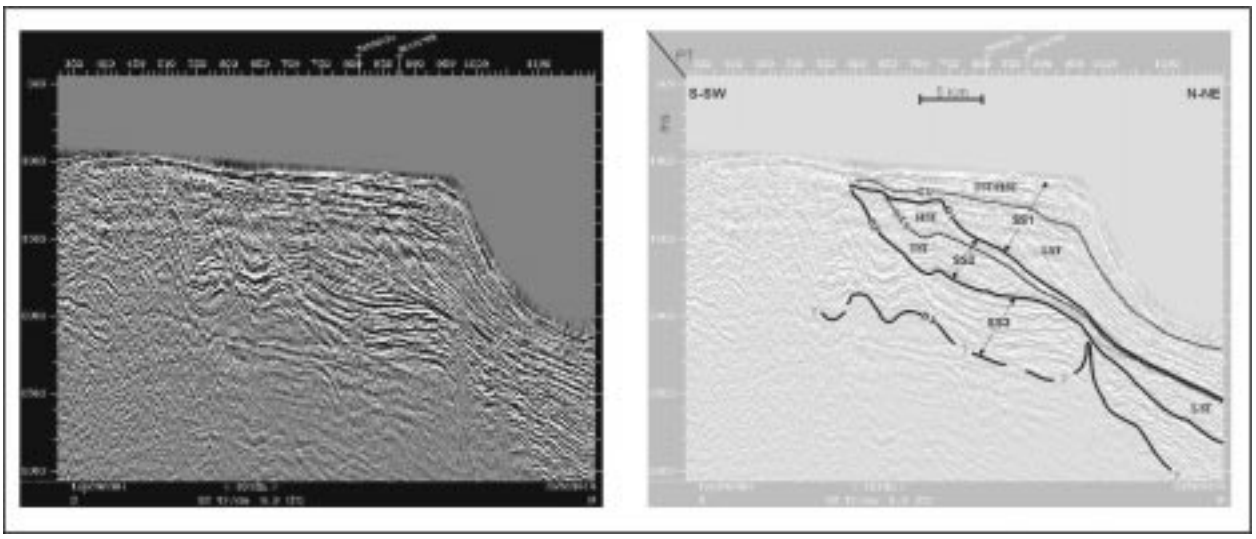

Figura 2 – Seção sísmica *dip* (SA500010).

certamente, depósitos de águas profundas de leques submarinos. Continente adentro, as reflexões de **SS3** terminam em truncamento estrutural no embasamento continental e, bacia adentro, em *onlap* distal no embasamento oceânico. O topo de **SS3** é caracterizado por um conspícuo truncamento erosivo, denominado discordância **D2**, que é também identificada por terminações em *onlap* e *downlap* dos refletores da seqüência **SS2** sobreposta. **SS3** apresenta-se como uma cunha sedimentar falhada e deformada. preenchendo *grabens* formados na fase rifte da bacia, como sugerido em Gamboôa & Maldonado (1990).

A seqüência **SS2** interpõe-se entre as discordâncias **D2** e **D1**, a qual é definida pelo truncamento erosivo *up dip* dos próprios refletores de **SS2** e pelas terminações em *onlap* dos refletores de **SS1**. **SS2** é subdividida em três tratos de sistemas, face à uma conspícua superfície de *downlap* (**DLS**), além dos padrões de configuração e de terminações das reflexões: a) de nível de mar baixo (*Lowstand System Tract* – **LST**), b) transgressivo (*Transgressive System Tract* – **TST**) e c) de nível de mar alto (*Highstand System Tract* – **HST**). Entre **D2** e a **DLS** é definido o **LST**, composto de montiformas com configuração *hummocky*, tornando-se mais contínuas e paralelas bacia adentro, constituindo leques de talude/fundo de bacia. Ainda entre **D2** e a **DLS** ocorre o **TST**, com configuração paralela/subparalela e contínuas e, também, *hummocky* (próximo ao topo), com mergulho suave bacia adentro. O **TST** deve conter fácies de retração submarina, constituída por uma sucessão de fácies que começa, provavelmente, em sua base com um *till* de alojamento, sobreposto por sedimentos glácio-marinhos, que, com a deglaciação ficam cobertos por sedimentos marinhos. A fácies *hummocky* no topo do **TST** pode estar relacionada a ciclos menores de avanço e recuo da geleira (próximo ao *highstand* eustático - transição **TST**/**HST**), podendo ser constituída por depósitos *ice-rafted* e de fluxos gravitacionais. Os refletores do **TST** e **LST** terminam, continente adentro, em *onlap* sobre **D2** e em *downlap* bacia adentro, mais para o fundo da bacia terminam em *onlap* distal ou em *downlap* contra a discordância **D3**. Entre a **DLS** e **D1** ocorre um trato de mar alto (**HST**), representado por clinoformas oblíquo-tangenciais de média continuidade, "downlapando" a **DLS**. Acima de **D1** assenta-se **SS1**, possuindo clinoformas sigmoidais-oblíquas, em distintas camadas de *topset* e *foreset*. Tal configuração indica um ambiente de alta energia, com alternância de processos construtivos (sigmóides) e *by pass* nos *topsets* (oblíquos). Em ambiente glaciais, tal configuração sugere deposição diretamente à frente da *grounding-line*. Lateralmente, os *foresets* das clinoformas variam de refletores fracos e baixa/média continuidade a fortes e contínuos no talude/sopé continental. Ainda no talude/sopé continental, observam-se montiformas com configuração *hummocky* que terminam, continente adentro, em *onlap* sobre refletores fortes e contínuos. Tais variações indicam uma transição entre numerosos escorregamentos e deslizamentos (reflexões fracas, média/baixa continuidade), passando para fluxo de detritos (reflexões fortes e contínuas abaixo do talude) que por sua vez geram correntes turbidíticas de alta densidade, erodindo a parte superior do sopé continental. Tal interpretação implica que a maior parte da deposição ocorre nos períodos de máximo glacial e no final destes períodos, quando o rápido suprimento de *till* na borda da plataforma produziria instabilidades no talude superior.

Alguns refletores de *foreset* de **SS1** terminam em *toplap*, abaixo de fortes refletores de *topset*, que terminam abruptamente na borda da plataforma, enquanto que, bacia adentro, terminam em *onlap* e *downlap* em **D1**. Os refletores de *topset* têm amplitude variável/continuidade média e são intercalados com refletores muito fortes e de alta amplitude, terminando abruptamente na borda da plataforma. Montiformas com configuração caótica ocorrem diretamente acima e abaixo das terminações destas reflexões fortes de alta amplitude. Estas reflexões forte que terminam na borda da plataforma abruptamente devem constituir, provavelmente, *till* subglacial, tais

terminações abruptas representam *till tongues*. Tais montiformas correspondem às associações de bancos de morenas com depósitos de deslizamentos/escorregamentos, nos momentos de retração da geleira (depósitos de *grounding-line*).

Infere-se uma superfície transgressiva (*Transgressive Surface* – **TS**) no limite entre os refletores de *topset* e *foreset* de **SS1**, baseando-se na diferença entre a configuração dos refletores de *topset* e *foreset*, onde os *foreset* constituiriam o trato de mar baixo (**LST**) de **SS1**, associados aos avanços da *grounding-line* até a borda da plataforma; enquanto os refletores de *topset* e *foreset* acima da **TS** corresponderiam a depósitos proglaciais de baixo ângulo, associados a ciclos menores de avanço/recuo das geleiras, variando para fácies marinho profundo intercaladas com depósitos *ice-rafted* e fluxos gravitacionais, causados por instabilidades na borda da plataforma/talude superior, consistindo em **HST**/**TST** indivisos, de **SS1**, do Recente. A inferência da **TS** é corroborada pelas abruptas terminações dos refletores de *topset*, que após alcançarem um máximo avanço em direção à bacia, passam a retroceder continente adentro. As fortes reflexões sub-horizontais são interpretadas como causadas por erosão sub-glacial e *till* de alojamento, indicando que o máximo avanço da geleira está cada vez mais em direção ao continente. Tal feição estaria associada a uma subida eustática. No topo de **SS1** ocorrem calhas/elevações, sugerindo *icebergs scour*, além de grandes canais associados à calhas glaciais.

A Figura 3 esquematiza o arcabouço estratigráfico da Bacia de Bransfield construído a partir desta análise sismo-estratigráfica, muito semelhante ao modelo clássico da Estratigrafia de Seqüências.

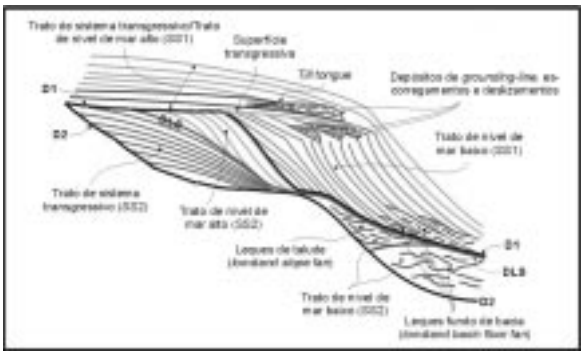


Figura 3 – Esquema para o arcabouço estratigráfico da Bacia de Bransfield proposto neste trabalho.

**Correlações estratigráficas**

A interpretação aqui efetuada foi correlacionada com outros estudos sismo-estratigráficos e dados de fontes diversas: a) margem continental ao redor da Antártica (Cooper *et al.*, 1991); b) Bacia de Bransfield (Gambôa & Maldonado, 1990 e Prieto *et al.*, 1999); c) bacias circum-vizinhas (Larter & Cunningham, 1993; Larter *et al.*, 1997; Rebesco *et al.*, 1997; Viseras & Maldonado, 1999); d) perfurações do DSDP/ODP na Península Antártica; e) curva de isótopo de oxigênio (Abreu & Anderson, 1998) e f) "Curva de Vail" (Haq *et al.*, 1988). Nesta correlação as seguintes premissas são assumidas: 1) a deposição glacial é síncrona na Bacia de Bransfield e em região circum-vizinha (*i.e.*, se a geleira avança em direção à bacia no Mar de Bellingshausen, também avançaria nas bacias de Bransfield e de Powell); 2) o avanço/recuo das geleiras estão associados à quedas e a subidas eustática, respectivamente, e 3) o maior volume de terrígenos que se depositam no talude/sopé continental ocorre durante o máximo glacial (avanço da *grounding-line* até a borda da plataforma) e no final destes períodos (*stillstand* e início da retração da *grounding-line*).

Desta forma, a partir das correlações, chegou-se às seguintes conclusões sobre a história do preenchimento sedimentar da Bacia de Bransfield: *1)* **SS3** corresponde à fase *rift* da bacia, como já sugerido por Gambôa & Maldonado (1990) e Prieto *et al.* (1999), sendo depositada após 20-21 Ma (Eomioceno), início de abertura da bacia segundo Barker (1983); *2)* **D2**, limite entre **SS3** e **SS2**, representa o primeiro grande avanço da geleira até a borda da plataforma, associado ao crescimento da geleira no Oeste Antártico (*West Antarctic Ice Sheet* - WAIS). As correlações com a curva de isótopo de oxigênio de Abreu & Anderson (1998), com a "Curva de Vail" (Haq *et al.*, 1987) e com os dados de Rebesco *et al.* (1997), sugerem que este avanço da geleira ocorreu em torno de 11 Ma; *3)* **SS2**, portanto, depositou-se sob um regime glacial, com um grande aporte sedimentar no talude/sopé continental, devido ao enorme poder erosivo e de transporte das geleiras e à grande quantidade de sedimentos que deveria existir no caminho da geleira (depositados durante o período pré-glacial). Isto explica as montiformas localizadas no sopé continental, depositadas através dos sistemas de *grounding-line*, interpretadas constituir o **LST** de **SS2**. O **TST** de **SS2** estaria relacionado à fase de recuo da geleira, sendo que, dentro desta retração de maior ordem de grandeza, ciclos menores de avanço e recuo da *grounding-line* forneceriam o aporte sedimentar necessário para a deposição deste trato de sistema, numa intercalação entre depósitos proglaciais de baixo ângulo (como descritos por Larter & Vanneste, 1995) com depósitos marinhos. O topo do **TST** e do **LST** de **SS2** é marcado por uma conspícua superfície de *downlap* (**DLS**). Correlações com os trabalhos de Larter & Barker (1989), Larter *et al.* (1997), Viseras & Maldonado (1999), ODP *Leg* 113 (*site* 696), ODP *Leg* 178 e com a "Curva de Vail", sugerem 4,6 Ma para a **DLS**. Acima da **DLS** sobrejaz o **HST** de **SS2**, indicando *stillstand* eustático. Os depósitos deste trato também estão associados à ciclos de menores de recuos e avanços da *grounding-line*. Neste contexto de *stillstand* as geleiras têm maior competência de avanço, depositando-se leques e deltas de *grounding-line*, conformando as clinoformas deste trato; *4)* O início da deposição de **SS1** está relacionada a um novo avanço da geleira até a borda da plataforma, dentro do período em que ocorre a formação das geleiras do Hemisfério Norte (+/- 3 Ma). O avanço da geleira, juntamente com deformações tectônicas (dobramentos), teriam causado o truncamento erosivo,

discordância **D1**, dos refletores do **TST** e do **HST** de **SS2**, sobre a qual é depositado um **LST**, com configuração de clinoformas sigmoidais-oblíquas, interpretadas como depósitos de frente de *grounding-line*, de acordo com os modelos de Boulton (1990), Larter & Cunningham (1993), Larter *et al.* (1997) e Prieto *et al.* (1999). As fortes reflexões com término abrupto próximo à borda da plataforma que são observadas dentro das camadas de *topset* nas seções sísmicas constituiriam erosão e *till* sub-glacial, enquanto que a diferença entre as reflexões de *topset* e *foreset* estariam relacionadas à uma nova subida eustática, com o máximo avanço da geleira cada vez mais em posições continente adentro. As reflexões de *topset*, portanto, representam depósitos de frente de *grounding-line* de baixo ângulo intercalados com depósitos marinhos, sempre influenciados por depósitos *ice-rafted*. O máximo avanço glacial é marcado por uma superfície transgressiva (*Transgressive Surface*–**TS**), marcada pela reflexão com término abrupto mais para dentro da bacia. Abaixo da **TS** está o **LST** de **SS1**, enquanto que acima ocorre os tratos **TST/HST** (indivisos), condizente com o atual nível de mar alto.

## Conclusões

Este modelo estratigráfico aqui elaborado (*vide* Figura 3) poderá certamente, ser aplicado de uma forma preditiva em outras bacias marginais da Antártica, desde que se considere, obviamente, os fatores locais.

Em síntese, as interpretações e correlações realizadas neste trabalho sugerem a seguinte datação para a deposição das seqüências: **SS3** (mais nova que 20-21 Ma e mais antiga do que 11 Ma); **SS2** (entre 11 e 5 Ma) e **SS1** (de 5 Ma até o Presente).

## Referências Bibliográficas


Abreu, V.S.; Anderson; J.B. 1998. Glacial eustasy during the Cenozoic: sequence stratigraphic implications. *AAPG Bulletin*, **82**(7), 1385-1400.

Birkenmajer, K. 1983. Late Cenozoic phases of block faulting on King George Island (south Shetland Islands, West Antarctica). *Bulletin de l'Academie Polonaise des Sciences, Sciences de la Terre*, **20**, 21-32.

Cooper, A.K.; Barrett, P.J.; Hinz, K.; Traube, V.; Leitchenkov, G.; Stagg, H.M.J. 1991. Cenozoic prograding sequences of the Antarctic continental margin: a record of glacio-eustatic and tectonic events. *Marine Geolgy*, **102**, 175-213.

Gambôa, L.A.P. & Maldonado, P.R. 1990. Geophysical investigations in the Bransfield Strait and in the Bellingshausen Sea – Antarctica. *In*: John, B.S. (ed.). *Antarctica as an Exploration Frontier – Hydrocarbon Potential, Geology and Hazards*, AAPG Stud. Geol. # 31, 127-141.

Haq, B.U; Hardenbol, J. & Vail, P.R. 1988. Mesozoic and Cenozoic chronostratigraphy and cycles of sea-level change. *In*: Wilgus, C.K. *et al.* (eds.). *Sea-level changes - an integrated approach*. Tulsa, SEPM, 71-108.

Larter, R.D. & Cunningham, A.P. 1993. The depositional pattern and distribution of glacial-interglacial sequences on the Antarctic Peninsula Pacific margin. *Marine Geology*, **109**, 203-219.

Larter, R.D; Rebesco, M; Vanneste, L.E; Gambôa L.A.P.; Barker, P.F. 1997. Cenozoic tectonic, sedimentary and glacial history of the continental shelf west of Graham Land, Antarctic Península. *In*: American Geophysical Union (ed.). *Geology and Seismic Stratigraphy of the Antarctic Margin, Antarct. Res. Ser.*, **71**, 1 – 27.

ODP (Ocean Drilling Program) 1998. Leg 178 Preliminary Report – Antarctic Glacial History and Sea-Level Change. Página da Web: http://www-odp.tamu.edu/publications/prelim/178_prel em 24/06/1999.

Prieto, M.J.; Ercilla, G; Canals, M; Batist, M. 1999. Seismic stratigraphy of the Central Bransfield Basin (NW Antarctic Peninsula): interpretation of deposits and sedimentary processes in a glacio-marine environment. *Marine Geology*, **157**, 47-68.

Rebesco, M; Larter, R.D; Barker, P.F.; Camerlenghi, A; Vanneste, L.E. 1997. The history of sedimentation on the continental rise west of the Antarctic Peninsula. *In*: Barker, P.F.; Cooper, A.K. (eds.). *Geology and Seismic Stratigraphy of the Antarctic Margin*, part 2. Antarctic Research Series, AGU, **71**, . 29-49.

Viseras, C. & Maldonado, A. 1999. Facies arquitectures, seismic stratigraphy and development of a high-latitude basin: the Powell Basin (Antarctica). *Marine Geology*, **157**, 69-87.

# Bottom deposits in the Central Scotia Sea: the importance of the Antarctic Circumpolar Current and the Weddell Gyre flows

*Andrés Maldonado(1), Antonio Barnolas(2), Fernando Bohoyo(1), Javier Hernández-Molina(3), Jesús Galindo-Zaldívar(4), Luiz Gamboa(5), Alipio José Pereira(5), José Rodríguez-Fernández(1), Luis Somoza(2), Emma Suriñach(6) George André Uller(7) and Juán Tomás Vázquez(3).*

*1 - Instituto Andaluz Ciencias de la Tierra. CSIC/Universidad de Granada, Spain*
*2 - Instituto Geológico y Minero de España, Madrid, Spain*
*3 - Facultad de Ciencias del Mar, Cádiz. Spain*
*4 - Departamento de Geodinámica. Universidad de Granada, Spain*
*5 – Petrobras S/A. Brazil*
*6 - Departament de Geologia Dinàmica i Geofísica. Universitat de Barcelona, Spain*
*7 – Universidade Federal Fluminense*

**Abstract**

The opening of a marine gateway between South America and the Antarctic Peninsula since the Late Eocene to Early Oligocene involved the disruption of the final barrier to the initiation of the Antarctic Circumpolar Current (ACC). The separation of the southern continents increased the thermal isolation of Antarctica and favored the accumulation of extensive ice sheets which reached progressively the shelf edge. The deep water from the Weddell Gyre flows northward into the Scotia Sea through corridors within the South Scotia Ridge and interacts with the ACC, resulting in large contourite waves and drifts. These deposits were largely developed from the Miocene and their distribution and extent highlight the importance of Antarctic deep water production, which in turn may had profound influences on the global circulation system and present climate.

## Introduction

The Scotia Sea is a small ocean basin developed as results of the final processes of the continental fragmentation of Gondwana and the Late Paleogene separation of the Antarctic Peninsula from South America (Livermore et al., 1994; Barker, 1995). During the 2000-2001 austral summer season a sector of the central and southern Scotia Sea, north of the South Orkney Microcontinent was investigated using swath bathymetry, multichannel and high resolution seismic profiles, together with magnetic field measurements. A segment of the sea floor was also mapped with the multibeam echo sounder fitted to the BIO HESPERIDES (Fig. 1). The oceanic sea floor according to the magnetic anomalies oriented E-W in the mapped area is about 13.6 to 20.2 Ma old (chron C5C to C6), from north to south (Tectonic Map of the Scotia Sea, 1985).

The area investigated with swath bathymetry is located at the exit of a major morphologic gap in the South Scotia Ridge, northward of the entrance to Jane Basin. The bathymetry ranges between 2500 in the SE corner and more than 3500 m in the northern sector. The sea bottom is accidented, with wide valleys, incised channels, depressions and areas of very irregular physiography.

## Countourite deposits

The swath bathymetry map reveals an irregular bottom relief and a variety of bedforms which are attributed to contourite deposits. Large drifts have an elongated and mounded morphology oriented in two predominant directions: N-S in the southern sector and NW-SE in the northern sector. These deposits are over 1 s (twt) thick in the center of the drift and they have a wedge geometry with reflectors converging towards marginal zones of non-deposition (Fig. 2). Contourite waves fields are also well developed. Most sediment waves are slightly asymmetrical and they migrated in the direction of the bottom current, either upslope or downslope, whereas the wave fields tend to be elongated in the direction of the current.

A contourite channel-levee fan occupies the central sector of the swath map. It is about 80 x 40 km and elongated in the downslope direction. Like turbidite fans, this system is developed from a main feeder channel and it is composed of several distributary channels and the associated levees.

The MCS profiles show strong basement reflections of the top of Layer 2 at a mean depth of 0.8 s twt beneath the sea floor, although locally the sedimentary cover of the igneous crust is absent. Four large amplitude, continuous reflectors can be recognized across most of the profiles. Seismic Unit I, at the top, is a rather thin sediment drape, some 0.5 s twt thick, which is attributed to the Quaternary. The other five units display high amplitude, discontinuous internal reflectors, characterized by wavy to subparallel internal configuration. Towards the base of each unit

are also observed oblique and sigmoid configuration which downlap the reflector boundary. Unit III shows densely packed reflectors of marked wavy configuration, whereas the top and bottom boundary reflectors depict erosional character. This unit is of Late Miocene to Early Pliocene age and reveals a marked cyclic pattern of deposition of alternating high and low energy periods. The overall seismic character of these units exhibit active bottom currents, which resulted in the development of large contourite wave and drift deposits over the entire area.

In this presentation we show that the opening of seaways around Antarctica not only allowed the installation of a strong circumpolar flow, but also triggered a high production of Antarctic deep water. This water was swept northward from the Weddell Gyre into the South Atlantic and this flow could be the thermal motor influencing the late Cenozoic circulation patterns, the cooling of the oceans since the Early Oligocene and, as consequence, the chilling of the world´climate.

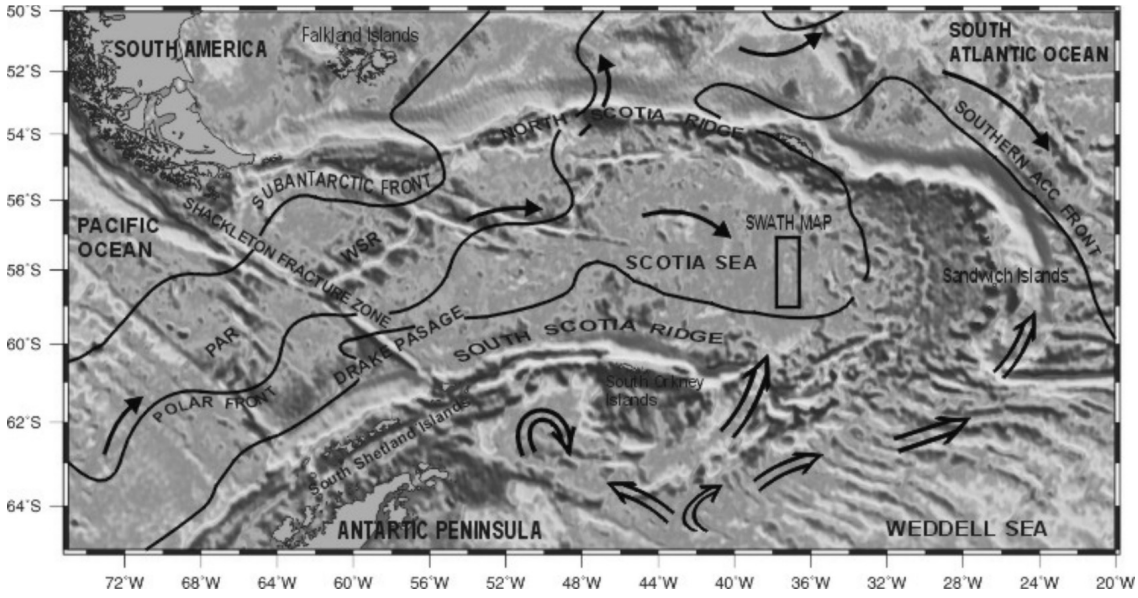


Figure 1- Simplified map from the GEOSAT gravimetric anomaly map recently released by the US Navy showing the distribution of the main oceanographic features. The ACC (arrows) and the WSBW (open arrows) flow directions are shown.

**Discussion and Conclusions**

The deposits in the central sector of the Scotia Sea result from the interplay between the northward flowing Weddell Sea Bottom Water (WSBW) and the eastward directed flow of the ACC. The initiation of the ACC following the opening of the Drake Passage is considered perhaps the most important event controlling the evolution of the Cenozoic climate and one crucial factor influencing the development of extensive Antarctic icesheets during the Miocene (Kennett, 1982; Barrett, 1996). More recently, however, it is contested if a deep circumpolar passageway alone is sufficient to produce a strong current and the subsequent permanent icesheets of the East Antarctic (Lawver and Gahagan, 1998).

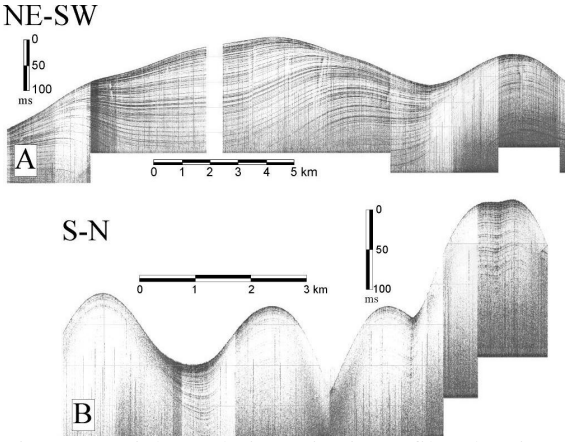


Figure 2.- High-resolution seismic profiles showing representative contourite drift (A) and large-scale contourite wave (B) deposits in the central Scotia Sea.

**References**

Barker, P.F., 1995, Tectonic framework of the East Scotia Sea. In: Taylor, B. (Eds), Backarc Basins: Tectonics and Magmatism. Plenum Press, New York, 281-314.

Barrett, P.J., 1996, Antarctic paleoenvironment through Cenozoic times: a review. Terra Antartica, 3, 103-119.

Kennett, J. P., 1977, Cenozoic evolution of Antarctic glaciation, the circum-Antarctic ocean, and their impact on global paleoceanography, J. Geophys. Res., 82, 3843-3860.

Lawver, L.A., Gahagan, L.M., 1998, Opening of Drake Passage and its impact on Cenozoic ocean circulation. In: Crowley, T.J., Burke, K.C., (Editors), Tectonic Boundary Conditions for Climate Reconstructions. Oxford Univ. Press, Oxford, 212-223.

Livermore, R., McAddo, D. and Marks, K., 1994. Scotia Sea tectonics from high-resolution satellite gravity, Earth and Planetary Science Letters 123, 255-268.

# Bransfield Strait development in the tectonic framework of NE Antarctic Peninsula

*Jesús Galindo-Zaldívar[(1)], Luiz Gamboa [(2)] and Andrés Maldonado [(3)].*
*1 - Departamento de Geodinámica. Universidad de Granada, Spain*
*2 - Petrobras S/A. Brazil*
*3 - Instituto Andaluz Ciencias de la Tierra. CSIC/Universidad de Granada, Spain*

**Abstract**

Bransfield Strait is an incipient oceanic back-arc basin developed between the South Shetland Block and the Antarctic Peninsula. The combined analysis of multichannel seismic profiles acquired during several oceanographic cruises and the satellite free air gravity anomaly map allow to establish the development of this basin. The structures show an along-strike evolution and they are heterochronous. The occurrence of an axial volcanism and the presence of a break-up unconformity reveal that the Central Bransfield Basin is an incipient oceanic basin. Continental extension was asymmetrical and developed a typical lower-plate passive margin in the Antarctic Peninsula and a starved upper plate margin along the South Shetland Block. This structure evolved from a low angle normal fault initiated in the continental margin of the Antarctic Peninsula with top-to-the-NW displacement. The hanging wall of this fault is the South Shetland Block, which moved northwestward from the Antarctic Peninsula margin. Thinning of the continental crust is also presently active in the Western and Eastern Bransfield basins, with formation of half-grabens and associate wedge structures generally opening northwestward. The initiation of Bransfield Strait and its present activity is as a combined consequence of the end of spreading in the Phoenix-Antarctic ridge (3.3±0.2 Ma) and the westward propagation of the transcurrent and transtensional tectonics active in the continental blocks of the South Scotia Ridge.

## Introduction

The two major plates in the study area are the Scotia and Antarctic plates, in contact via a left-lateral transpressive fault zone boundary located along the South Scotia Ridge (Fig. 1). This boundary extends northwestward across the Drake Passage as a prominent submarine ridge between the South Chile Trench and the South Shetland forearc, called the Shackleton Fracture Zone. The southern end of the Shackleton Fracture Zone is subducted below the South Shetland forearc. The South Shetland Block may be considered as a crustal element independent from the Antarctic Plate.

The Bransfield Strait is a NE-SW elongated basin that lies between the northwestern tip of the Antarctic Peninsula and the South Shetland Block, and is widely interpreted as an extensional marginal sea associated with active subduction at the South Shetland Trench (Pelayo and Wiens, 1989; Gamboa and Maldonado, 1990; Barker and Austin, 1998). The South Shetland Trench is the last conspicuous expression of a subduction zone that existed all along the western margin of the Antarctic Peninsula. In addition, it is proposed that the rift of the Bransfield Strait merges eastward into an active transcurrent fault zone within the South Scotia Ridge (Galindo-Zaldivar et al., 1996). Meanwhile, González-Casado et al. (2000) propose that the Bransfield Basin develops only as a consequence of the sinistral transcurrence between the Scotia and Antarctic Plates.

The West Scotia and the Phoenix-Antarctic Ridges, extend across the central sector of the Drake Passage (Fig. 1). The Phoenix Plate ocean floor was subducted beneath the Antarctic Plate continental lithosphere at the South Shetland Trench, while farther northwest new ocean floor was created at the Phoenix-Antarctic Ridge, which migrated southward. New bathymetric and magnetic anomaly data show that extinction of the last remaining Phoenix Ridge segments of the once-extensive Phoenix-Antarctic spreading center occurred at the time of magnetic chron C2A (3.3 ± 0.2 Ma), synchronous with a ridge-trench collision south of the Hero Fracture Zone (Livermore et al., 2000).

Good markers for understanding the recent tectonic evolution of the area are the elongated bodies of Cretaceous mafic rocks located along the Antarctic Peninsula. These rocks are associated with large magnetic anomaly bands known as the Pacific Margin Anomaly or West Coast Magnetic Anomaly. The single elongated anomaly that is recognized in the southern region of the Antarctic Peninsula is divided into two branches in the northern Antarctic Peninsula by the opening of the Bransfield Strait.

## The Bransfield Strait structure

A combined set of MCS profiles from Brazil, Spain, Japan and China have been used to determine the main features of the structure of the Bransfield Strait area. The Bransfield Basin has a lens shape and can be divided into three subbasins: Western, Central and Eastern.

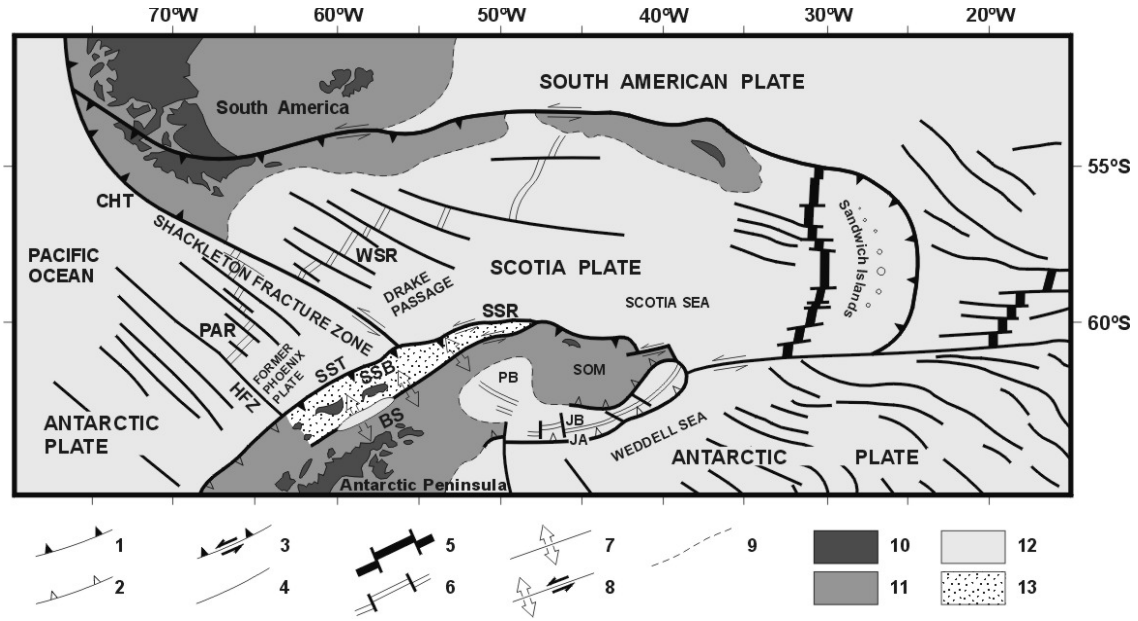


Figure 1 - Tectonic map of the Scotia Arc. 1, active subduction zone. 2, inactive subduction zone. 3, transpressive fault zone. 4, fault zone. 5, active spreading ridge. 6, inactive spreading ridge. 7, active extensional zone. 8, active transtensional fault zone. 9, continental-oceanic crust boundary. 10, emerged continental crust of South America and Antactic plates. 11, submerged continental crust. 12, oceanic crust. 13, South Shetland Block. BS, Bransfield Strait. CHT, Chile Trench. PAR, Phoenix-Antarctic Ridge. HFZ, Hero Fracture Zone. SST, South Shetland Trench. SSB, South Shetland Block. SSR, South Scotia Ridge. PB, Powell Basin. SOM, South Orkney microcontinent. JB, Jane Bank. JA, Jane Arc.

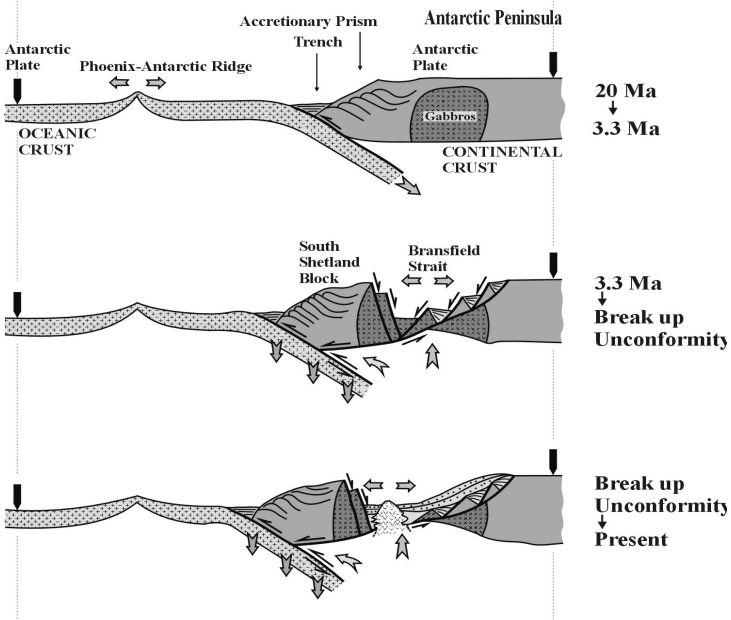


Figure 2.- Tectonic model for the development of the Bransfield Strait and the South Shetland Block.

Only incipient rifting occurred south of Deception Island in the Western Basin. This region is affected, however, by intense normal faulting that created rotated blocks on the continental crust. A fairly thick synrift sequence is observed in half-grabens. The sedimentary fill shows wedges opening towards the NW. Some faulting affects the seafloor, indicating active tectonics and present-day rifting. In addition, the profiles show a recent stage of compression, which develops large folds in the basin filling.

The Central Bransfield Basin extends from Deception Island to the Bridgement Islands, both interpreted here as outcrops of an incipient spreading center that exists along the axis of the basin with associated magnetic anomalies. The southeastern margin presents structures and sedimentary fill that in many ways resemble the features observed along passive margins, with development of syn rift and post rift sequences. In this part of the basin the continental crust was thinned in response to the NW-SE extensional tectonic regimen, which continues up to present as shown by earthquake focal mechanism data (Pelayo and Wiens, 1989). A low angle crustal fault dipping towards the NW, and that probably continues below the South Shetland Islands, served as the detachment plane for the synthetic normal faults that cut a synrift sequence deposited along the Antarctic Peninsula side of the basin. The synrift sequence can be seen in MCS data and the sedimentary fill of the half-grabens has wedge shapes opening towards the SE. In addition, there is a well developed drift sequence that is bounded at its base by a break-up unconformity, occurring only at the central part of the Bransfield Basin. The stretched continental crust forms a band about 30 km wide along the southern margin of the basin, whereas a narrow, steep slope topography marks the passage from the shelf along the South Shetland Islands to the axial area of this part of the Bransfield Basin.

The incipient spreading center along the Bransfield Basin is interrupted by a transform fault near the northern tip of King George Island.

The crustal structure in the axial part of the central Bransfield Basin has motivated several studies. In an earlier investigation using seismic refraction, Ascroft (1972) proposed the existence of a stretched continental crust intruded by an axial volcanic ridge below, and Moho depths of the order of 14 to 20 km were obtained. Later researches obtained much greater Moho depth values up to 30 km in the same area. Later, Grad et al. (1997), using OBS data, obtained a model of the crustal structure at the Bransfield Basin that, while indicating Moho at depths of 30 km, showed the presence of a high velocity layer (Vp = 7.3 – 7.2 kms) at the axial portion of the Bransfield Strait. Torres (1997) modeled the crustal structure at the Central Bransfield Basin using magnetic, gravimetric and seismic data to describe a crustal structure similar to that proposed by Ascroft (1972) whereby a shallow Moho exists below the basement high at the central region of the basin.

The seismicity in the region is concentrated at the ends of the Central Basin at Deception and Bridgement Islands. The focal earthquake mechanisms determined for shallow and intermediate seismicity (Pelayo and Wiens, 1989) indicate NW-SE extensional stresses compatible with the opening of the Bransfield Strait.

The Eastern Bransfield Basin extends northward of Bridgement Island to a region just south of Elephant Island. The structural style of this sector has features similar to those observed in the Western Bransfield Basin: steep normal faults occur along the northern margin. The Eastern Bransfield Basin is characterized by the development of half-grabens with sedimentary wedges opening towards the NW, indicating an extensional or transtensional regime. In addition, most of the sediments of the half-grabens show open, large folds indicative of a recent compressional deformation.The deposits representing the synrift phase of the basin are cut by numerous normal faults, some of them affecting the present-day seafloor morphology (Fig. 2).

**Conclusions**

The Bransfield Strait is an asymmetrical backarc basin whose opening is probably related to a low angle normal fault with top-to-the-NW displacement, for which the South Shetland Block constitutes the hanging wall (Fig. 2). The margin adjacent to the Antarctic Peninsula presents all the features associated with a lower plate passive margin, such as the development of landward tilted half-grabens, the presence of a break-up unconformity, and the deposition of an oceanward dipping “drift” sequence. However, the margin near the South Shetland Islands is typical of an upper-plate margin: poorly nourished, sharp and with high angle faults. The extension is more developed in the Central Bransfield Basin, where a volcanic axis is recognized as the expression of a young spreading center, and there is possibly incipient oceanic crust. In the Bransfield basin extremities, the present-day deposits represent the synrift sequence, and extension continues to progress.

The Bransfield Basin probably develops as a consequence of two interacting processes. The main one is related to the end of the oceanic spreading at the Phoenix-Antarctic Ridge at Middle Pliocene times

(3.3 Ma) and the subsequent development of a roll-back mechanism that produces the northwestward migration of the South Shetland Block (Fig. 2) . The second process that takes place in the region is the propagation of the sinistral transcurrent deformations associated with the Scotia/Antarctic Plate boundary (Fig. 1) that propagated through the continental blocks, becoming transtensional inside the South Scotia Ridge and extensional in the Bransfield Strait.

**References**

Ascroft, W.A.,1972, Crustal structure of the South Shetland Islands and Bransfield Strait, Br. Antarct. Surv., Sci. Rep. 66, 1-43.

Barker, D.H.N. and Austin, J.A., 1998, Rift propagation, detatchment faulting, and associated magmatism in Bransfield Strait, Antarctic Peninsula, J. Geophys. Res. 103, 24017-24043.

Galindo-Zaldívar, J., Jabaloy, A., Maldonado, A. and Sanz de Galdeano, C., 1996, Continental fragmentation along the South Scotia Ridge transcurrent plate boundary (NE Antarctic Peninsula), Tectonophysics 242, 275-301.

Gamboa, L.A.P. and Maldonado, P.R., 1990, Geophysical investigations in the Bransfield Strait and in the Bellinghausen Sea- Antarctica. In: Antarctica as an Exploration Frontier- Hydrocarbon Potential, B. St. John. Ed., Geology and Hazards, Am. Assoc. Petr. Geol. 31, 127-141

González-Casado, J.M., Giner-Robles, J.L. and López-Martínez, J., 2000, Bransfield Basin, Antarctic Península: Not a normal backarc basin, Geology, 28, 1043-1046.

Grad, M., Shiobara, H., Janik, T., Guterch, A. and Shimamura, H., 1997, Crustal models of the Bransfield Rift, West Antarctica, from detailed OBS refraction expreriments, Geophys. J. Int., 130, 506-518.

Livermore, R., Balanyá, J.C., Barnolas, A., Galindo Zaldívar, J., Hernández, J., Jabaloy, A., Maldonado, A., Martínez, J.M., Rodríguez-Fernández, J., Sanz de Galdeano, C., Somoza, L., Suriñach, E. and Viseras, C., 2000. Autopsy on a dead spreading centre: the Phoenix Ridge, Geology, 28, 607-610.

Pelayo, A.M. and Wiens, D.A., 1989, Seismotectonics and relative plate motions in the Scotia Sea region, J. Geophys. Res. 94, 7293-7320.

Torres, L.C., Gomes, B.S. and Gamboa, L.A.G., 1997, Determinacao da Espessura Crustal na Margem Ativa da Regiao Antártica, 5th International Congress of the Brazilian Geophysical Society, Sao Paulo, Brazil, Expanded Abstract, 1, 67-69.

# Continental crust fragmentation, small basin development and deep water circulation in the southern Scotia Sea (Southern Atlantic)

*Jesús Galindo-Zaldívar[(1)], Andrés Maldonado[(2)], Antonio Barnolas[(3)], Fernando Bohoyo[(2)], Javier Hernández-Molina[(4)], Luiz Gamboa [(5)], Alipio José Pereira [(5)], José Rodríguez-Fernández[(2)], Luis Somoza[(3)], Emma Suriñach[(6)] George André Uller [(7)], and Juán Tomás Vázquez[(4)].*

*1 - Departamento de Geodinámica. Universidad de Granada, Spain*

*2 - Instituto Andaluz Ciencias de la Tierra. CSIC/Universidad de Granada, Spain*

*3 - Instituto Geológico y Minero de España, Madrid, Spain*

*4 - Facultad de Ciencias del Mar,Cadiz. Spain*

*5 – Petrobras S/A. Brazil*

*6 –Departament de Geologia Dinàmica i Geofísica. Universitat de Barcelona, Spain*

*7 - Universidade Federal Fluminense*

## Abstract

The development of the Scotia Plate between the South American and Antarctic plates since the Oligocene has produced the fragmentation of the former continental crustal strip that connected South America and the Antarctic Peninsula. This fragmentation developed numerous small oceanic basins bounded by blocks of stretched continental crust, which resulted in the present-day conspicuous structure of the Scotia Arc and the neighbouring areas. Seismic, gravity, magnetic and multibeam profiles were recorded in Protector Basin during the SCAN 2001 cruise on board of the B/O Hesperides. This basin of Middle-Late Miocene age constitutes a good example of small oceanic basin bounded by thinned continental crust. A profile of the southern basin shows the spreading ridge and the symmetrical oceanic magnetic anomalies. The basin, however, northward is very asymmetrical and ends by the closure of both continental margins. The Scotia Plate is in fact a complex mixture of oceanic and continental crust fragments that determines the deep water circulation in the region.

## Introduction

The Scotia Sea in the southern Atlantic Ocean reveals a complex mosaic of tectonic and bathymetric features (Fig. 1 and 2). The Scotia Plate is the largest crustal element of this sea and accommodates in the boundaries the sinistral transcurrent motion between the South American and Antarctic plates. The Scotia Plate is bounded to the north by the North Scotia Ridge; to the west by the Shackleton Fracture Zone and to the South by the South Scotia Ridge (Livermore et al., 1994; Maldonado et al., 2000). The smaller Sandwich Plate is individualised in the eastern Scotia Sea by an active spreading ridge (Fig. 1).

The opening of the Scotia Sea since the Oligocene conditioned the breakup of the continental connection between South America and the Antarctic Peninsula (Barker et al., 1991). Numerous continental blocks developed during this opening are now dispersed around the Scotia Sea. The continental blocks located at the southern boundary of the Scotia Plate form the South Scotia Ridge.

Several small oceanic basins are recognized in the region as result of this evolution. Two of the most important basins are the Powell and Jane basins. Powell basin formed during the eastwards drifting of the South Orkney microcontinent from Eocene-Oligocene up to Early Miocene, whereas Jane Basin constitutes a back-arc basin developed from Early up to Middle Miocene (Maldonado et al., 1998). The end of the oceanic spreading and the migration of the boundary to the South Scotia Ridge conditioned the incorporation of these structures to the Antarctic Plate.

The objectives of the SCAN 2001 cruise of the B/O Hesperides during the 2000-2001 Antarctic summer concentrated in the determination of the tectonic style of the Scotia Plate near the Scotia-Antarctic plate boundary, in addition to the study of deposits that may reveal the deep water circulation patterns. During this cruise, multichannel seismic, gravity, magnetic and multibeam profiles were obtained in the Protector Basin and Pirie Bank areas (Fig. 2).

## The Protector Basin and the Pirie Bank in the tectonic framework of the Scotia Plate

The Scotia Plate is an oceanic plate with numerous fragments of stretched continental crust formed by the activity of several spreading ridges. The main ones are the West Scotia Ridge and the Scotia-Sandwich Ridge. The magnetic anomalies of the Drake Passage show that spreading of the West Scotia Ridge started in Oligocene and ended after magnetic chron C5A (probably at about 6 Ma) due to the shifting of the spreading center to the eastern Scotia Sea (Barker et al., 1991; Maldonado et al., 2000). The Sandwich-

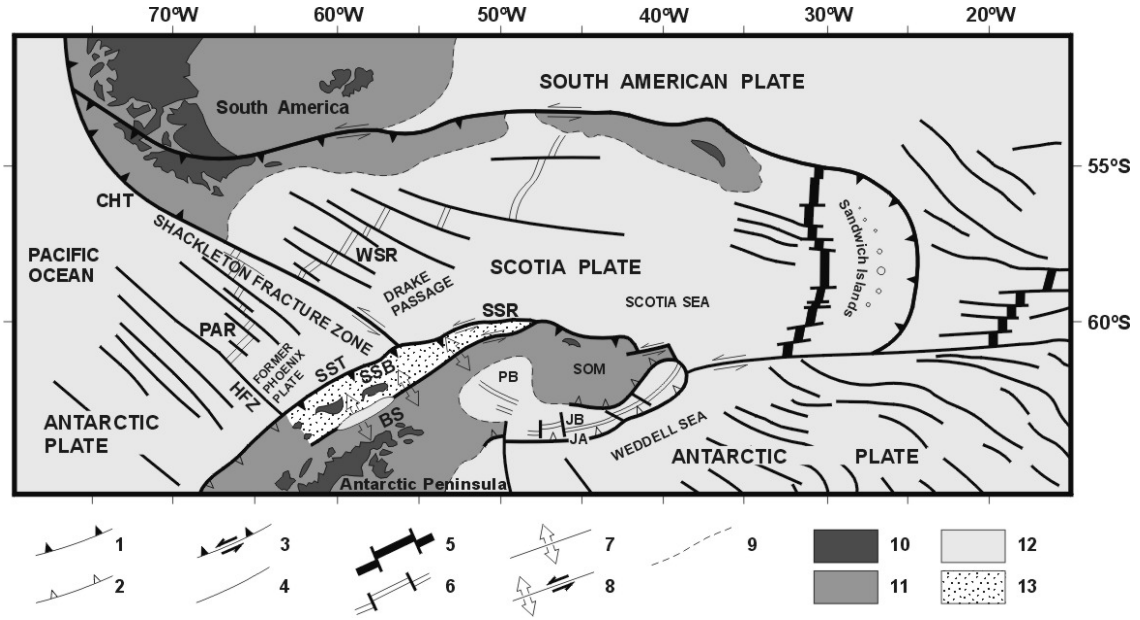


Figure 1 - Tectonic map of the Scotia Arc. 1, active subduction zone. 2, inactive subduction zone. 3, transpressive fault zone. 4, fault zone. 5, active spreading ridge. 6, inactive spreading ridge. 7, active extensional zone. 8, active transtensional fault zone. 9, continental-oceanic crust boundary. 10, emerged continental crust of South America and Antactic plates. 11, submerged continental crust. 12, oceanic crust. 13, South Shetland Block. BS, Bransfield Strait. CHT, Chile Trench. PAR, Phoenix-Antarctic Ridge. HFZ, Hero Fracture Zone. SST, South Shetland Trench. SSB, South Shetland Block. SSR, South Scotia Ridge. PB, Powell Basin. SOM, South Orkney microcontinent. JB, Jane Bank. JA, Jane Arc.

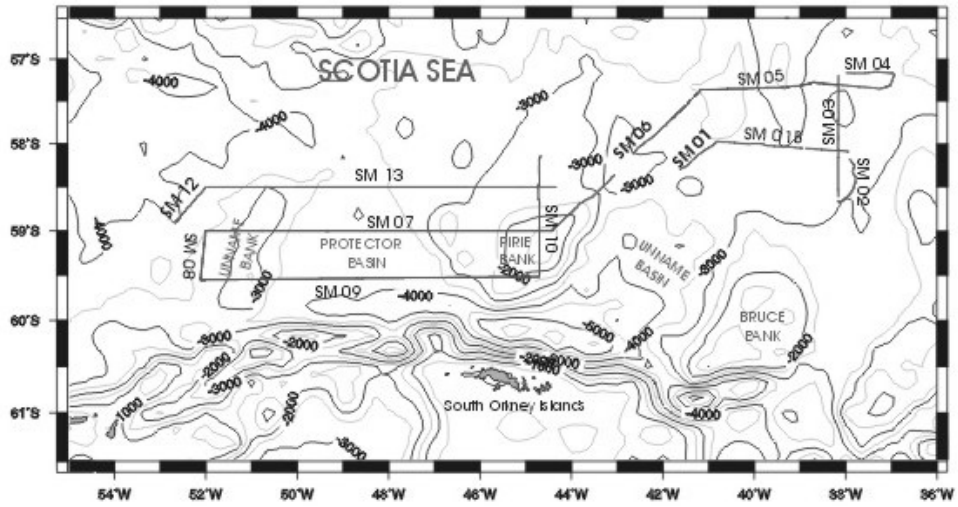


Figure 2 - Track lines of SCAN 2001 cruise.

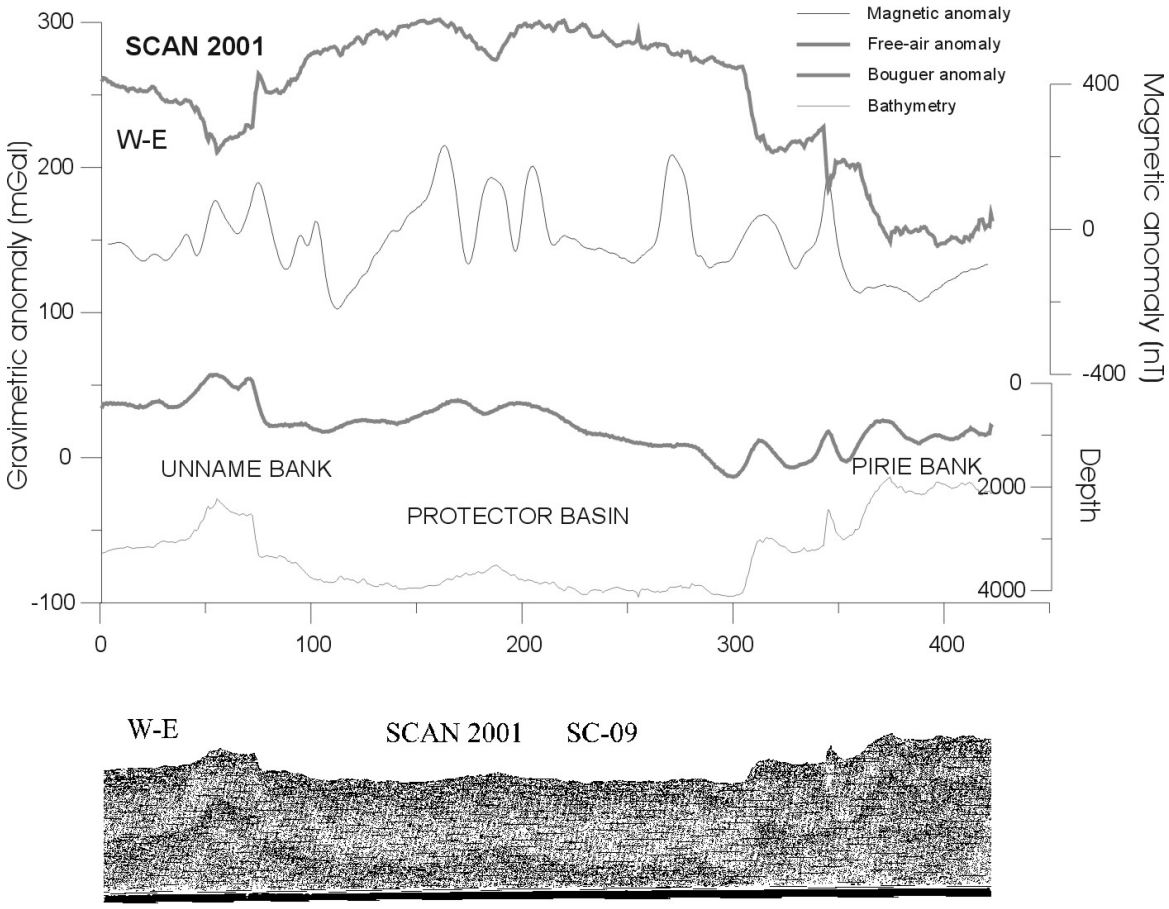


Figure 3 - SM09 profile across the Protector Basin. Bathymetry, Bouguer, Free-air, magnetic anomaly and seismic profile.

Scotia spreading ridge is presently active and has created the youngest oceanic crust of the Scotia Plate.

In addition to these ridges, other smaller ridges are found in the basins located between the continental blocks of the Southern and central Scotia Sea. The Protector Basin is a small oceanic basin formed at the western margin of Pirie Bank (Figs. 2, 3). The spreading ridge has an approximate N-S trend and the opening was in an E-W direction. The magnetic anomalies and the seismic profiles obtained in a southern transect allow to recognize a single central ridge. The spreading was symmetrical taking into account the length from the ridge to the basin margins and the magnetic anomalies. Initial identification of magnetic anomalies indicates a Middle-Late Miocene age for the development of the basin. However, the features of this basin are very different in a northern profile. The basin ends northwards by the closing of the continental margins and becomes asymmetrical. Between Pirie and Bruce banks, there is another basin with similar features to those of Protector Basin. Northwards of these banks, in the central Scotia Sea, the bathymetry and free air gravity data indicates a similar tectonic style with continental banks surrounded by oceanic crust.

In addition to the extensional deformations and oceanic spreading, the Scotia Sea has also undergone compressional tectonics. The most representative compressional structures are represented by the reverse faults and overthrust developed at the northern boundary of the South Orkney microcontinent over the Scotia Plate (Galindo-Zaldívar et al., 1996). Moreover, the oceanic crust of Scotia Plate show internal deformations, as in the West Scotia Ridge that was affected by a thrust developed after 6 Ma(Galindo-Zaldívar et al., 2000; Maldonado et al, 2000).

The basement highs developed by continental blocks or deformed oceanic crust, act as a barrier for sea bottom currents. In the region around Pirie and Bruce banks, there is a complex interaction of the bottom waters from Weddell Gyre flow and the Antarctic Circumpolar Current. Contouritic deposits are found between the continental crustal blocks that indicate two main current directions and the interaction between these two flows.

**Conclusions**

The Scotia Plate is formed by a complex mosaic of oceanic and stretched continental crustal blocks that were fragmented and amalgamated between the Oligocene and Upper Miocene times. The continental blocks formed the continental strip that connected South America and the Antarctic Peninsula.

Protector Basin is an oceanic basin developed by the stretching of the continental crust located at the western border of Pirie Bank during the Middle-Late Miocene times. This basin shows a southern symmetrical cross section, whereas it is largely assymetrical northwards and ends by the approximation of the two continental margins. Other similar small oceanic basins between continental blocks are developed in the southern and central Scotia Sea, like the basin located between Pirie and Bruce banks.

The tectonic evolution of the area produced a complex bathymetry with elevated banks and depressed oceanic basins. In this region interacts the Antarctic Circumpolar Current and the bottom water from the Weddell Gyre developing a complex host of contourite deposits.

**References**

Barker, P.F., Dalziel, I.W.D. and Storey, B.C., 1991, Tectonic development of the Scotia Arc region. In: Tingey, R.J. (Ed.). Antarctic Geology. Oxford University Press, Oxford, 215-248.

Galindo-Zaldívar, J., Jabaloy, A., Maldonado, A. and Sanz de Galdeano, C., 1996, Continental fragmentation along the South Scotia Ridge transcurrent plate boundary (NE Antarctic Peninsula), Tectonophysics 242, 275-301.

Galindo-Zaldívar, J., Jabaloy, A., Maldonado, A., Martínez-Martínez, J.M., Sanz de Galdeano, C., Somoza, L. and Suriñach, E., 2000, Deep structure of the area of intersection between the Shackleton Fracture Zone and the West Scotia Ridge (Drake Passage, Antarctica), Tectonophyscis, 320, 123-139.

Livermore, R., McAddo, D. and Marks, K., 1994. Scotia Sea tectonics from high-resolution satellite gravity, Earth and Planetary Science Letters 123, 255-268.

Maldonado, A., Zitellini, N., Leitchenkov, G., Balanyá, J.C., Coren, F., Galindo-Zaldívar, J., Lodolo, E., Jabaloy, A., Zanolla, C., Rodríguez-Fernández, J. and Vinnikovskaya, O., 1998, Small basin development along the Scotia/Antarctica plate boundary and northern Weddell Sea, Tectonophysics 296, 371-402.

Maldonado, A., Balanyá, J.C., Barnolas, A., Galindo-Zaldívar, J., Hernández, J., Jabaloy, A., Livermore, R., Martínez, J.M., Rodríguez-Fernández, J., Sanz de Galdeano, C., Somoza, L., Suriñach, E. and Viseras, C., 2000, Tectonics of an extinct ridge-transform intersection, Drake Passage (Antarctica), Mar. Geophys. Res., 21, 43-68.

# Deep-water Submarine Hazards on the Southern Santos and Northern Pelotas Basins

*Luciana Martins Lima, Lagemar-Universidade Federal Fluminense, Brazil, luciana@igeo.uff.br*
*Cleverson Guizan Silva. Lagemar-Universidade Federal Fluminense, Brazil, cleverson@igeo.uff.br*

**Abstract**

Deep-water sedimentary processes in the Southern Santos and Northern Pelotas Basins were investigated based on the analysis of seismic reflection profiles and 3.5 kHz echograms, to demonstrate the influence of downslope and alongslope processes in both sediment distribution and bedforms.

The main observed submarine hazards are associated with downslope seabed creep and growth faults at the continental slope, resulting in a rough topography over acoustically transparent, deformed sediments. Large slump deposits were also documented, at the end of the continental slope, as well as extensive turbidite deposits, covering large areas of the São Paulo Plateau.

**Introduction**

Submarine mass transport refers to the downslope movement of material, containing various water amounts, for which gravity is the driving force (Cook *et al.*, 1982). It can be divided into rockfalls, slides and different types of sediment gravity flows, classified in accordance with the water content, support mechanism and mechanical behavior, being debris flow and turbidity flows the two end members representing plastic and fluid behavior respectively.

The initiation of the sediment instability is associated with a variety of factors occurring during or after deposition, including large sedimentation rates, steep gradients, presence of gas within the sediments, salt and mud diapiric movements, earthquakes, faults, bioturbation, erosion by bottom currents and waves and sea-level oscillations.

The presence of several features indicative of deep-water sediment instability in southern Santos and northern Pelotas Basins was reported by Mello (1988) and by Silva *et al.* (1999). The later authors observed several faults and escarpments in areas of steep gradients of the continental slope in Santos Basin, giving rise to slump scars, creep and slump deposits, as well as turbidite deposits distributed along the São Paulo Plateau.

In this work, the integration of new 3.5 kHz data with older seismic information was used to map the main morphological features indicative of seabed instability and to characterize the main submarine hazards.

**Study Area**

The study area is located in the southern Santos and northern Pelotas basins, offshore the states of Rio de Janeiro, São Paulo, Paraná and Santa Catarina, in the meridional Brazilian continental margin, among latitudes 24$^o$ and 30$^o$ S and longitudes 43$^o$ and 50$^o$ W. The two basins are limited by a tectonic lineament constituted by the Florianópolis High and the São Paulo Volcanic Ridge, along the continuity of the Rio Grande Fracture Zone (Figure 1).

Contrasting morphologies are observed on the two basins as a result of its geological and tectonic evolution and the action of equally distinct sedimentary processes. In Santos Basin, the São Paulo Plateau is the most distinct province presenting an irregular topography, resulted from intense salt diapirism. The southern limit of salt occurrence coincides with the end of the Plateau and the São Paulo volcanic ridge. Greater depths are observed in Pelotas Basin, forming a smaller rounded depression, limited to the west by the continental slope and to the east by the Rio Grande Rise. A large sedimentary drift, covered by an extensive field of stationary mudwaves is located in this depression, and resulted from the action of the Antartica Bottom Current (Silva *et al.*, 1999).

**Data Set and Results**

The 3.5 kHz data was collected in 1998, during an oceanographic expedition aboard the R/V Knorr from Woods Hole Oceanographic Institute. This data set was integrated with older seismic lines, collected by different institutions and compiled from the National Geophysical Data Center. The complete geophysical survey tracklines are depicted in figure 2.

The main morphological features are illustrated in figure 2, as well as the areas of occurrence of the principal sedimentary processes and deposits. The outer continental shelf and shelf edge in Southern Santos Basin presents ubiquitous erosive features, giving rise to a steep continental slope, where distinct creep and slump processes and deposits are observed. As a result, the seabed is contorted and folded, generating a pressure ridge presented in the base of the slope in depths around 2000 m. Distinct, circular to elliptical collapse structures are found in the upper slope, in water depths ranging from 400 to 900 m. These structures are 400 to 1000 m in diameter and have 40 to 75 m of relief, being aligned to growth faults parallel to the regional isobaths. Figueiredo Jr. *et al.* (1999) associated these features to hydrocarbon or gas seeps, controlled by faults under the influence of salt diapirs. A large salt ridge at the end of the continental slope marks the beginning of the São Paulo Plateau that is characterized by a rough topog-

raphy, where numerous ponded basins, controlled by salt domes and ridges, are covered by turbidite deposits. The pervasive occurrence of salt domes is responsible by the elevated nature of the Plateau. Many diapirs are almost reaching the present seafloor and some collapse structures are observed probably associated with the dissolution of the salt by the ocean water.

The Florianópolis High is a prominent structural feature, limiting Santos and Pelotas Basin. This structure, on the outer shelf and upper slope is characterized by deeply faulted blocks, where the upper prograding sedimentary layers are eroded away, leaving submarine exposures of the older hard substratum.

The continental slope at Pelotas Basin is equally steep, presenting regular bottom topography, with sub-parallel sedimentary layers, interrupted by several linear growth faults. An extensive contourite deposit covered by a large field of mudwaves dominates the continental rise. The nature and origin of these bedforms were addressed by Silva *et al.* (1999) who considered the action of the North Atlantic Deep Water and the Antartica Bottom Water in the reworking and re-sedimentation of the bottom sediments, forming the sedimentary waves.

## Conclusions

The reconnaissance of the morphological features along the continental slope and rise in southern Santos and northern Pelotas Basins revealed the distinct nature of the sedimentary and erosional processes and the main submarine potential hazards in the area. These are associated with submarine sediment instability, related to seabed creep and slump, generating slump deposits and debris flow deposits as well as turbidite currents and associated deposits. Other distinct features are related to growth faults and collapse structures, which might be genetically associated. Contrasting with the irregular topography of the seabed along the São Paulo Plateau, the continental rise on the Pelotas Basin is deeper and dominated by constructional features, related to a large contourite drift and associated mudwaves field.

## References


Cook, H. E.; Field, M. E. and Gardner, J. V.; 1982. Continental Slopes. In: Peter Scholle and Darwin Spearing Eds, Sandstone Depositional Environments. AAPG Memoir 31, 329 – 364 p.

Figueiredo Jr, A. G.; Brehme, I.; Barbosa, C. F.; Baptista Neto, J.; A.; Silva, C. G.; 1999. Sea-floor depressions in Paraná continental shelf, Santos Basin. 6th International Congress of the Brazilian Geophysical Society, Rio de Janeiro. Boletim de Resumos Expandidos (Digital - CD).

Mello, G. A.; 1988. Processos Sedimentares Recentes na Bacia do Brasil: setor Sudeste-Sul. Dissertação (Mestrado em Geologia e Geofísica Marinha) – Universidade Federal Fluminense, 172 p.

Silva, C. G.; Neto, J. A. B.; Brehme, I. & Figueiredo, A. G.; 1999. Características Sísmicas das Feições de Movimentos de Massa do Talude Continental da Porção Sul do Platô de São Paulo. 6th International Congress of the Brazilian Geophysical Society, Rio de Janeiro. Boletim de Resumos Expandidos (Digital CD).

Silva, C. G; Baptista Neto, J. A.; Brehme, I; Figueiredo Jr, A. G.; 1999. Morfologia das ondas de lama ao sul do Platô de São Paulo, com base em batimetria de varredura e 3,5 kHz. 6th International Congress of the Brazilian Geophysical Society, Rio de Janeiro. Boletim de Resumos Expandidos (Digital - CD).


## Acknowledgments

To CNPq who provided the scholarship for the first author at the Marine Geology and Geophysics M.Sc. Program of the Universidade Federal Fluminense.

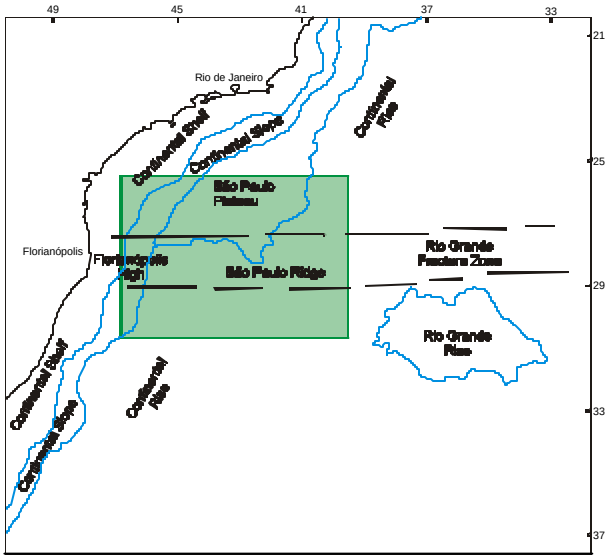


Figure 1 – Location of the study area.

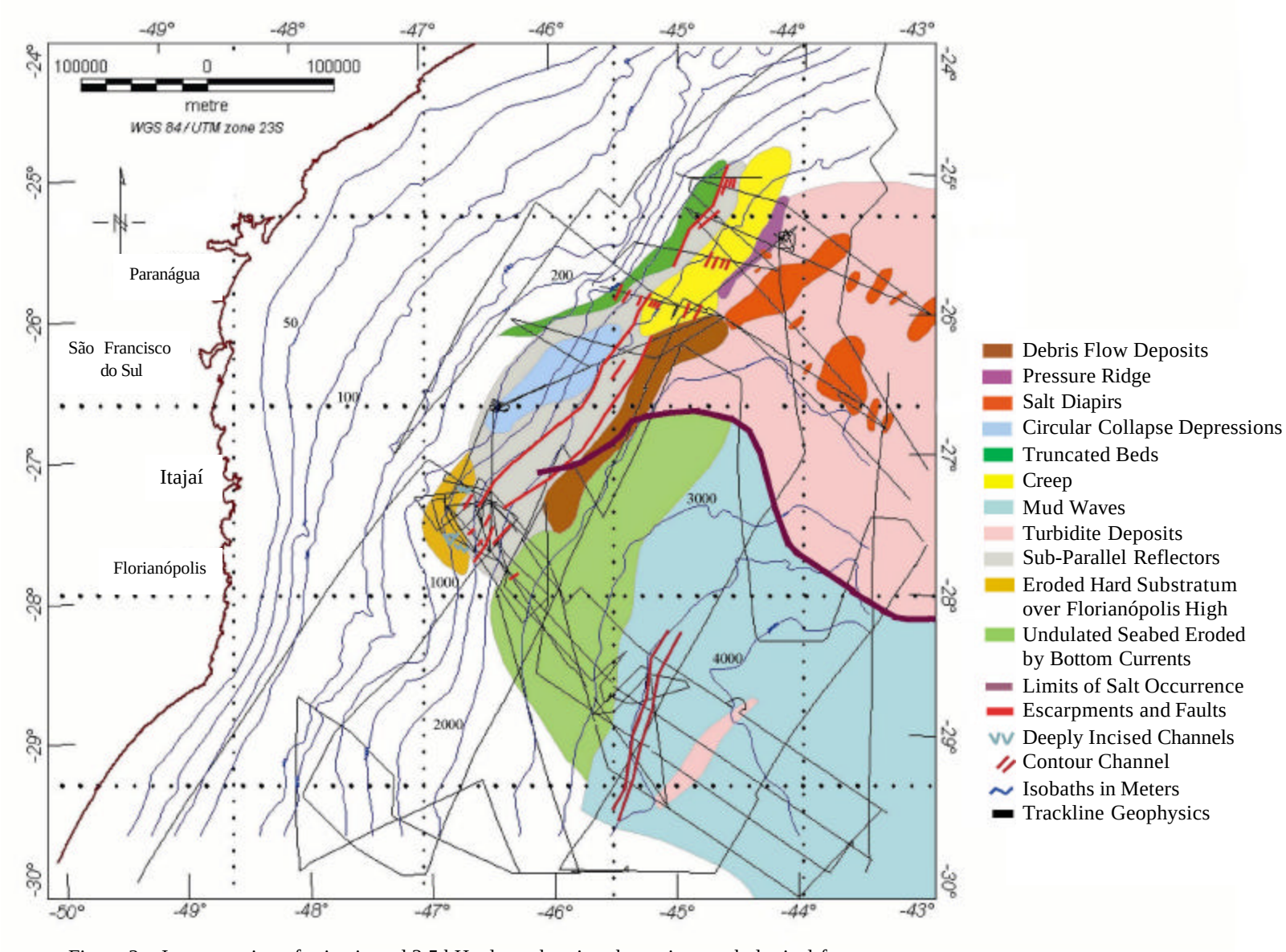


Figure 2 – Interpretation of seismic and 3.5 kHz data, showing the main morphological features, submarine deposits and sedimentary processes.

# Gravity and Seafloor Age along the Ascension Fracture Zone

*Sandra H. A. J. Quental[1] (squental@igeo.uff.br), Sidney L. M. Mello[1], Marcelo Sperle Dias[2] and Jorge J. C. Palma[1]*
*[1]Departamento de Geologia, Laboratório de Geologia Marinha - Universidade Federal Fluminense, Niterói, RJ*
*[2]Departamento de Oceanografia - Universidade do Estado do Rio de Janeiro, RJ*

**Abstract**

Based on bathymetric, satellite gravity and seafloor isochron data, we investigate the structure of the Ascension Fracture Zone (AFZ). The AFZ is a double trough fracture zone, which is generally continuous until the northeastern Brazilian Continental Margin. The northern trough is quite remarkable for most of its length, while the southern one is less pronounced. However, structural highs are usually observed bounding the southern through. Particularly, close to the margin there is a quasi E-W linear crustal basement high, which defines the Maceió Lineament. The main changes in the fracture zone strike occur at about 60-70, 40-50 and 20-30 m.y. An analysis of the free-air gravity anomalies and seafloor age along the fracture zone shows that the wavelength of the gravity anomalies widens with the increasing age of the oceanic crust, while their amplitudes show no linear relationship with the age. The slope of the gravity anomalies on the younger side of the fracture zone is steeper than that on the older side for age offsets varying from 3 to 14 m.y. Therefore, the shape of the gravity anomalies across the AFZ is generally asymmetric. Apparently, the AFZ follows a pattern, in which the basement highs on the younger side of the fracture zone as well as the widening and the asymmetry of the gravity anomalies can be predicted by differential subsidence and lateral heat flow. Further a flexural model using two interfaces (water/crust and crust/mantle) with a constant crustal thickness shows that major volcanic edifices to the south of the AFZ can be younger than the surrounding oceanic crust, while other structural highs are denser than normal oceanic crust. Both structures may be a result of the stress field near the fracture zone, which in one side could have facilitated magma upwelling due to brittle failure and on the other allowed tectonic uplifting of deeper oceanic crust and mantle rocks.

**Introduction**

The oceanic fracture zones (FZ) are features that separate lithospheric plate segments of distinct ages and hence different regional depths [e.g., *Heirtzler and Le Pichon*, 1965; *Heitzler et al*., 1968]. These structures perpendicularly offset the midocean ridge axis and may extend their strike to the continental margins, where their peculiar morphology is usually disguised by terrigenous sedimentation, specially when it is intense [*Guazelli and Carvalho*, 1981].

Since oceanic lithosphere cools with its increasing distance from the ridge spreading center, it gets denser, thicker and subsides. That is why a crossing profile over a FZ reveals a contrast in depth and lithospheric thickness, reflecting the age offset between its two sides. This differential subsidence is consequently related to the lithospheric thermal history and age, leading to the development of distinct structures in the provinces delimited by FZs.

The Ascension Fracture Zone (AFZ) was mapped in its transform area by *Van Andel et al* [1973], who defined an offset of 230 km separating two segments of the Mid Atlantic Ridge (MAR). *Gorini* [1981], *Palma et al*. [1984] and *Palma* [1989] extended its morphological trace to the Brazilian northeastern continental margin. Extensive crests and valleys with widths between 10 to 30 km and topographic variations of 1800 to 2250 m characterize the AFZ.

According to *Brozena et al.* [1985] and *Palma et al.* [1984], this is a double FZ [e.g., *Fleming et al*., 1970; *Gorini et al.*, 1984], since a structural high separating two valleys can be distinguished in the MAR region. The structural high and both valleys (down to 4000 m deep) can be traced westwards for hundreds of kilometers [*Palma et al.*, 1984].

This morphostructural configuration is generally maintained towards the oceanic basin, but from 29ºW to the continental margin, the strike of the AFZ becomes hardly distinguished because of the thick sedimentary cover and to the regional complexity of the oceanic basement [*Palma et al*., 1984].

Here we study the western structure of the AFZ based on bathymetry, gravity anomaly profiles and seafloor age across the fracture zone from the midocean ridge to the continental margin seafloor age. Further we apply a simple flexural model to investigate the structure of large volcanic edifices nearby the AFZ.

**Data set**

We compiled bathymetric data from Noc. Almirante Camara (cruises AC83AB, AC83AA, AC86AA, AC86AC) from the GEODAS/NGDC Database (version 4.0). Satellite free air gravity [*Sandwell and Smith*, 1997] was obtained in 2-minute grid through ftp to *topex.ucsd.edu/marine_grav* (*Figure 1*). Seafloor gridded age data were obtained

from *Muller et al.* [1997] and are also available from the NGDC.

**Data Analysis**

The Free-air gravity map (*Figure 1*) shows the structure of the AFZ. The positive gravity anomalies indicate basement structural highs while negative anomalies correspond to structural basins, some of which probably filled with sediments. Basement highs are conspicuous features only to the south of the AFZ.

Eleven cross strike profiles (240 km interval) display gravity anomaly and age offset variation along the AFZ *(Figure 2)*. Profiles are referred to the axis of the structural high that separates the two fracture zone throughs. The troughs are linear features as deep as 4000-5000 m that extends until the margin.

We examine gravity by looking at the amplitude and wavelength of the anomaly with the increasing age of the oceanic crust and age offset varying from 3 to 14 m.y. The maximum amplitude is the difference between the lowest value in the through and the peak on the old side of the fracture zone [e.g. *Wessel and Haxby*, 1990], while the wavelength of the anomaly is the distance between the two peaks in both sides of the fracture zone. This analysis shows a widening tendency for the wavelength of the gravity anomaly with an increasing seafloor age and no evident relationship between the signal amplitude and the age offset. Only three profiles show a structural step between the two sides of the fracture zone. Close to the ridge axis it is of the order of 19 mGal and decreases to 5 mGal in the ocean basin. The slope of the gravity anomaly on the young side of the fracture zone is usually steeper (+ 0.6 mGal/km) than that on the old side.

**Modeling**

We selected two profiles to investigate the thermomechanical behavior of the lithospheric structures across the AFZ. One at the Maceió Lineament, surveyed by the Noc Almirante Camara (cruise AC83AB) and another approximately at 21°W obtained by a R/V Vema (cruise V3101).

We use a 2-D flexural model accounting for 2 interfaces: water/oceanic crust and crust/mantle, assuming constant density values of 1.03, 2.90, and 3.30 g cm$^{-3}$ respectively. It solves the General Flexure Equation for a continuous plate floating over a fluid of low viscosity , which is

$$\frac{\partial^2}{\partial x^2}\left[\frac{D\partial^2 w}{\partial x^2}\right] + \frac{P\partial^2 w}{\partial x^2} + \Delta\rho_2 g w(x) = \Delta\rho_i g h(x)$$

where $w$ is the geometry of the Moho, $P$ is the pressure exerted on the elastic plate, $\Delta\rho$ is the density contrast of the interface, $h$ is the geometry of that interface, and $D$ is the flexural rigidity of the plate, given by

$$D = \frac{ET_e^3}{12(1-\sigma^2)}$$

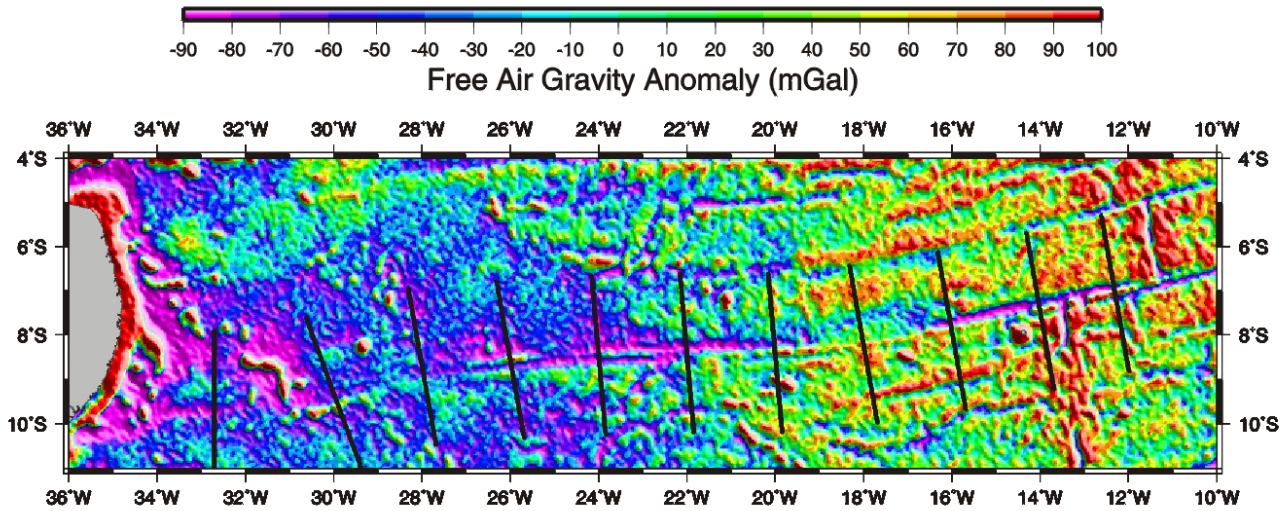


Figure 1 – Satellite free-air gravity map displaying location of selected profiles.

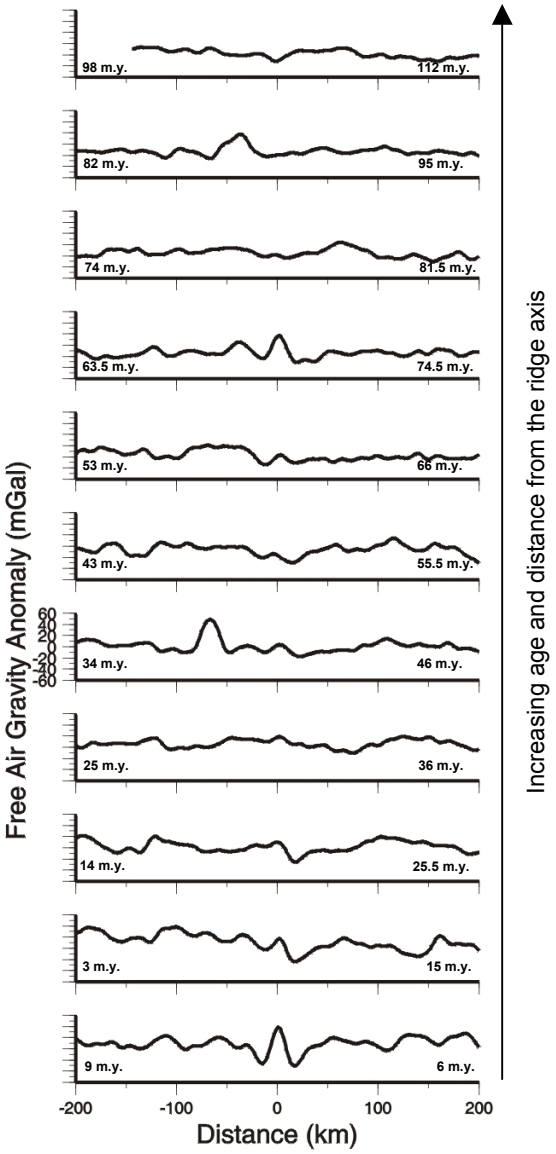


Figure 2 – Free-air gravity profiles selected for analysis, displaying crustal age in both sides of the Ascension fracture zone.

where $E$ is the Young's modulus, $\sigma$ is the Poisson's ratio, and $T_e$ is the elastic thickness of the plate.

The numerical solution for (1) [*Banks et al.*, 1977] is

$$w(k) = \frac{\Delta\rho_1}{\Delta\rho_2}\left[1 + \left(\frac{k^4 D(k)}{\Delta\rho_2}\right)\right]^{-1} h(k),$$

which allows predicting the geometry of the Moho.

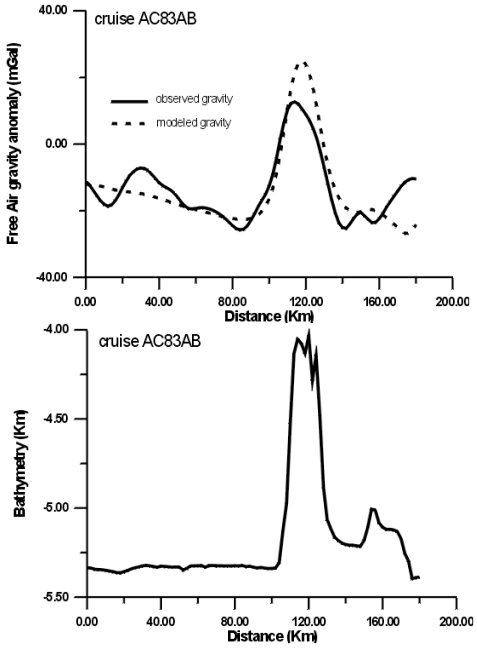


Figure 3 – a (top): Observed and modeled free-air gravity for profile extracted from cruise AC83AB and b (bottom): respective bathymetry.

The individual gravity effect of all interfaces is computed by *Parker's* [1973] equation

$$F\left[\Delta g_i(x)\right] = -2\pi G \Delta\rho_i e^{-kz_i} \sum_{n=1}^{\infty} \frac{\left|\overline{k}\right|^{n-1}}{n!} \cdot F\left[h_i^n(x)\right]$$

where $G$ is the gravitational constant (=6.67 x $10^{-11}$ N $m^2$ $kg^{-2}$), $\Delta\rho_i$ is the density contrast, $z_i$ is the depth average value, and $h_i(x)$ is the geometry of interface $i$. The total gravity effect of the model is then computed by the inverse FFT of the sum of individual gravity effects calculated in the frequency domain.

*Figure 3a* shows the gravity effect of the Maceió Lineament for an elastic thickness of 5 km. This probably implies that the volcanic emplacement of part of the lineament is relatively younger than the surrounding oceanic crust (~ 10 m.y). The observed misfits are mainly related to the simplification of the model, which did not consider either a sediment cover or a 3-D effect. The gravity effect of a structural high at 21°W was also observed, being underestimated by the model for different elastic thickness. In this case, such high seems to be an outcrop of denser crustal rocks. In fact, tectonic uplifting of deeper crustal rocks and mantle has been reported along of many fracture zones [e.g. Bonatti, 1994; *Hecknian et al.*, 2000].

## Conclusions

The continuous basement high to the south of the AFZ as well as the signature of the gravity anomalies with respect to crustal age suggests that the structure of the fracture zone follows a pattern that is predicted by differential subsidence and lateral heat flow models [e.g. *Sandwell and Schubert*, 1982]. Apparently, the Maceió Lineament was formed on newly oceanic lithosphere, as indicated by the low elastic thickness. On the other hand, other structures to the south of the AFZ are not necessarily of volcanic origin and could result of tectonic uplifting.

**Acknowledgments.** We would like to thank Dr. Dan Metzger from the NOAA for providing us GEODAS CD-ROM v. 4.0. For all processing and gridding of data we used the Generic Mapping Tools – GMT (P. Wessel & W.H.F. Smith, http://gmt.soest.hawaii.edu).

## References

Banks, R. J.; Parker, R. L.; Huestis, S. P. Isostatic compensation on a continental scale: Local versus regional mechanisms. *Geophys. J. R. Astr. Soc.,* **51**: 431-452, 1977.

Bonatti, E. et al., Transform migration and vertical tectonics at the Romanche fracture zone, equatorial Atlantic, *J. Geophys. Res*., **99**: 21779-21802, 1994.

Brozena, J.M.; Cherkis, N. Z.; Vink, G. E.; Kovacks, L. C.; Pirmez, C. A SeaBeam study of the Ascension Fracture Zone and adjacent Mid-Atlantic Ridge segments. *EOS*, **66** (18): 355, 1985.

Fleming, H. S.; Cherckis, N. S.; Heirtzler, J. R. The Gibbs fracture zone: a double fracture zone at 52° 20' N in the Atlantic Ocean. *Mar. Geophys. Res.*, **1** (1): 37-45, 1970.

Gorini, M. A. The tectonic fabric of the equatorial Atlantic and adjoining continental margins: Gulf of Guinea to Northeastern Brazil. *Estruturas e Tectonismo da Margem Continental Brasileira, e suas Implicações nos Processos Sedimentares e na Avaliação do Potencial de Recursos Minerais* (Relatório Final). Rio de Janeiro: PETROBRAS/ CENPES/DINTEP. Série Projeto REMAC, **9**: 11-116, 1981.

Gorini, M. A et al. Características morfotectônicas da zona de fratura dupla Bode Verde e o seu traçado em direção aos montes submarinos da Bahia. *In: Anais do XXXIII Cong. Bras. Geol.*, Rio de Janeiro, RJ, SBG, **4**: 1615-1628, 1984.

Guazelli, W. and Carvalho, J. C. Estruturas da margem continental leste brasileira e das áreas oceânicas e continentais, adjacentes. *Estruturas e Tectonismo da Margem Continental Brasileira, e suas Implicações nos Processos Sedimentares e na Avaliação do Potencial de Recursos Minerais*. Rio de Janeiro: PETROBRAS/CENPES/DINTEP. Série Projeto REMAC, **9**: 117-143, 1981.

Heirtzler, J. R. and Le Pichon, X. Crustal structure of the mid-ocean ridges, 3, Magentic Anomalies over the mid-Atlantic ridge. *J. Geophys. Res*., **70**: 4013, 1965.

Heirtzler, J. R.; Dickson, G. O.; Herron, E. M.; Pitman III, W. C. e Le Pichon, X. Marine magnetic anomalies, geomagnetic field reversals, and motions of the ocean floors and continents. *J. Geophys. Res*., **73**: 2119-1236, 1968.

Hekinian, R. et al., Submersible observations of Equatorial Atlantic mantle: The St. Paul Fracture Zone region, Marine Geophysical Researchers, **21**: 529-560, 2000.

Muller, R. D.; Roest, W. R.; Royer, J.-Y.; Gahagan, L. M.; Sclater, J. G. Digital isochrons of the world's ocean floor. *J. Geophys. Res.*, **102**: 3211-3214, 1997.

Palma, J. J. C. Mapeamento morfoestrutural do segmento ocidental da Zona de Fratura de Ascensão e porções adjacentes da crista da Cordilheira. Rio de Janeiro, diss. mestrado, *Univ. Fed. do Rio de Janeiro (UFRJ)*, 150 p., 1989.

Palma, J. J. C.; Brozena, J.; Mello, S. L. M.; Carvalho, J. C. Mapeamento morfoestrutural preliminar da Zona de Fratura de Ascensão até a margem continental nordeste brasileira. In: *Anais do XXXIII Cong. Bras. Geol.*, Rio de Janeiro, RJ, SBG, **4**: 1643-1654, 1984.

Parker, R. L. The rapid calculation of potential anomalies. *Geophys. J. R. Astr. Soc.,* **31**: 447-455, 1973.

Sandwell, D. T. and Schubert, G. Geoid height-age relation from Seasat altimeter profiles across the Mendocino fracture zone. *J. Geophys. Res*., **87**: 4657-4667, 1982*b*.

Sandwell, D. T. and Smith, W. Marine gravity anomaly from Geosat and ERS-1 satellite altimetry. *J. Geophys. Res*., **102**: 10039-10054, 1997.

Van Andel, T. H., Rea, D. K., Von Herzen, R. P., Hoskins, H. Ascension Fracture Zone, Ascension Island, and the Mid-Atlantic Ridge. *Geol. Soc. America Bull*., **84**: 1527-1546, 1973.

Wessel, P. and Haxby, W. Thermal stresses, differential subsidence and flexure at oceanic fracture zones.. *J. Geophys. Res.*, **95** (B1): 375-391, 1990.

# Improving Interpretation of Seafloor Geology from the Integration of Conventional Marine Geology Tools and 3D Seismic

*Viana, A.R., Almeida, C.W., Schreiner, S., Hercos, C.M., Almeida Jr., W., Machado, L.C.R., Miller, D.J., Machado, R.P.*

*PETROBRAS - Marine Geology Team*

**Abstract**

Use of 3D-seismic surface mapping has proved to be a rapid and efficient method of identifying the major seafloor features that affect both oil exploration and production processes. Accuracy of this method still remains uncertain where no ground-truth tools are employed. Integrating tools of conventional oceanographic surveys dedicated to near surface geology interpretation and 3D-seismic is the best method to reduce uncertainties and calibrate the inversion of seismic amplitude in lithology. Recognition of the application of 3D-seismic data as a tool for hazard evaluation in deep waters was early performed by the Marine Geology section of Petrobras, which integrated that technique with the latest available technology of data interpretation and visualization. The need of calibrating seismic data induced the application of different methods of ground-truthing, comprising video and still-frame photography of the seafloor, several sample acquisition, surface and deep-towed side-scan sonar imaging and 3.5 kHz sub-bottom profiles. The gathered data was analyzed to determine the nature and extension of surface and near surface features. Major features such as mass movement deposits, thick shallow sand accumulations, active fault movement and the presence of shallow gas and chemosynthetic communities are investigated by the combination of those different tools with a high accuracy and reliability. This article presents a case of integrating different marine geology tools in order to calibrate 3D-seismic maps, such as physiographic, bathymetric and amplitude/lithologic maps. In order to better image the attributes some up-to-date visualization methods derived from remote sensing techniques were employed providing astonishing sea-floor landscapes.

**Tools and methods**

A series of conventional and non-conventional methods of marine geology were used in this study in order to identify the extent of their use in the characterization of the near-surface geology. It follows a brief comment on some of them.

Long range side-scan sonar records are a fine tool to perform regional and semi-detailed seafloor studies and general characterization of the recent geology. The backscatter patterns are usually associated to grain size and compaction degree of the sediments and to the roughness of the seafloor. The penetration of its high frequency source (around 100 kHz) depends on those soil characteristics, varying from a few centimeters to a few meters. Few studies have been performed in order to associated the extent of the beam penetration.

Regional studies with 3.5 kHz sub-bottom profiles were formerly performed by Kowsmann et al. (1996). Around 380km of sbp lines, 4km apart spaced covered the study area. The main physiographic features and sedimentary deposits were interpreted in accordance with the characteristics of the returning echo based on the criteria proposed by Damuth (1980).

Six-meter long piston cores were retrieved along the study area for many interests. The cores are split into two halfs, photographed and analyzed for sedimentology and biostratigraphy purposes.

Mapping the seafloor from 3D-seismic yields the possibility of creating physiographic and amplitude maps. The physiographic map derived from a coherence algorythm (dip maps) highlights discontinuities in a image. It detects differences in dip across a horizon using a different algorithm from that used in calculating a dip map. Elaborating dip maps involves the mathematical comparison of points around a single sample point in a original map. The coherence algorithm compares sets of samples on either side of each sample point (three samples on either side of a point in both directions). The result is a plane connecting the results of the 3X3 computation at each sample of the original horizon, which reproduces the original topography of the mapped horizon. In the analysis of amplitude maps is important to remember that inherent to the seismic method is its capability of registering changes of the physical characteristics of the investigated soil through the record of the relationship between the acoustic impedance (pv , where p = density of the rock/sediment, v = sound velocity propagation) of the different layers crossed by the sound wave. The acoustic impedance contrast between two media (in our case sea water

and bottom sediments) can be analyzed from the seismic amplitude maps.

The understanding of the seafloor morphology has been revealed as an important step in the comprehension of the evolution of the recent geology. The development of visualization techniques resulting both from the seismic interpretation tools and from the remote sensing procedures provided high quality images of the seafloor. In this study the software ER-Mapper was used to construct an algorithm with bathymetric and amplitude data coming from 3d-seismic. The original files in the .xyz grid format were converted in .ers ER-Mapper format. The algorithm is a list of instructions or processing commands that the program uses to transform the input data into an image that can be visualized both in 2D and 3D views. Vertical exaggeration is an artifact to better visualize subtle forms of the submarine relief.

**Case Study**

A 3D-seismic dataset from the southeastern Brazilian margin was selected in order to perform the comparison with conventional geo-marine tools. Initially, a physiographic map derived from the 3D-seismic is elaborated via a coherence algorithm. This map reproduces fair confidently the sea-floor topography as stressed by Almeida et al. (2001). The long-range side-scan sonar records produced quite confident seafloor images which were used as guidelines for further studies. A polarity inversion on the sonar records were performed aiming to correlate low backscatter (in general associated with sandy sediments) with light gray and high backscatter (finer-grained sediments) with dark gray (Fig. 1). Highly rough textures were associated to complex seafloor topography developed by outcropping/sub-outcropping mass movement deposits.

The association of backscatter patterns to depositional styles were also corroborated by 3.5 kHz records. Light gray sonar records corresponds to prolonged echofacies, usually associated to sand deposits, and some short hyperbolas within this facies were related to shallow and narrow channels (Fig. 2). The rough topography, initially associated to mass movement deposits, as such as the salt-controlled relief (escarpments) are marked by the long-tailed hyperbolas.

A hand-guided interpretation of the sonar records were compared automatic textural classification in order to evaluate the efficiency of the method (Bentz et al., 2000). Several classes were depicted (Fig. 3) and then compared with 3D-seismic amplitude maps (Fig. 4). The amplitude was extracted from the first reflection, which corresponds to a positive peak in Petrobras convention. Thus all amplitude values at the seafloor are positive. The amplitude maps indirectly suggest different sediment styles as proposed by Almeida et al. (2001) and their use as an accurate tool depends on the calibration with direct measurements. As a first step, a comparison between sonar record and amplitude map is performed and it is observed a close relationship between the high amplitude values with low backscatter areas, while high backscatter corresponds to low amplitude values. With the objective of calibrating all geophysical tools with ground-truthing data several piston cores were retrieved in the study zone (Fig. 4).

The sonar facies interpretation was corroborated by the sediment cores, what would indirectly corroborate the analysis for the 3D-seismic amplitude. Nevertheless a direct correlation is imperative in order to actually confirm the interpretation of sedimentary facies via seismic maps. A first analysis of the comparison of amplitude versus lithology was performed by Torres and Machado (2000). Following studies confirmed the correlation between high amplitude values with sand deposits and low amplitude values to fine-grained sediments (Fig. 4). The fine-grained sediments at the seafloor have higher porosity than the coarse-grained ones slowering the sound velocities. Gas-charged coarse-grained sediments become very soft bottoms also inducing a sound speed slowering. High amplitude values were also found in zones of outcropping of consolidated sediments, where the acoustic energy travels slightly faster than the surrounding and softer seafloor. A fuzzy, low amplitude pattern is observed at areas where mass flow deposits occur. An excellent visualization of the depositional system is obtained by coupling seismic interpretation tools with remote sensing software. By that mean, 3D panoramas are obtained with the coupling of bathymetric and amplitude data upon one single layer and with the performance of vertical exaggeration (Fig. 5). Video and still-frame photography supplemented and supported the observations above. A continuous research must be made in order to calibrate the largest number of amplitude anomalies.

Up to know, the approach presented in this study has proved that integrating different tools is by far the most confident method for seafloor and near surface geology investigation. Also, 3D-seismic based geohazard assessment has proved to be a rapid and quite accurate method which can be used as a by-product of the conventional exploration data.

References

Almeida Jr.,W., Viana, A. R., Almeida, C.W., Silva, F.B. and Gambôa, L.F.P., 2001.Improving Seafloor Mapping of Brazilian Offshore Deepwater from 3D Seismic. Int. Geoph. Congr., SBGf, Salvador, Expanded Abstract

Bentz, C.M., Sant'anna, M.V., Machado, L.C.R., Miller, D.J., and Viana, A.R., 2000. Textural analysis and classification of Campos Basin sonar data to improve seafloor characterization. 31st Int. Geol. Congr., IUGS, Rio de Janeiro, Abstracts.

Kowsmann, R. O.; Schreiner, S.; Murakami, C. Y.; Piauilino, P.O.V.; Barrocas, S.; Miller, D.J.; Rizzo, J.G., 1996. Ecofacies de 3,5 Khz do talude da Bacia de Campos e do Plato de Sao Paulo adjacente. Cong. Brasil. Geologia, 39., Salvador, v. 3, p. 463-465

Torres, R.B. and Machado, L.C.R., 2000. Caracterização do fundo marinho através do estudo integrado de dados geológicos e geofísicos em ambiente GIS - Bacia de Campos. GIS- Brasil 2000, Abstracts, Curitiba.

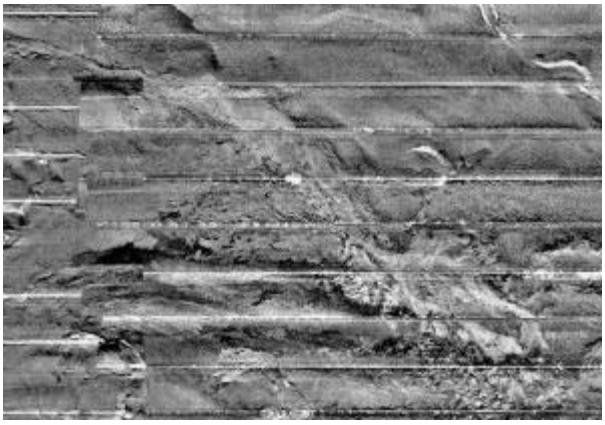

Figure 1: Side-scan sonar mosaic illustrating the main features described in the text. 1 and 2 are low backscatter areas related to the development of a submarine channel and lobe system; 3 is a moderate to high backscatter are probably related to mud deposits; 4 is a high backscatter area related to the rough topography of mass movement deposits and 5 is a high backscatter pattern associated to salt-controlled relief. Inset indicates area represented in Fig. 3. Red line indicate the position of the 3.5 kHz record of Fig. 2.

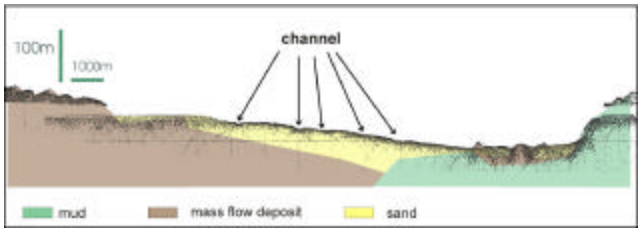


Figure 2: 3.5 kHz echofacies interpretation indicating different depositional styles. See discussion in the text.

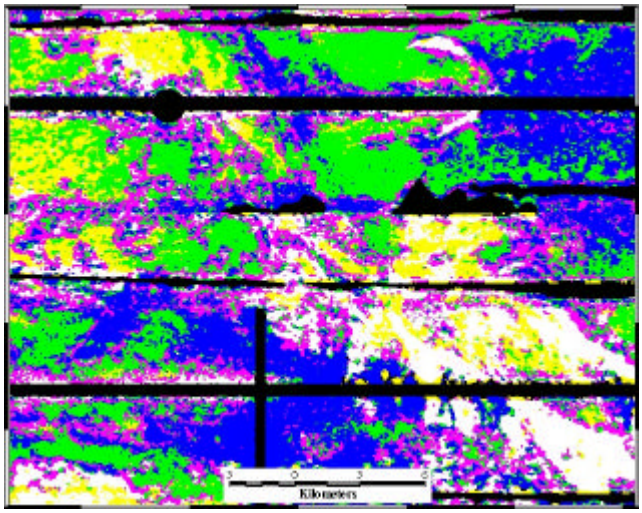


Figure 3: Textural classes identified by remote sensing techniques applied upon side-scan sonar images (Bentz et al., 2000). The method constrained the analysis to five classes selected by their backscatter pattern.

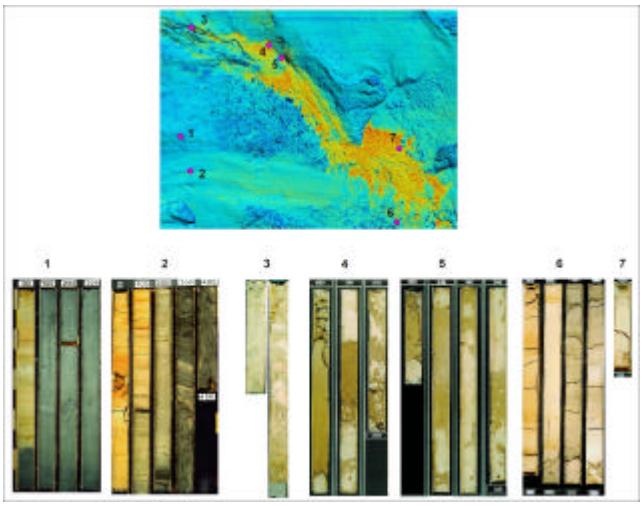

Figure 4: Amplitude values draping the edge detection map of the seafloor derived from 3D-seismic data. Red and yellow correspond to high amplitude values and correspond to the sonar facies 1 and 2 in Fig. 1. Blue and dark blue correspond to fine-grained sediments (sonar textures 3 and 4 in Fig. 1). The fuzzy dark blue texture is interpreted as blocks from mass movement deposits and is associated to the sonar texture 4 in Fig. 1. An imbricated system of channels is observed in the upper left corner of the figure. Divergent channels are observed in the lower right area (high amplitude area) and are interpreted as distributary channels in a complex of amalgamated channels and lobe deposits. The elongated left-to-right light yellow amplitudes in the lower area is interpreted as the deposits of low-density, almost laminar density flows. Bold circles indicate the location of 1 to 7 piston cores used in the calibration of the geophysical indirect tools. Core 1 retrieved silty mud with intercalation of fine-grained millimeter to centimeter thick sand layers; core 2 retrieved marly sediments overlaying diamictites (debris-flow deposit), cores 3, 4, 5 and 7 retrieved turbiditic coarse to fine-grained sands; core 6 retrieved intermingled silty mud, fine-grained sand and diamictites. The sediment types retrieved fit very well with the amplitude values derived from the 3D-seismica data and with the backscattern patterns from the side-scan sonar.Figure 2: Dip attribute - Coherence map calculated from dip extracted from interpreted seafloor

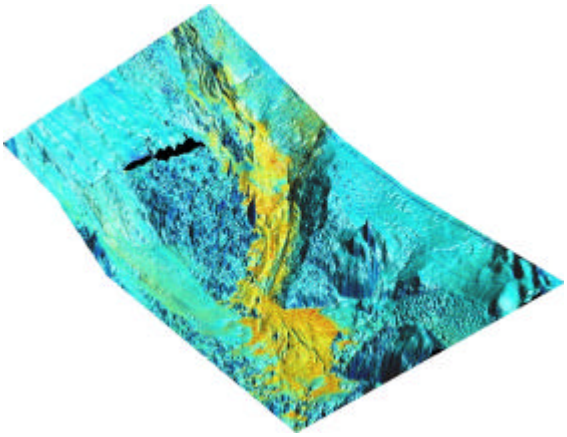

Figure 5: 3D-perspective of the study area performed by coupling topographic and seafloor amplitude values from 3D-seismic with a remote sensing software (ER-Mapper). The image has a large vertical exaggeration which enhances the observation of delicate physiographic features and their relationship with the seafloor amplitude variations. This image highlights the irregular topography associated to mass movement deposits (1), the braided-channel system in the upper portion of the figure (2), the lobate pattern of the area of amalgamated distributary channels and depositional lobes (3), the smooth relief developed by the "almost laminar" (?) density flow (4) and the salt-controlled escarpments (5).

# Seafloor Mapping 3D Seismic
# Improving Seafloor Mapping of Brazilian Offshore Deepwater by the use of 3D Seismic

*Waldemar de Almeida Jr., Adriano R. Viana, Cleide W. de Almeida, Fernando Barbosa da Silva, e Luiz Antônio Pierantoni Gambôa, PETROBRAS S/A, Brazil*

**Abstract**

The use of 3D-seismic surface mapping has proved to be an adequate and reasonably accurate method for proper imaging the deep-water seafloor and the near surface sedimentary column. Attributes such as time, amplitude and dip attitude derived from 3D-seismic surveys are the basis for a thorough assessment of geohazard evaluation. The development of new techniques of mapping using seismic data and the updated application of available technology have provided the tools to improve the knowledge of the sea-floor of the deepwater realm where the Brazilian offshore oil industry is facing new challenges. This article presents the application of this methodology on a Brazilian deepwater 3D-seismic dataset where complex interplay between tectonics and sedimentation controls the depositional patterns. The detailed identification of the mapped elements demonstrates the suitability of this technique. The resultant maps add reliability to the interpretation of the surface and near surface geology

**Introduction**

The migration of oil findings towards deeper and deeper water has enhanced the need for more reliable geohazards assessment. Previously used techniques such as single channel HR seismic, sub-bottom profiler, side-scan sonar and piston coring have proved their efficiency but the acquisition of specific data for this purpose is very expensive. However, the updated use of existing technology and the large areal coverage coupled with the increasing quality of 3D-seismic data yielded a viable alternative to investigate the seafloor at minimum extra costs and with greater definition of the existing features and processes. Thus, with no additional data one can obtain good resolution data maps which associated with some basic concepts on rock properties and seismic data response allow detailed interpretation of recent or almost recent geological processes. These products are of major importance both for the petroleum exploration industry as well as for understanding the events responsible for shaping the sedimentary basins. Such approach has being increasingly applied by the oil industry (Pressler and Walker, 1999; Roberts et al., 2000) and has several potential applications such as: geotechnical characterization of the sea bottom; geohazards assessment; detection of faults cropping at the surface (with strong implications on hydrocar-bon migration, trapping and sealing mechanisms), and for the understanding of recent deep-water depositional systems.

The technique is based on accurate mapping of the sea bottom on a 3D survey. It was developed from the need of a fast and efficient method to characterize the submarine physiography, to detect faults cropping at the sea bottom, to estimate the characteristics of the shallow sediments and, finally, to evaluate the presence of abnormal fluids in the near-surface sediments. It can be performed by mapping the reflector that corresponds to the seafloor at every line and trace, using at first automatic horizon detection programs and then refined by the interpreter. Considering the reflector (seafloor) has a positive reflection coefficient the mapping is done on the positive peak. Following this step, the amplitude values are extracted from the data extraction and the amplitude and dip attributes maps are produced. The first is the maximum amplitude in a half wavelength window around the tracked time event. The second involves a mathematical comparison of points around a single point in an original image, highlighting discontinuities in it. A new understanding of the seafloor topography and a general overview on the sediments distribution can be gained from the integrated interpretation of these maps and seismic sections. As a premise for understanding the sediments characteristics via seismic amplitude attributes it was considered as a general rule that the fine-grained sediments have low positive amplitude and the coarse-grained sediments (sand and gravel) have high amplitude values. Some complications must be considered in this simple model: outcropping of consolidated sediments must have high amplitudes at the seafloor, while the presence of light fluids (oil and gas) will reduce the amplitude values. When seafloor samples are available, a ground-truth calibration of the seismic mapping is obtained.

**Case Study**

A data set was retrieved from a 3D-seismic survey along the southeastern Brazilian margin (interval sampling 4 ms and 25x25m spaced shot points) in order to illustrate the methodology described above. The interpretation is only based on seismic data. The product of the two-way-travel time map with the sound propagation speed in ocean water (generically

adopted as 1500m/s) results on the bathymetric map (Figure 1). The surveyed area is comprised in water depths ranging from 2000 to 2500m (2666 to 3333 milli-seconds). Deep waters are a well known environment for good seismic data quality. The coherence maps (dip attributes maps) are a fine tool for the visualization of the seafloor topography (Figure 2). Several features are observed such as narrow channels, escarpments, flat/smooth areas, crenellated seafloor. These features when coupled with the maximum amplitude map (Figure 3) provide a reasonable basis for the interpretation of the local surface geology. The amplitude map indicate areas of possible sand-rich (red and yellow colors in Figure 3) and mud-rich deposits (blue and green).

**Interpretation of sedimentary features**

Both manual or automatic controlled methods of textural classification of images (Bentz et al., 2000), frequently used in remote sensing, can be applied to the amplitude map in order to identify the main depositional features (Figure 4). Interpretation of the maps is supported by the analysis of seismic lines. Sand-rich areas are characterized by stronger amplitudes and small dip (Figure 4, facies A). They occur both in channeled and fan-shaped geometries and seem to be the most recent sedimentary deposits in the surveyed area. In the channeled area, strong amplitudes are associated to cut-and-fill features where lateral discontinuities interrupts parallel, strong amplitude seismofacies. In the fan-shaped areas (a complex of amalgamated lobes and distributary channels) the lateral continuity of the strong parallel reflections are well marked and typical of sand-rich zones. The escarpment and high relief flanking the sand-rich area is related to salt diapiric structures modifying the seafloor topography (Figure 4, facies B). High dips and weak amplitudes are observed in this area. A disturbed/rough topography (irregularities more than 20m high), are related to weak amplitudes and to a chaotic seismofacies (Figure 4, facies C) and interpreted as mass movement deposits probably composed of diamictites, with large blocks being uplifted during flow evolution and frozen at its top (elutriation process). Intermediate amplitude values associated to an elongated geometry can hypothetically be associated to low-concentration, fine grained turbidite deposits or to sandy slurry flows (Figure 4, facies D). All these patterns can also be seen on the 3 different seismic sections (Figures 5, 6 and 7) located on Figure 4. Faults can hardly be detected on bathymetric maps while their identification on dip maps is very conspicuous. It is important to notice that footprints originated from the acquisition and/or processing steps, specially in the acquisition direction (east-west) does not compromise the interpretation.

**Complementary work**

The goal of this article was to present a technique to map the seafloor and interpret the shallow geology as a byproduct of regular 3D seismic exploration surveys. Application of these studies are very clear in defining safe drilling and production operations and enhances our perception of continental margins processes. The next step needed for an even better interpretation is to develop a ground-truth calibration in order to better correlate the indirect measurements with the actual lithologies.

One must be aware when applying this technique to deeper horizons. Only easy-to-track horizons can be mapped using automatic detection algorithms. For the more general case, it would be preferable to work with time and surface crops of coherency volumes that will certainly give correlated results but at a higher cost and machine time.

**Conclusions**

It was our objective to present the usefulness of 3D seismic-derived attribute maps in the understanding of the near surface geology. The data set used in this exercise was conventionally acquired with main parameters of 4 ms interval sample and 25x25m grid. Higher frequency data sampled at intervals of 2 ms with a finer spatial grid will improve the method resolution. Provided that good quality 3D seismic data is available to explore a given area, much can be gained with the extraction and interpretation of the seafloor seismic attributes.

This approach will certainly lead us to a new era of understanding the recent sedimentary processes. The magnitude of seafloor fluctuations, slope failures deposits, deep water circulation and facies distribution at the continental margins will be much more reliably understood. This knowledge will also be used to better understand the processes that rule the deposition of older sediments, improving the task of finding new targets for hydrocarbon exploration

**References**

Bentz, C.M., Sant'anna, M.V., Machado, L.C.R., Miller, D.J., and Viana, A.R., 2000. Textural analysis and classification of Campos Basin sonar data to improve seafloor characterization. 31st Int. Geol. Congr., IUGS, Rio de Janeiro, Abstracts.

Pressler, R. R., Walker, D.B., 1999. Integrating deep tow and conventional 3D seismic for deepwater sea-floor imaging. Offshore, July, 98-100.

Roberts, H., Coleman, J., Hunt, Jr, J., and Shedd, W.W., 2000. Improving interpretation of seafloor geology, biology from remote sensing. Offshore, September, 126-128,181.

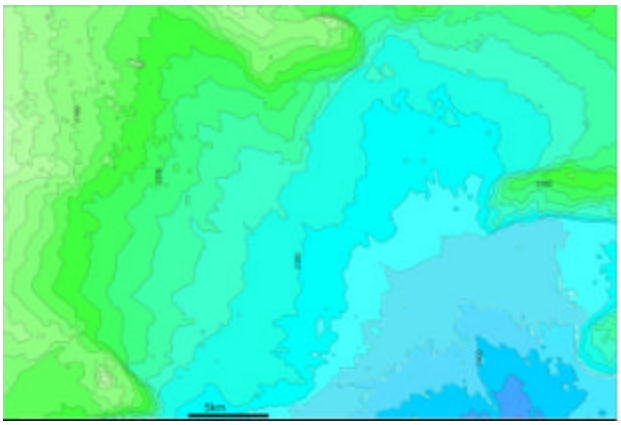

Figure 1: Bathymetric map produced from the 3D seismic data. Interval contour = 25m

...

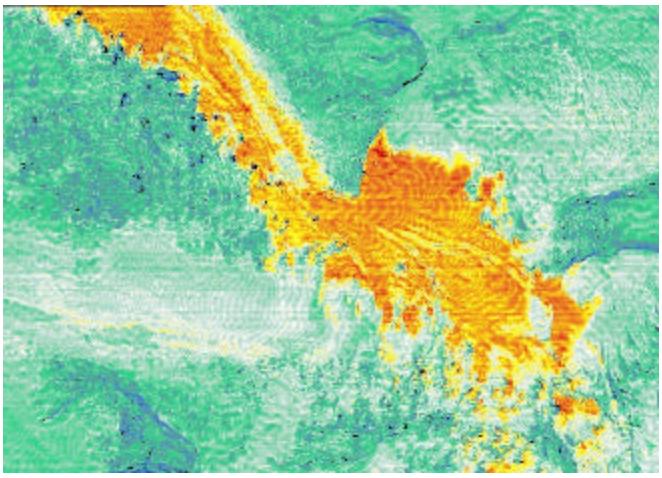

Figure 3: Maximum positive seismic amplitude strength at the seafloor. Red and yellow corresponds to the highest amplitudes, blue and green to the lowest ones

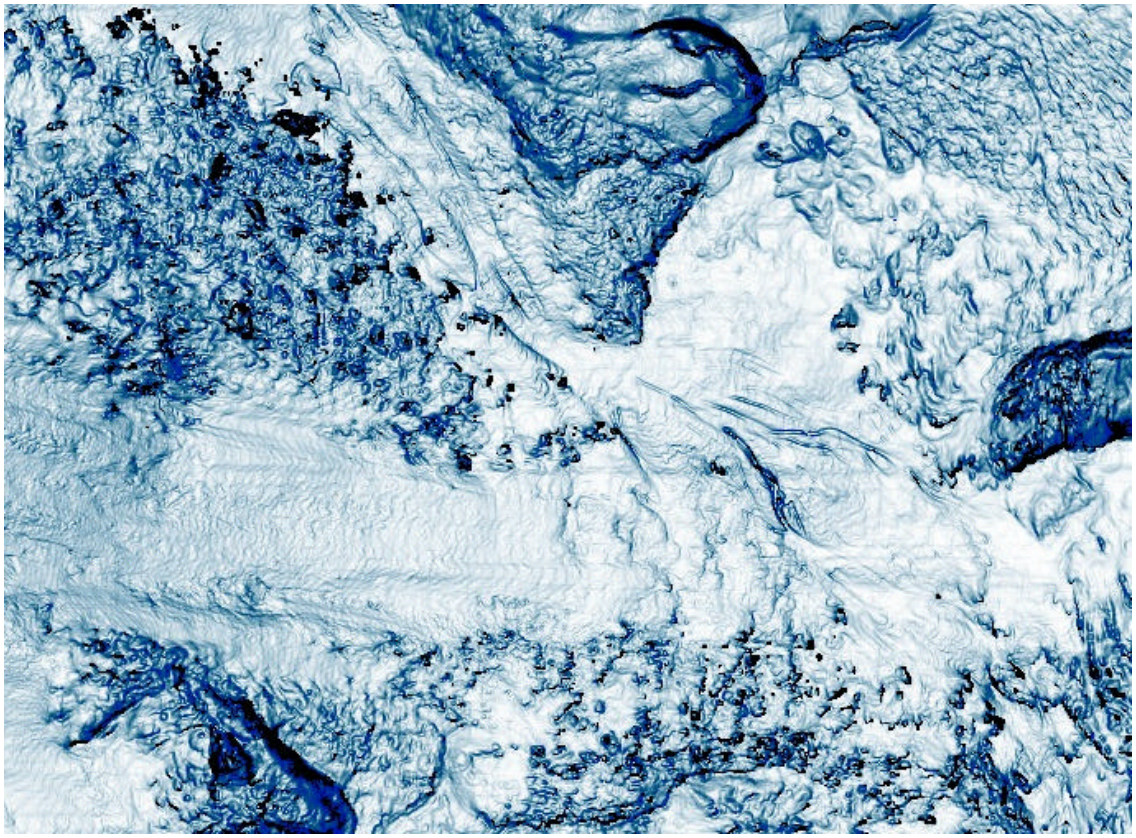

Figure 2: Dip attribute - Coherence map calculated from dip extracted from interpreted seafloor

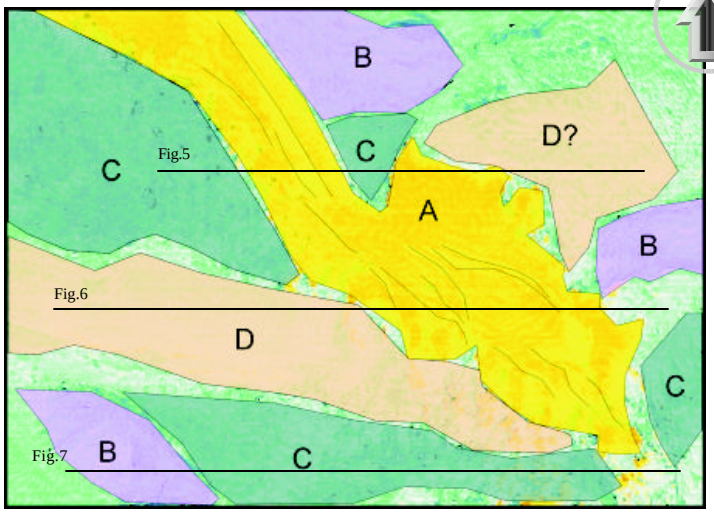


Figure4.Interpretationofthemaindetectedfeatures.A,B,Cand Daretexturalclassescorrespondingtodifferentamplitudevalues. Narrowlinesindicatechannelsandlineaments.

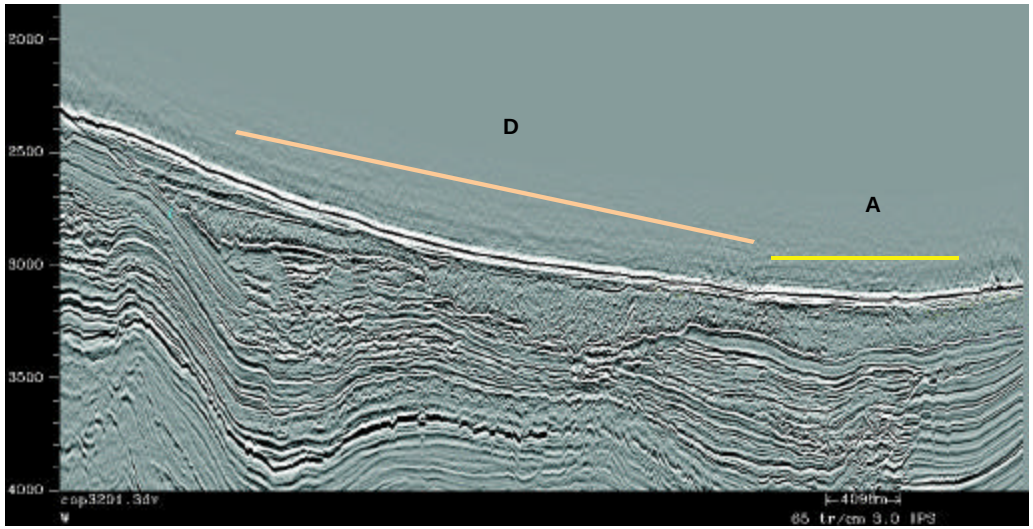


Figure6.Fromlefttoright:moderateamplitudereflectionsprobablyassociatedtohighlydiluted turbiditeflowsorslurryflows(D)overlyingchaoticseismofacies(debrisflowdeposits);highamplitu depositspossiblyassociatedtoasand-richcomplexofamalgamatedlobesandchannels(A), Observethewidespreadextensionofthechaoticfaciesimmediatelybelowthesurfacesedimen

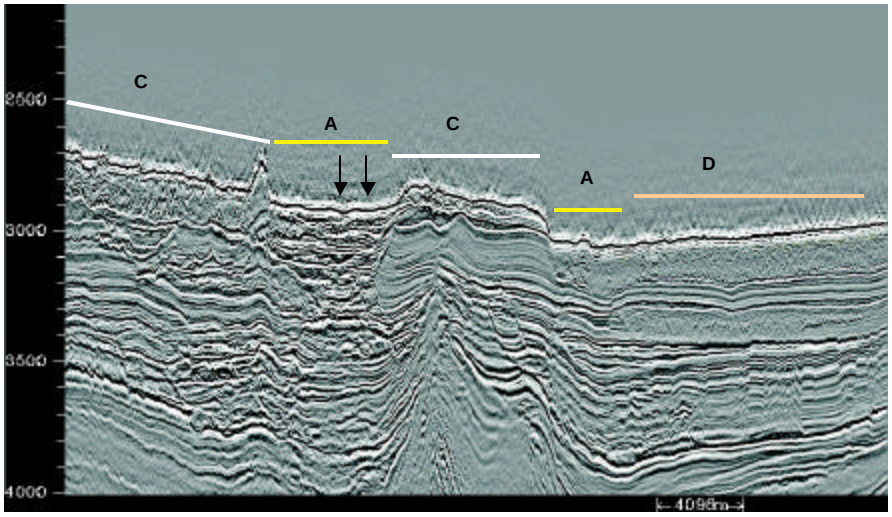


Figure5.Fromlefttoright:Roughsurfaceassociatedtodebrisflowdepositswithchaotic seismofacies (C), largeclastsarethrowntowardsthe top of thedepositsduringflow evolution;highamplitudedepositspossiblyassociatedtochannelfillbycoarse-grained sediments(A),arrowsindicatesmallchannelsinsidethemainconduit;elevatedrelief related to underlying salt diapir movement and with associated escarpments is observedatthecenteroftheseismicprofile;moderateamplitudereflectionsprobably associated to highly diluted turbidite flows or slurry flows (D) overlying chaotic seismofacies(debrisflowdeposits)

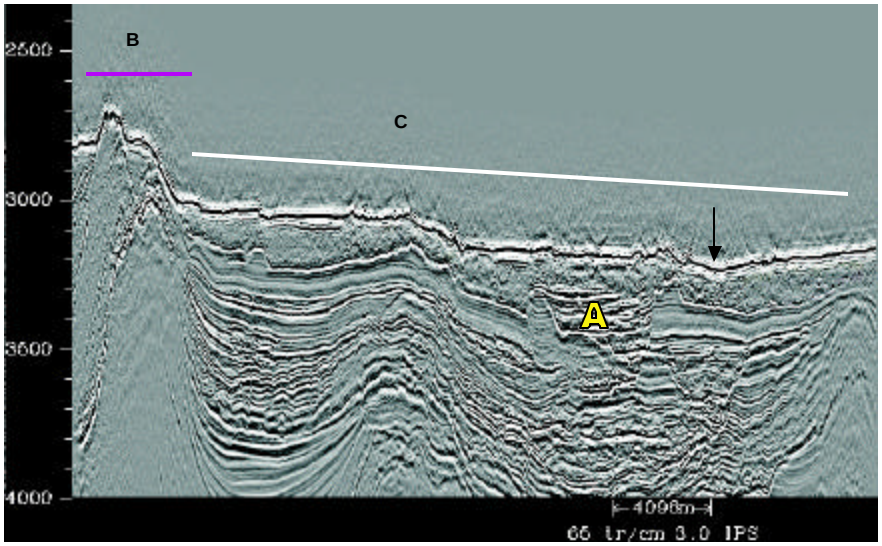


Figure7.Fromlefttoright:Elevatedreliefrelatedtounderlyingsaltdiapirmovement(B)with associatedescarpments;Roughsurfaceassociatedtodebrisflowdeposits(C),arrow correspondstoafaintindicationofpresenceofchannelconduitsconnectingthesand-rich lobeupstreamtodeeperenvironment.Underlyinghighamplitudesassociatedtocutandf patternsuggestsancientdownstreamcontinuationofthesand-richturbiditechannel(A).

# Integration of Shipborne Gravity and Satellite Altimeter Data for the Representation of the Gravity Field in the Northern Brazilian Margin

*Eder Cassola Molina, IAG-USP, Brazil (eder@iag.usp.br)*


## Abstract

The integration of GEOSAT GM satellite altimeter data, shipborne and land gravity data by least squares collocation was used in order to calculate an integrated representation of free-air anomaly and geoid height in the northern brazilian margin (52°W-30°W, 6°S-6°N). The comparison of the preliminary results with data from an independent LEPLAC-V leg shows that this technique can be very useful in the representation of the gravity field, allowing the adequated use of different kind of data.


## Introduction

The Earth's gravity field elements represent a valuable tool in the detection and study of oceanic features and continental margin structure. The classical approach to represent the gravity field in this region is the use of shipborne gravity data, that have a high precision but usually a limited spatial distribution. Since the late 1980's the use of satellite altimeter data has improved the knowledge of the gravity field over the oceanic areas providing a global coverage, with some problems in the regions near the continental area. The integration of these data, heterogeneous in kind and precision, is a powerful technique to represent the gravity field in the continental and adjacent oceanic area.

## The gravity field representation by least squares collocation

The elements associated with the gravity field, mainly free-air anomaly and geoidal heights, can be adequately integrated by least squares collocation (Moritz, 1980, de Sá et al., 1993, Molina, 1996), with significative advantages regarding the spatial distribution of these data. The main advantages of this method are:

- all the elements associated with the gravity field can be used to calculate any element the gravity field, provided that the covariance functions are known;
- the calculation of the gravity field can consider the input data accuracy;
- the calculated elements estimated variances may be used to identify higher or lower confidence areas due to the data distribution and/or original data quality.

The main limitation of the method is that the covariance functions between all the elements involved in the calculation have to be known, what is not an easy task in most cases, mainly due to heterogeneous distribution of data.

Least squares collocation consists in determining an approximating function $\hat{T}$ from linear functionals $L_i$ applied to the anomalous potential T. Applying the appropriated linear functionals to $\hat{T}$ one can calculate the corresponding element of the gravity field (e.g., $\Delta g$, N). The mathematical model is (Moritz, 1980)

$$t = AX + s + n \qquad (1)$$

where t is the vector containing the observations, A is a known fully populated matrix, X is the vector of parameters that expresses the deterministic component of the data, s is the vector of the anomalous field signals. and n is the vector of observational errors. The signals n can be calculated by applying linear functionals to the anomalous potential T. By removing the proper deterministic component of the data, generally by a geopotential model truncated at an adequated degree, the model can be expressed as

$$t = s + n \qquad (2)$$

with

$$s = L_i T \qquad (3)$$

In this work, the represented elements are gravity anomalies, expressed by

$$\overline{\Delta g}_r = \overline{\Delta g} - \overline{\Delta g}_d = -\left.\frac{\partial T}{\partial r}\right|_P - \frac{2}{R} T_r + n \qquad (4)$$

and geoidal heights,

$$N_r = N - N_d = \frac{T_r}{\gamma} + n \qquad (5)$$

where the subscript r means the stochastic component, calculated by removing the deterministic component of the gravity field, denoted by the subscript d, R is the Bjehammar's sphere radii and $\gamma$ is the earth's mean free air gravity anomaly (Molina, 1996).

The system given by (1) has the formal solution in the form

$$\hat{s} = C_{st}\, C_{tt}^{-1}\, t \qquad (6)$$

and the associated variance can be expressed by

$$\sigma_s^2 = C_0 - C_{st}^T\, C_{tt}^{-1}\, C_{st} \qquad (7)$$

where Ctt is the autocovariance matrix of the observations t and Cst is the cross-covariance matrix associated with the signal s and the measurements t. If the experimental errors of the measurements are available, the variance of the errors can be adequately included in the matrix Ctt (Moritz, 1980).

## THE DATA

The dataset used in this study includes satellite altimeter data, shipborne gravity data and continental gravity data. These data are described below and the data distribution is shown in Figure 1. In order to calculate the integrated model, all data had a deterministic component removed by subtracting the corresponding value calculated by the geopotential model EGM96 (Rapp and Lemoine, 1998) truncated at degree 180. This component was subsequently restored to the gravity field calculated values.

### Shipborne gravity data

The GEODAS marine database (NGDC, 1991) and EQUANT I and II legs available in the region were processed and converted to a suitable format for retrieving and processing. The database was constructed based on the procedure used by *xsystem* (Pal Wessel, personal communication), which makes the storing, retrieving and processing of marine geophysical data in an efficient way. After being stored, all data were submitted to an analysis to remove erroneous data points, by an automatic procedure that detected points with a directional gradient higher than a permissible limit specified, and visual inspection, comparing gravity, magnetics and bathymetry along the legs in order to correct or eliminate bad data. The internal crossover errors were calculated to determine the consistency and overall accuracy of each leg. This kind of problem was investigated in detail by Wessel & Watts (1988), and consists in calculating the differences of gravity values in the intersection of two tracks. The analysis of the internal crossover errors detects if there is a systematic component and/or a temporal drift affecting the leg. Calculating these quantities, one can correct each of the legs to eliminate such effects. Even with this procedure, some points still remain with large crossover errors. This could be attributed to an inadequated Eötvös correction, which depends essentially on the ship positioning. So, if one considers each track independently, corrections to each track that has at least two crossover points can be calculated to minimize the overall crossover errors. This approach was used by Prince & Forsyth (1984), and permits the detection of shifted tracks that could cause serious problems when using the data, by generating erroneous gravity features in the digital model. After this procedure, if some cruise remained with large crossover errors, it was discarded. The dataset obtained was processed to investigate the distribution of the external crossover errors, in order to garantee the dataset consistency.

The distribution of the crossover errors shows some legs with unrealistic large values that were discarded. The selected dataset was analysed to check its consistency, and the corrections for each track were calculated and applied to the data (Molina, 1996). This adjustment procedure removed spurious data points, homogeneized the data, and permitted to estimate the rms for this dataset, assuming that the external crossover error of each cruise is representative of its accuracy. The corrected marine gravity dataset for the study region consists of 7,718 free-air anomaly shipborne data points.

### Satellite Altimetric Data

The GEOSAT Geodetic Mission altimeter data were processed in order to obtain an altimetric dataset in the northern brazilian region. All the corrections avaliable in the Geophysical Data Records were applied, obtaining a one-second-averaged sea surface height (SSH) dataset, comprising near 150,000 data points in the region.The points which did not satisfy the usual quality criteria for satellite data (Sandwell & McAdoo, 1990) were discarded.

This altimetric dataset has a very dense spatial distribution, with an average of one data point each 5 km between the tracks, and a denser distribution alongtrack, what makes it feasible for a good representation of the gravity field in the region.

### Continental Gravity Data

The continental data available in the study area (52°W-30°W, 6°S-6°N) comprises over 6,400 gravity stations, referred to IGSN71 (IAG, 1974), with geographical coordinates, orthometric heights, free-air and Bouguer anomalies calculated using the 1967 theoretical gravity formula and 2.67 g $cm^{-3}$ for Bouguer density. The data were carefully analysed to exclude data points affected by large errors in the dataset (Sá et al., 1993). In general, the overall precision for these data is better than 0.5 mGal for free-air anomaly. To prevent problems in the representation in areas devoid of data, the digital gravity model obtained by Sá et al. (1993), interpolated at 0.5 degree, was used to fill in continental regions where no data were available.

## THE INTEGRATED MODEL

### Covariances determination

Empirical covariances of the residual free-air anomaly were computed, adjusted and propagated to obtain the covariances between the elements involved in the calculation of the free-air anomalies and geoidal heights. The methodology used is described in Knudsen (1987) and Molina (1996). In order to ensure the covariances are isotropic within an adequate radius, allowing them to be used into the representation by least squares collocation, two-dimensional covariances were calculated and the results show that, within a range of at least 100 km, this assumption is reasonable.

### Model calculation

The model calculation consisted in dividing the region around each 3.5 arc min block in 10 sectors, and searching the 20 nearest data points, 2 by sector, to avoid directional bias. The appropriate covariances were interpolated from the tabulated covariances, so the equations (6) and (7) could be used to estimate the free air anomaly and geoid heights and the associated variances for each 3.5 arc min cell. As the represented anomalous potential $\hat{T}$ is harmonic outside the geoid masses, the linear functional given by (5) represents in fact height anomalies, associated to the quasi-geoid surface, and not geoid heights values, associated to the geoid surface. In practice, however, the differences between height anomalies and geoidal undulations is usually within 0.1 m in continental areas, as noticed by Sjöberg (1993); in the oceans, both values are the same. So, depending upon the use of this variable, it can be considered equivalent to geoid height. The calculated height anomaly is shown in Figure 2, and the free-air anomaly is represented in Figure 3.

## DISCUSSION AND CONCLUSIONS

Although marine gravity data has achieved an expressive increase in quality in the last decade, the data distribution is usually adequated only to investigate limited regions of the oceanic crust. Satellite altimeter data, however, showing a global data distribution, can be used to represent the gravity field all over the oceans, but the methodology to convert altimeter data in gravity anomalies presents some problems, mainly near the coastlines, due to noise in the data. One additional problem is that the use of these data independently does not permit the integration with gravity land data to investigate continental margin features. The least squares collocation method described in this work is a powerful technique that can be used to calculate the gravity field elements.

In order to make a preliminary evaluation of the integrated model accuracy, a comparison of the free-air anomaly calculated with the integrated model with the values of a LEPLAC-V leg, not used in the model calculation, is shown in Figure 4. The good agreement between the predicted and the actual free-air anomaly in this preliminary test shows that this technique can be used to achieve good results in the integration of continental and oceanic data, derived from gravity and satellite altimeter, exploring the best characteristic of each kind of data.

### References

Knudsen, P., 1987. Estimation and modelling of the local empirical covariance function using gravity and satellite altimeter data. Bulletin Géodésique 61, 145-160.

Moritz, H., 1980. Advanced Physical Geodesy. Abacus Press, Wichmann.

Molina, E.C., 1996. Ajustamento e integração de dados gravimétricos e de altimetria por satélite na representação do campo de gravidade no Atlântico Sul. PhD Thesis, IAG-USP, 200pp.

Prince, R.A., Forsyth, D.W., 1984. A simple objective method for minimizing crossover errors in marine gravity data. Journal of Geophysical Research 49, 1070-1083.

Rapp, R.H., Lemoine, F., 1998. The development of the joint NASA GSFC and the National Imagery and Mapping Agency (NIMA) geopotential model EGM96. NASA/TP-1998-206861, GSFC, Greenbelt, MD.

Sá, N.C.de, Ussami, N., Molina, E.C., 1993. Gravity Map of Brazil 1. Representation of Free-Air and Bouguer Anomalies. Journal of Geophysical Research 98, 2187-2197.

Sandwell, D.T., McAdoo, D.C., 1990. High-Accuracy, High-Resolution Gravity Profiles From 2 Years of the Geosat Exact Repeat Mission. Journal of Geophysical Research 95, 3049-3060.

Sjöberg, L. E., 1993. Techniques for geoid determination. In: Vanícek, P., Christou, N.T., Geoid and its Geophysical Interpretations. CRC Press, USA, pp. 33-56.

Wessel, P., Watts, A.B., 1988. On the accuracy of marine gravity measurements. Journal of Geophysical Research 93, 393-413.

Acknowledgments

I would like to thank the personnel of the National Imagery and Mapping Agency (NIMA) for their contribution of state-of-the-art spherical harmonic synthesis software for modeling various components of the earth's gravity field with EGM96, Brian Beckley and the NASA GSFC staff by helping with retrieving of GEOSAT GM data, Per Knudsen for fruitful discussing about covariances adjustment, Pal Wessel & Walter Smith for GMT software, and Naomi Ussami for useful discussions during the course of all the stages of this work.

For high resolution images and additional details, please visit
http://www.iag.usp.br/geofisica/docentes/eder/north.html

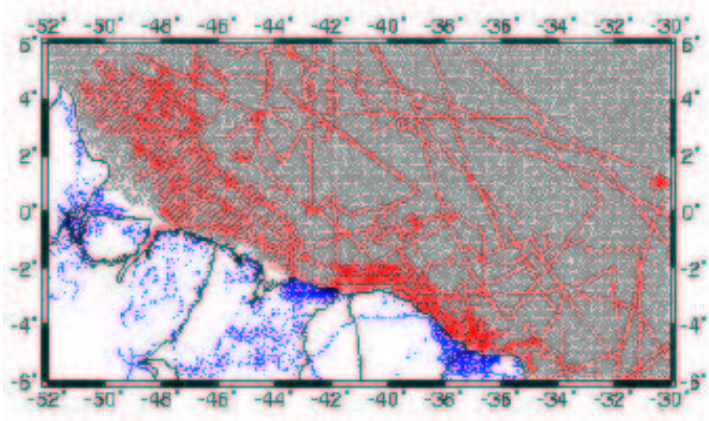

Figure 1 – Data distribution in the study area area (52°W-30°W, 6°S-6°N). Gray dots represent GEOSAT GM altimeter data, red dots are shipborne marine gravity data, and blue dots represent land gravity data.

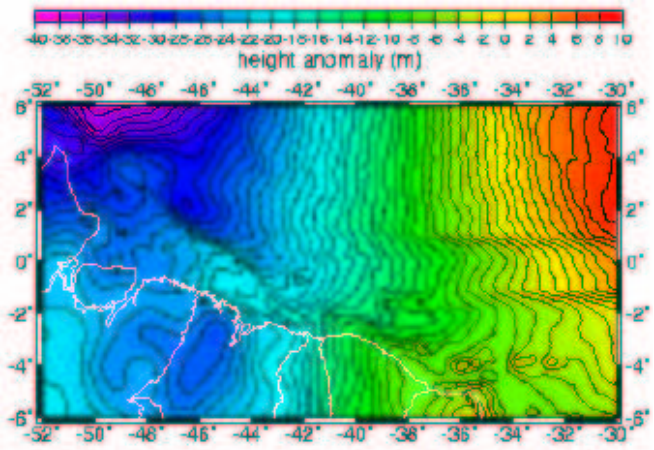


Figure 2 – Representation of the integrated height anomaly in the northern brazilian region. Contour interval: 1 m.

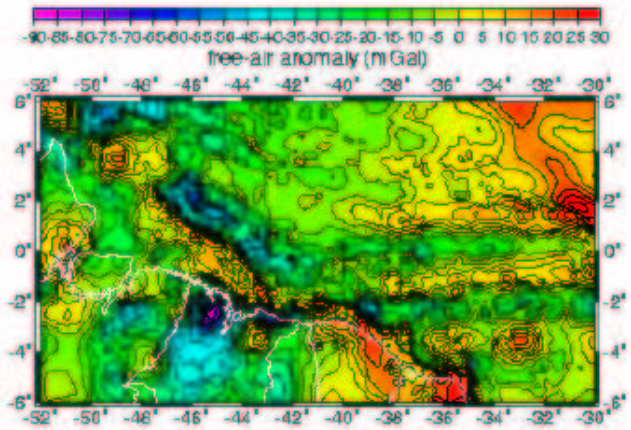


Figure 3 – Representation of the integrated free air anomaly in the northern brazilian margin. Contour interval: 5 mGal.

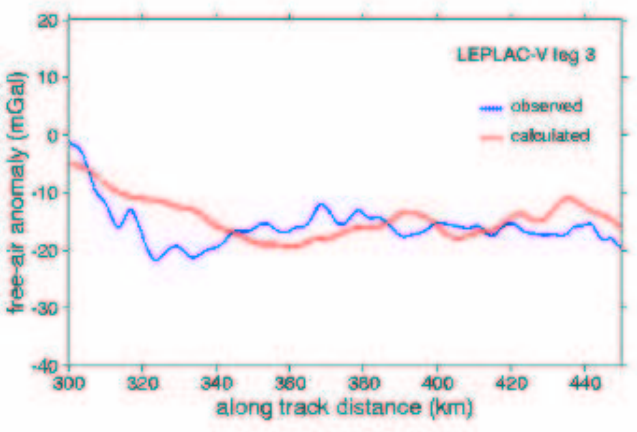


Figure 4 – Comparison between a segment of a LEPLAC-V leg and the values predicted by the integrated model in the northern brazilian continental margin. Blue symbols represent the observed values, and red symbols the corresponding estimated values using the technique described in this work.

# MODELING THE GENESYS AND EVOLUTION OF VOLCANIC RIFTED BASINS: CONSTRAINTS FROM SOUTHEASTERN BRAZILIAN CONTINENTAL MARGIN

***MARCELO SPERLE, GEOSCIENCE INSTITUTE / RIO DE JANEIRO STATE UNIVERSITY, sperle@uerj.br***
***GARRY D. KARNER, LDEO - COLUMBIA UNIVERSITY, garry@ldeo.columbia.edu***
***LUÍZ F. S. BRAGA, OBSERVATÓRIO NACIONAL – CNPq, braga@on.br***

**Abstract**

The quantitative relation among the first order parameters controlling the basement topography distribution at divergent continental margins could be investigated through the development of a thermo-mechanical model, including the effects of the pre-rift mantle plume, lithospheric rifting, erosion in the rift escarpment and sedimentation in the marginal basin.

The regional basement topography of southeast Brazil, including the Brazilian highlands, coastal ranges and the continental margin could be conveniently modeled by this simple integrated tectonophysical model. The modeling was constrained by a number of geophysical data such as: topography/bathymetry, gravity, heat flux and apatite fission track data.

In this work we discuss the modeling results, its application to some transects crossing the southeast Brazilian margin and how it might be used as an interesting tool in evaluating the genesis and evolution of rift basins at divergent continental margins.

**Introduction**

A major controversy exists over whether extended continental lithosphere, associated with rift basins at divergent continental margins, possesses mechanical strenght or flexural rigidity during rifting Several studies using gravity anomalies over rifted basins and passive margins have concluded that the flexural rigidity of continental lithosphere remains negligible once it is extended, although low strenght has been attributed to the normal faulting of the crust and high heat flow in extended regions (Royden and Keen, 1980). Also little rationale has been given for why flexural rigidity should remain low after rifting. Moreover, other studies have concluded from gravity data that the morphology of rifted basins and their flanking topography are an expression of regional isostatic compensation Weissel and Karner, 1989; Ebinger et al., 1991) wich, in fact, requires that the extended lithosphere possesses finite mechanical strenght.

The answer for these questions are very important for basin analysis since it controls a number of important aspects for the oil industry as: basement depth and morphology, stratigraphy and heat flow.

Thus the main goal of this work becomes one of devising tests to discriminate between zero and finite *Te* across extensional basins and forward modeling the crustal shape and time-line stratigraphy of extensional basins and their respective free-air gravity anomalies for determinating the relationship between the topographic/bathimetric, basement and moho reliefs. Fundamental to any forward-modeling analyses is the need to define exactly what loads are being applied, or removed from the lithosphere.

In general, studies investigating the mechanisms responsible for the formation of rift flank topography have concentrated on young rift systems such that the present day flank topography had not suffered significant erosion. To test for the existence of rift flank topography at an old rifted margin, we have investigated the tectonic evolution of the coastal mountain ranges bordering the southeast Brazilian margin using a simple two-dimensional mechanical model to determine the flexural response of the lithosphere due to tectonic unloading, induced by extension, and subsequently by erosion of the rift topography and sedimentation in the adjacent basin. Thermocronologic data such as fission-track ages from Apatite, high resolution topography/bathimetry, marine and continenatl gravity data and seismic profiles are used to constrain the models.

**Theoretical Background**

Volcanic rift basins are located at divergent margins adjoined by major erosional escarpments wich separate uplands intracontinental areas (showing relative low rates of erosion and subdued relief) from coastal areas with much greater relief and higher rates of erosion. These escarpments are found along the divergent margins of eastern Australia, southearn Africa, western India, Red Sea and Gulf of Suez, Madagascar and also at southeast Brazil. Although these margins have diverse ages of formation, varying from Neogene for the Red Sea, late Cretaceous for

southeast Australia, to early Cretaceous for southern Africa and southeast Brazil, each one exhibits in common: (1) steeper slopes facing the rift or ocean basin, (2) a topographic culmination ot tableland at, or just inland from, the present location of the escarpment, and (3) a gradual decrease in elevation to a regional topographic level at some distance inland.

Different hypothesis exist to explain the topography adjacent to rift basins. Most of them rely on some type of thermal process engendered by lithospheric rifting to drive flank uplift. However in the case of Southeast Brazil and Southern African margins, any thermal support for rift flank uplift should have dissipated long ago, because extension ended at those margins in Late Jurassic/Early Cretaceous time.

A number of studies have hypothesized that the flexural rebound of the lithosphere in response to its tectonic unloading during extension may play a dominant role in the generation and permanent support of rift flank topography (Weissel and Karner, 1989; Braun and Beaumont, 1989; Ebinger et al. 1991). Implicit in these studies is that the extended lithosphere maintains significant flexural strenght during and after extension despite localized, but intense, fracturing of the crust by normal faults and the proximity to high heatflow regimes.

**Methodology**

.

. As discussed by Weissel and Karner (1989), Ebinger et al. (1991) and Karner & Driscoll (1993) flexural rebound of the lithosphere in response to tectonic unloading during extension might be the dominant process by wich rift flank topography is generated. Therefore the formation of rift basins and their flanking topography can be quantitatively modeled as the sum of the relief created by crustal-scale faulting, for example by instantaneous slip along a bounding planar or listric normal fault, to produce a “kinematic topography” or hole wich is in turn modified by the isostatic response of the lithosphere. The isostatic response to crustal thinning is to produce a rebound or “isostatic topography”. This rebound will tend to be regionally developed around the region undergoing extension, thereby resulting in permanent rift flanks that eventually are modified by sedimentation and erosion/denudation processes, while the moho will similarly be flexurally modified.

In the modeling approach we first specify a kinematic description of lithospheric extension by simple slip along a low angle fault above the detachment horizon (Wernicke and Burchfiel, 1982; Hall et al., 1984; BIRPS and ECORS, 1986). that produces a “hole” in the surface of the lithosphere due to the collapse of the hanging wall block. This deformation results in the thinning of the lithosphere and the pertubation of the geothermal gradient. We then calculate the isostatic reponse of the lithosphere to the density perturbations introduced by the kinematics of extension. Then we calculate the isostatic response of the water and sediment infilling into the rift basin and the isostatic effects of the pos-rift erosion. The fundamental assumptions here are that the kinematic and isostatic aspects of lithospheric extension can be treated separately and that the isostatic response of the lithosphere is analogous to the flexure of a thin elastic plate floating on a fluid substrate.

**Discussion and Results**

Both before and during the opening of the South Atlantic, widespread basaltic extrusions dating from about 160 to 120 Ma (Renne et al., 1992) outpoured in the regions of the Paraná and Karro basins, and over the regions that would subsequently become the offshore Campos and Santos basins. Tholeitic basalts constitute the basement of both the Campos and Santos basins in addition to intruding the rift sediments and early post-rift sediments to at least Santonian age. The climax of this major eruptive episoide of basalt production was marked a period of active rifting of the continental crust in the lower Cretaceous that produced a sucession of rift basins along the Brazilian margin.

Boreholes in the onshore part of the Campos Basin have drilled through 600 m of tholeiitic basalts and penetrated acid Precambrian igneous rocks similar to the granitoid rocks that outcrop along the coast. These same Precambrian rocks form the coastal Serra do Mar and Serra da Mantiqueira mountains.

Despite of the Campos and Santos basins have been studied for many decades by Petrobras (the Brazilian oil company) there is a paucity of stratigraphic and geochronological data avalaible for the scientific community wich limit our control on the evolution of the sedimentation history. Nevertheless we tried to parametrize our model by using one refraction and some seismic reflection profiles that, in a general sense, can be taken as an approximate representation of the basin geometry and the crust thickness in the region.

The flexural strenght of the lithosphere was determined by modeling the total morphological shape (both the flanks and rift basin) across regions of continental extension. Fundamental to this analysis is that the rift flank topography represents the flexural

rebound of the lithosphere in response to extension (Weissel and Karner, 1989). This assumption was tested by modeling the free-air gravity anomaly.

The free-air gravity anomaly is proportional to the magnitude of deviatoric stress in the lithosphere and can be a powerful constraint on the strenght of the lithosphere during and after extension. This is because the various crustal and lithospheric mantle loads engendered by rifting must be compensated. In defining the form of this compensation we are actually describing the flexural state of the lithosphere.

Density variations arising from the geometry of the isostatically deformed surface and crust-mantle interfaces are the major contributors to the free-air gravity anomaly over the rift basin. Second order contributors include the anomalous temperature strucuture of the lithosphere within the extended zone, the variation of sediment density with depth due the effects of compaction, and the variable bathimetry towards the basin. Free-air gravity anomalies within extensional provinces are an important key to understanding the mechanical behaviour of the lithosphere and therefore represent a major observational constraint in studies of rift basin development.

As we can see from the model results the calculated topography, basement, gravity anomalies and fission track distribution are in good agreement with the related observational data.

The flexural response of the lithosphere for the surface loads has been calculated in the wavenumber domain by using Fourier transforms. A crustal thickness of 35 km is assumed for all models. Densities used are 3.33 g/cm$^3$ for mantle, 2.80 g/cm$^3$ for crust, 2.20 g/cm$^3$ for sediments and 1.03 g/cm$^3$ for sea water. The best elastic thickness obtained for the rift fase was 30 km and the marginal escarpment retreat was obtained for an erosional rate of 1 km/m.y.

**Conclusion**

The regional topography of southeast Brazil, including Paraná Basin, Serra do Mar and Serra da Mantiqueira, could be conveniently modeled by a simple tectonophysical model. This model was constrained by a number of geophysical data such as: topography, gravity, heat flux, bathymetry, and apatite fission track data. In this work the theorical results from the modeling of one transect crossing the southeast Brazil and its adjoinning continental margin is discussed together along with recent geological, geophysical and geochemical evidences of neotectonism in this area.

The results sugest that the topography of southeast Brazil and its tectonic significance are related to the interplay of the juro-cretaceous magmatism in the Brazilian Highlands, mesozoic rifting in the coastal areas, differential erosion in the marginal escarpments and sedimentation in the marginal basins. The models allows the definition of a number of fundamental parameters for basing analysis and the oil industry and might be used as an important tool in volcanic rifted margins.

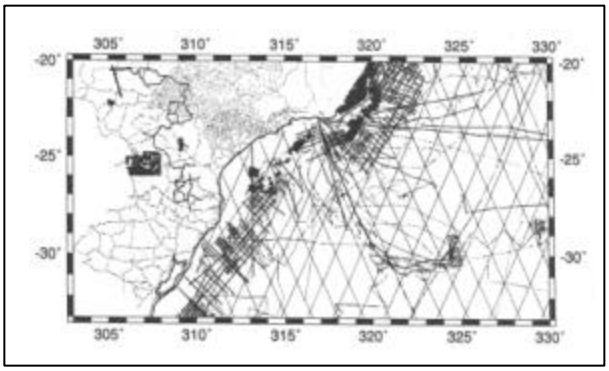


Fig. 1 – Distribution of gravity and topographic station in the southeast Brazil and adjoining continental margin.

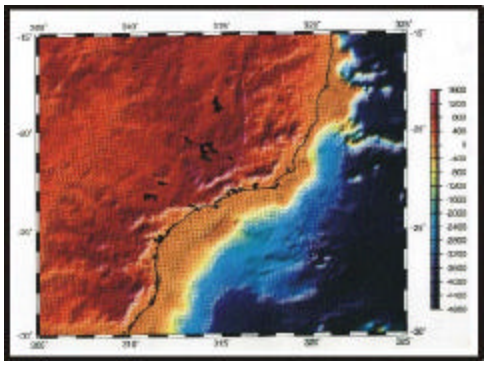

Fig. 2 – Topographic/bathymetric map from the southeast Brazil and adjoining continental margin.

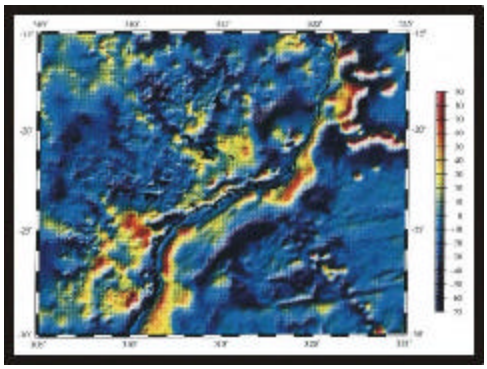

Fig. 3 – Free-air gravity map from the southeast Brazil and adjoining continental margin.

## Modeling the Genesys and Evolution of Volcanic Rift Basins

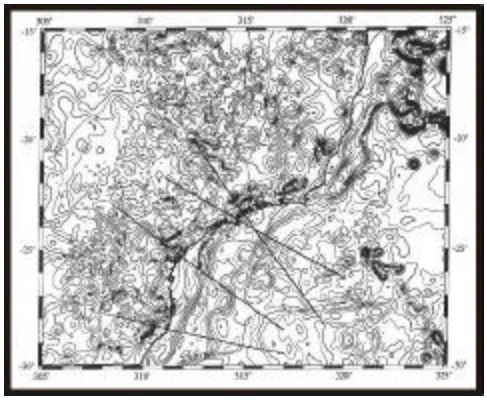

Fig. 3 – Free-air gravity map from the southeast Brazil and adjoining continental margin showing the modeled transects.

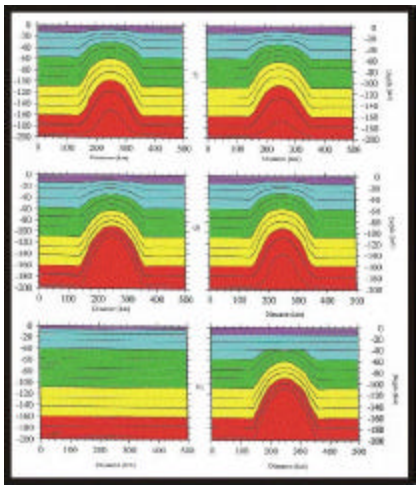

Fig. 4 – Simulation of the transient temperature structure of the continental lithosphere due to the Tristão da Cunha Mantle Plume (Pre-rift phase)

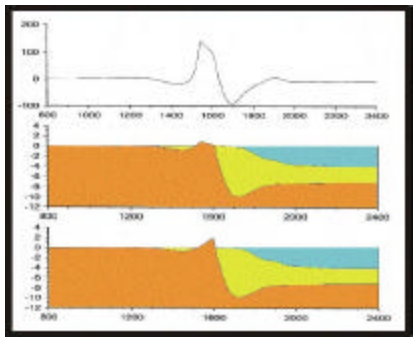

Fig. 5 – Integrated model showing the initial and final configuration of the continental margim together with its calculated free-air gravity anomaly.

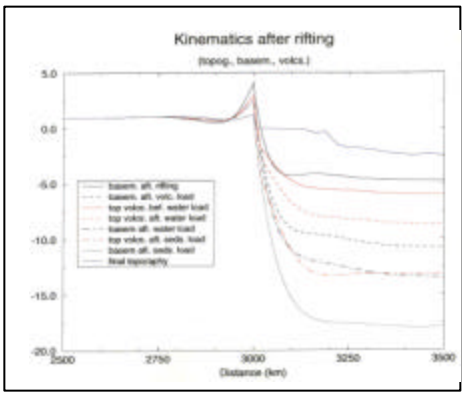


Fig. 6 – Kinematics of the basement interface after rifting considering the water, sediment and volcanic loadings.

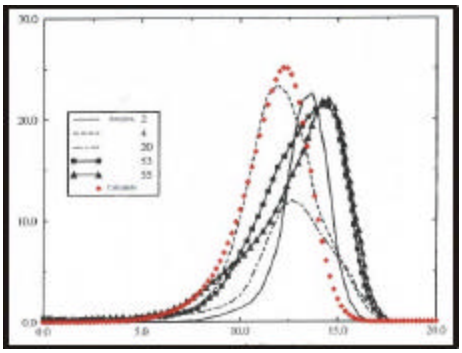

Fig. 7 – Model for the fission-track length and distribution from the apatites samples located at the coastal mountain ranges

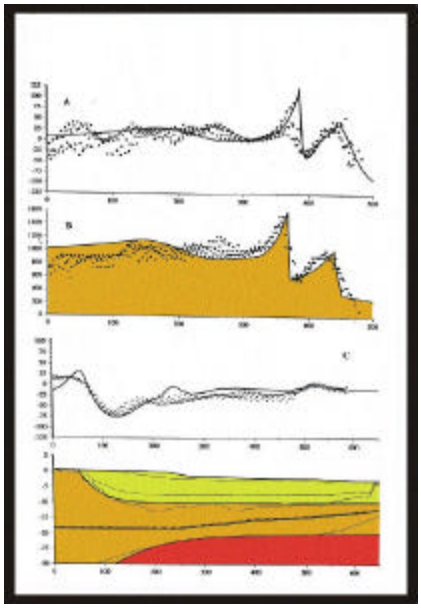

Fig. 8 – Integrated final lithospheric model for transect ***A*** crossing the southeast Brazilian continental margin. Note the good agreement between the gravity and topography data and those calculated from the model.

# Morphostructure and Gravimetry of Eastern Brazilian Continental Rise

*Ivo Bruno M. Pessanha*[1] *ivo@igeo.uff.br* ***Jorge J. C. Palma***[1]**,** *Marcelo Sperle Dia*s[2]**,**
*(1) LAGEMAR – Depto. de Geologia, IGEO/UFF (2) Depto. de Oceanografia, UERJ*

**Abstract**

Eastern Brazilian continental margin shows outstanding features, such as seamounts, ridges, sectors of abnormally widened continental shelf, besides igneous bodies regionally inserted in the sedimentary sequences. The widespread distribution of these features indicates conspicuous magmatic activity in the area. The small number of available petrologic, radiometric data and local gravity modelling results suggest that this is a post-rift mainly alkaline magmatic province of eocene age.

The genesis of these features has been ascribed for a few independent magmatic sources. However there is a striking coincidence of the area of magmatic province with the Complexo Geoidal Leste Brasileiro (CGLB), a long wavelength high of the gravity field recently derived from satellite altimetry.

The relationship between the regional tectonic framework and the CGLB, along with the absence of a topographic bulge to explain the gravity high arise the hypothesis that magmatic and gravity anomalies are both manifestations of a mantle upwelling under this whole region.

# MORPHOSTRUCTURE OF SÃO PAULO FRACTURE ZONE IN WESTERN EQUATORIAL ATLANTIC

*Valeria B. Perales, valeria@igeo.uff.br, Jorge J. C. Palma, jorge@igeo.uff.br, Susanna E. Sichel,susanna@igeo.uff.br*
*Depto de Geologia – LAGEMAR UFF, Niterói, RJ*

**Abstract**

São Paulo Fracture Zone (ZFSP) is a prominent linear structure of the Equatorial Atlantic seafloor that consists of a set of alternate troughs and ridges transversal to the Mid Atlantic Ridge (MAR), separating different levels of oceanic basement.
Based on multi-channel seismic data of Leplac Project, associated with free-air anomalies derived from satellite altimetry of the sea surface, it was defined the extension of the ZFSP, as well as the main structures that compose most of its western limb.
The ZFSP is very well defined in the crest of the MAR where it offsetts the axis segments ca. 630 km. In this area the main morphologic features are two transform valleys and the central rift valley offset by the transforms. The western inactive limb of the ZFSP is a ~200 km wide E-W swath of terrains bounded to the north and south by transverse ridges. These terrains are structured in two striking throughs as deep as 500 m each separated by a nearly continuous basement high, characterizing a double fracture zone. In the middle of the research area superimposed to the main E-W alignment, secondary directions N-S and NW-SE are represented by two outstanding ridges of origin not well understood yet.
Free-air gravity anomalies show the continuity of the northern ridge and intermediate basement high up to the Brazilian continental rise (~45°W). Farther westernwards the intermediate basement high lines up with a gravity high associated to the normal fault that forms the southern boundary of the Foz do Amazonas basin in the continental shelf.

# Parasound Data Interpretation on Amazon Submarine Delta

*Guisela Santiago Grossmann, Lagemar-Universidade Federal Fluminense, Brazil,guisela@igeo.uff.br*
*Alberto Figueiredo Jr., Lagemar-Universidade Federal Fluminense, Brazil, alberto@igeo.uff.br*
*Jurandyr Schmidt, Petrobras, jschmidt@petrobras.com.br*

**Abstract**

Amazon submarine delta is the main feature of the Amazon shelf. This area is influenced by several energetic forces, such as the large tidal amplitudes, the North Brazilian Current, the Trade Winds and specially by the enormous water discharge from the Amazon River.

Parasound Echosounder data, in a cooperative scientific program between Fluminense Federal University and Bremen University on board of R/V Meteor, cruise 34, leg 4 in 1996. Has frequency of the 4 kHz and were processed with Sesuit Software.

Parasound Echosounder System has decisive advantages over standard 3.5 kHz systems, among them, provide a higher depth resolution; different colors of the amplitude signal can be relating it with the grain size; and the reflected signal can be digitized, stored on a computer tape, and comparisons be made with the physical properties measures on sediment cores.

A important characteristic observed in Parasound record in Amazon submarine delta is laterally continuous sub-bottom reflectors by dozens meters. This sub-bottom reflectors are plan-parallel and its echos amplitudes are well distinguished. Is possible to found in several records, trapped gas appears masking the underlying reflectors.

**Introduction**

The Amazon River with a basin of drainage of $7x10^6$ $km^2$ can reach 354.793 $m^3s^{-1}$ at maximum water discharge (Figueiredo *et al.*, 1993). Sediment transport is approximately $1.2x10^9$ tons $yr^{-1}$ (Meade *et al*., 1985) and with such sediment load, the river builds up a submarine delta that extends until the external platform (Figueiredo *et al*., 1972). Besides river discharge, this region is also under the influence of the North Brazilian Current (NBC), flowing in northwest direction, deviating the discharge of the Amazonas River in this direction; strong tidal currents and northeast trade winds. All these factors interact on the shelf, causing a differential sediments distribution along the shelf (Costa, 1997), influencing its sedimentary evolution (figure 1).

This study has the objective processing digital seismic data of the echossonda and sub-bottom profiler Parasound and to interpret them to understand nature of the interbedded and interlaminated sands and muds and also occurrence of gas.

**Geomorphology and sedimentation of the Amazon Continental Shelf**

Sedimentation in the Amazon continental shelf is controlled by the discharge of Amazon River, estuarine circulation and tides. These act in the distribution and deposition of the sediments, resulting in sedimentary deposits possessing both fluvial and marine characteristics.

The locus of sedimentation occurs at a turbidity maximum due the flocculation. Suspended-sediment concentrations within the turbidity maximum can become very high, forming nearbed zone of fluid mud. The upper portion of the fluid mud is mobile, the lower portion is stationary, and below these is the cohesive seabed (Jaeger *et al*., 1995).

Superficial distribution of the sediments in the amazon shelf, to northwest of the river Para, it is marked by the presence of terrigenous sediments, composed by mud in the inner shelf and sands in the outer shelf. Carbonate sediments are restricted to the external shelf and they concentrate in front of the Amazon mouth (Costa, 1997).

The Amazon submarine delta is the main feature on the shelf. From the offshore river mouth it runs in northwest direction, being wider in front of the Amazon mouth (300 km) and becoming narrower toward Cape Orange, where it is only 50 km wide. The total length is approximately 650 km (Figueiredo *et al*., 1992).

It is a well defined submarine delta, where the topset, foreset and bottomset divisions can be identified. The foreset is characterized by the presence of clinoforms and its inclined strata attest a progradation of this feature.

Due to this clinoform structure, beginning in approximately 10 m of depth and extending the until the isobath of 70 m or 80 m, the Amazon submarine delta has potential to form deposits of about 60 m of thickness (Figueiredo *et al.*, 1995).

**Parasound Echosounder System**

The importance of being able to investigate the sedimentary structure of the seabed has led to the development of various types of low-frequency echosounders wich have been used to good effect as sub-bottom profilers (Grant *et al*., 1990).

These systems typically have used frequencies of around 3,5 kHz. The use of such low frequencies implies the employment of large transducers and wide beam-widths. This in turn leads to the genera-

tion of side echoes which interfere with the desired sediment echo (Grant *et al*., 1990).

The Parasound Echosounder System offers new possibilities in subbottom profiling. The system is based on the parametric principle. In addition to the transmission of a first signal with a fixed primary frequency, 18 kHz, a second primary frequency, between 20.5 and 23.5 kHz, is simultaneously radiated. The secondary frequency ranges between 2.5 and 5.5 kHz, respectively. The low secondary frequency is only generated in the central part of the beam which is the narrow beam angle of the primary frequencies (Kuhn *et al.*, 1993) and free of side echoes.

Utilization of the parametric effect has decisive advantages over standard 3.5 kHz systems.

- The relatively small beam angle of about $4^0$ increases the spatial resolution vertically and laterally and difraction patterns are strongly reduced in the echogram, increasing the resolution of sedimentary morphology (Kuhn *et al.*, 1993).
- Due to the high primary frequencies, a comparable short pulse length can be radiated. This, combined with the low secondary frequency, leads to higher depth resolution.
- Varying the second primary frequency and pulse length, the operator can select either for maximum penetration or maximum depth resolution
- The reflected signal can be digitized and comparisons be made with the physical properties measures on sediment cores (sound velocity, wet bulk density, porosity, magnetic susceptibiity), and with synthetic seismograms calculates from these data (Kuhn *et al*, 1993).
- The different colors of the amplitude signal can be relating it with the grain size.

A disadvantage of the Parasound system, is that due to the small beam angle only very weak bottom signals are reflected to the ship in areas with steep topography (Kuhn *et al.*, 1993).

**Data Collection**

The digital sub-bottom data, collected by Echosounder Parasound System, were obtained by the team of the University of Bremen, onboard the R/V *Meteor*, during the leg 34/4, in April of 1996. These data were processed by the software Sesuit - version 1998 of the University of Bremen.

In these data two waves, 18 kHz and 22 kHz were emitted simultaneously and a signal of the difference frequency, 4 kHz, was generated. The source used by the equipment is sweep type, consists of a pulse emitted with growing frequency and with defined length.

**Seismic Processing**

The difficulty in a seismic processing is related to the geologic complexity and to the acoustic impedance. A seismic processing consists of some basic stages as: geometry, data edition, filter applied, deconvolution, NMO and migration (Yilmaz, 1987).

The software used for the seismic processing is Sesuit - version 1998 of the University of Bremen.

As the data don't surpass many dozens of meters, the processing was simplified. An automatic gain control was applied to enhance the seismic sign, the noise was subtracted and a mute was applied.

**Data Interpretation**

The figure 2 shown a profile that characterize the presence of gas and the bedding of the sediment layers.

This profile, near the Amazon mouth, is characterized by plan-parallel and laterally continuous sub-bottom reflectors. This continuity can be observed by dozens of meters. The plan-parallel reflectors possess different echo amplitudes that are associated with alternation of sand and mud beds. This alternation could be caused by river discharge or by variations of tide. This sub-bottom reflectors are overlaying an irregular surface, probably relict sands, topographically discordant of present bottom.

Trapped gas appears masking the underlying reflectors and shows an abrupt lateral discontinuity. Absence of organic matter or trapping strata could be associated with this discontinuity.

**Conclusions**

This work shows that the Parasound data has great quality and is possible have a good characterization of the first dozens meters of Amazon submarine delta due to better depth resolution in the first layers of the sediment.

Important characteristics of this feature that can be studied better with the Parasound System are the continuity of the sub-bottom reflectors, gas location and identification of the sand and mud beddings.

**References**

Costa, E.A., 1997, Caracterização de ecofácies e processos sedimentares da Plataforma Continental Amazônica: MSc. Thesis, Fluminense Federal University, 138pp.

Figueiredo Jr., A.G., 1993, Modelo de sedimentação atual da Plataforma Amazônica. Thesis for full professor for selective process, Fluminense Federal University, 42pp.

Figueiredo Jr., A.G. & Nittrouer, C.A., 1992, Distribuição de caráter de eco de 3.5 kHz na Plataforma Continental do Amazonas. Anais do 37$^{0}$ Cong. Bras. de Geologia, 1: 201-202.

Figueiredo Jr., A.G. & Nittrouer, C.A., 1995, New insights to high-resolution stratigraphy on the Amazon continental shelf. Mar. Geol., 125:393-399.

Grant, J.A. & Schreiber, R., 1990, Modern Swathe Sounding and Sub-Bottom Profiling Technology for Research Applications: Atlas Hydrosweep and Parasound Systems. Mar. Geoph. Res., 12: 9-19.

Jaeger, J.M. & Nittrouer,C.A.,1995, Tidal controls on the formation of fine-scale sedimentary strata near the Amazon River mouth. Mar. Geol., 125: 259-281

Kuhn, G. & Weber, M.E., 1993, Acoustical characterization of sediments by Parasound and 3,5 kHz systems: Related sedimentary processes on the southeastern Weddell Sea continental slope, Antarctica. Mar.Geol., 113: 201-217.

Yilmaz, Ö., 1987, Seismic Data Processing. Society of Exploration Geophysicists, 526p.

**Acknowledgments**

We would like to thank the National Petroleum Agency (ANP) for supporting G. Grossmann thesis and Dr. Gerold Wefer (Bremen Univ.) for our participation on Meteor cruises and collection of data.

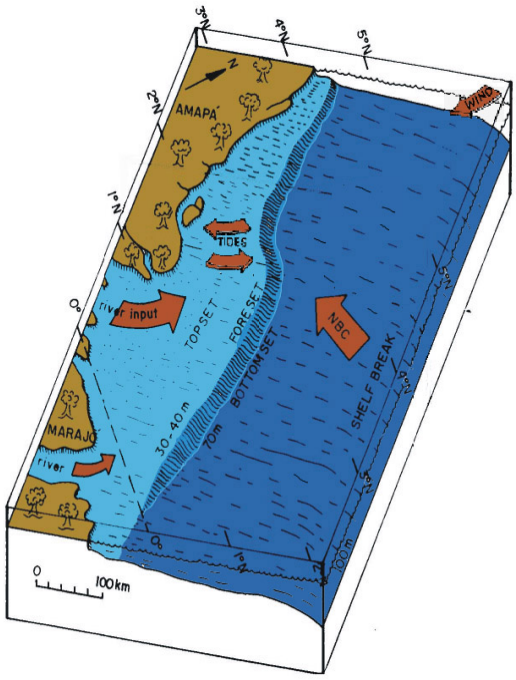


Figure 1 – Geometry of the Amazon submarine delta and the acting oceanographic processes.

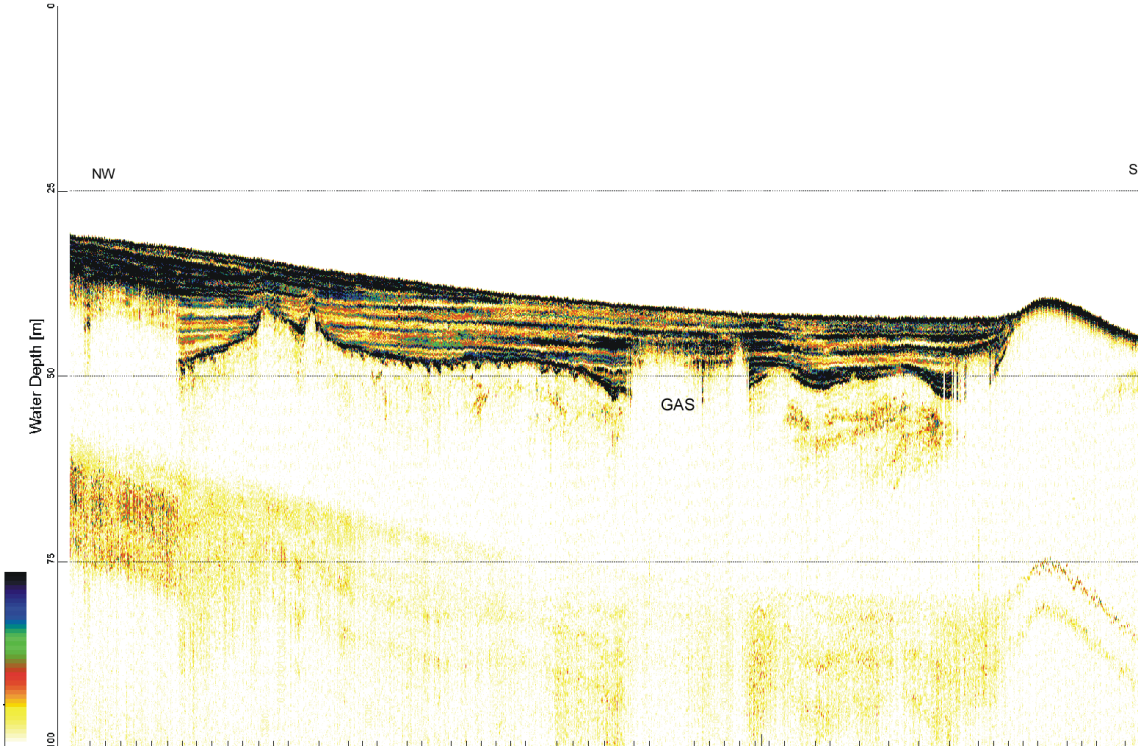


Figure 2 – Parasound record in Amazon submarine delta. Plan-parallel and laterally continuous sub-bottom reflectors overlaying a irregular surface. Trapped gas appears masking the underlying reflectors.

## South Atlantic Ocean

# Salt tectonics, volcanic centers, fracture zones and their relationship with the origin and evolution of the South Atlantic Ocean: geophysical evidence in the Brazilian and West African margins.

*Webster Ueipass Mohriak, Petrobras – E&P – Corp/Exp/TSP*

**Abstract**

Interpretation of regional gravity, magnetic and seismic data of the offshore region from the platform toward the continental-oceanic crustal boundary in ultradeep water regions of the Campos, Santos and the conjugate basins in the Angola margin indicate that the rift architecture along the South Atlantic sedimentary basins is highly controlled by fracture zones and volcanic centers. Both along the Brazilian and West African margins the crustal limit is a tectonic feature of utmost importance for petroleum exploration in deep waters, and the integration of different geophysical tools suggest new models for the early phase of sedimentation along the divergent margins. Basement-involved structural features probably related to extensional tectonics, as well as salt tectonics structures, were previoulsy interpreted to occur only on continental crust. However, analogies with other sedimentary basins and integrated interpretation of the geophsysical data suggest that these features might be interpreted both on continental and oceanic crust. The characterization of fossil volcanic ridges probably associated with early oceanic spreading centers indicate a mechanism of formation of volcanic rifted margins by progressive oceanic spreading center indentation along rifted continental crust. This mechanism, which shows some similarities to the present-day structures observed along the Afar region, is associated with propagators advancing from the southern (Pelotas) towards the northern (Campos) provinces, with right-lateral steps.

**Introduction**

The understanding of rift structrures and salt tectonics in the ultradeep water provinces of the South Atlantic (bathymetries exceeding 2,000 m) constitute one major challenge for regional basin analysis and petroleum exploration (Jackson et al., 2000). In the South Atlantic, pre-salt source rocks and post-salt reservoirs are usually linked by migration pathways related to salt tectonics, and thermal maturation of source rocks is also dependent on the thermal conductivities of salt and overburden strata, sedimentation history, and by heat flow anomalies associated with magmatic activity through time.

Several recent works have analyzed rift and salt tectonics styles in the deep water region of the South Atlantic continental margins, particularly Chang et al., 1992; Souza et al., 1993; Demercian et al., 1993; Fonck et al., 1998; Jackson et al., 1998, Jackson et al., 2000; Mohriak et al., 1999, Marton et al., 2000). This work will focus mainly on the interpretation of regional potential field data (gravity and magnetics) and also on seismic profiles in the southern part of the Eastern Brazilian margin, which will be used as a guideline to interpretation of the tectonic domains and structural styles observed in a regional transect from the platform towards the oceanic crust domain both along the Brazilian and West African margins.

**Geophysical Data: Gravimety and Magnetic Anomalies**

Potential field data (e.g., Geosat) show that the southeastern region of Brazil is characterized by a negative Bouguer anomaly near depocenters in the platform, and by increasing positive anomalies from the shelf towards the deep water region. Volcanic plugs are characterized by linear anomalies that usually follow E-W trends along transform faults and NW trends along possible leaking fractures or shear zones (Souza et al., 1993). The boundary between continental and oceanic crust may be interpreted by modelling the gravity anomalies and comparing with the regional seismic profiles (Bassetto et al., 2000). Major magnetic anomalies also indicate that different basement domains and structures extend from oceanic towards continental crust.

**Geophysical Data: Seismic Interpretation**

Figure 1 (modified from Dias, 1993) schematically shows of the regional distribution of the rift phase sediments in the Eastern Brazilian sedimentary basins.Figure 2 (modified from Schobbenhaus et al., 1984 and Mohriak et al., 2000) shows an alternative interpretation of the tectonic framework of the Southeastern Brazilian margin based on potential field and seismic interpretation of the margin, including the oceanic crust structures in the São Paulo Plateau. Figure 3 (modified from Macedo, 1990 and Gladczenko et al., 1997) shows alternative interpretations of a transect extending

from the onshore region of the Santos Basin towards the crustal limit.

Four tectonic compartments associated with sedimentary basins can be identified along these profiles: 1) the onshore continental domain of the intracratonic Paraná Basin; 2) the offshore (shelf-to-upper-slope) continental domain characterized by crustal thinning and syn-rift phase sediments; (3) the offshore (lower slope to bathyal depths) continental to transitional crust domain characterized by syn-rift sediments, salt tectonics and volcanic wedges associated with seaward-dipping wedges; and (4) the ultradeep water region characterized by compressional salt tectonics, reduced syn-rift sediments, and presence of volcanic wedges associated with seaward-dipping reflectors in the transition to a pure oceanic crust (Cainelli and Mohriak, 1999). The oceanic region is characterized by major features such as the Florianópolis Fracture zone and the Abimael ridge (Figure 2), probably associated with early phases of oceanic crust formaion and spreading (Mohriak et al., 2000), and several other magmatic structures usually observed in pure oceanic crust (e.g., Reston et al., 1999).

**Tectonic Interpretation**

Some similarities in rift structures and tectonics styles are observed in conjugate margins across the South Atlantic when seismic data in the Eastern Brazilian margin are compared with equivalent regional profiles in the West African margin (Jackson et al., 1998; Jackson et al., 2000; Marton et al., 2000; Mohriak et al., 1999). Previous geodynamic models for evaporite deposition in the South Atlantic suggested that syn-rift sediments and salt layers were contemporaneously deposited across the conjugate margins, and the salt basins were subsequently split apart as a consequence of oceanic crust inception and continental drift (e.g., Asmus and Baisch, 1983; Asmus, 1984). The data provided by the regional profiles in the ultradeep water region of conjugate basins indicate that the deposition of Aptian salt post-dates the rift-phase along the Brazilian and West African margin, as suggested by by Fonck et al., 1998 and Marton et al., 2000. The salt distribution is highly asymmetric, with some segments characterized by very wide salt provinces (example, Campos and Santos basins), as a function of preferential emplacement of oceanic ridges along one of the margins (Mohriak et al., 1999; Jackson et al., 2000). The boundary between continental and oceanic crust is characterized by igneous features, particularly intrusive plugs, volcanoes, wedges of seaward-dipping reflectors extruded during inital stages of oceanic crust emplacement, fracture zones, and fossil spreading centers. This interpretation indicate a mechanism of formation of volcanic rifted margins by progressive oceanic spreading center indentation along rifted continental crust, with some similarities to the present-day structures observed along the Afar region, where two branches of oceanic crust formation are associated with propagation of the Red Sea and the Gulf of Aden rifting between Africa and Saudi Arabia (Manighetti et al., 1998). In the South Atlantic this mechanism was probably associated with oceanic ridge propagators advancing from the southern (Pelotas) towards the northern (Campos) provinces, with right-lateral steps.

**References**

Asmus, H.E., 1984. Geologia da margem continental brasileira. In: Schobbenhaus, C., Campos, D.A., Derze, G.R. and Asmus, H.E. (coord.), Geologia do Brasil, Ministério das Minas e Energia/DNPM, Brasília, 1984, p. 443 - 472.

Asmus, H.E. and Baisch, P.R., 1983. Geological evolution of the Brazilian continental margin. Episodes, vol. 1983, n. 4, p. 3 – 9.

Bassetto, M., Alkmin, F.F., Szatmari, P. and Mohriak, W.U., 2000. The oceanic segment of the southern Brazilian margin: morpho-structural domains and their tectonic significance. In: W. U. Mohriak and M. Talwani (eds.), Atlantic rifts and continental margins, AGU Geophysical Monograph 115, p. 235-259.

Cainelli, C. and Mohriak, W.U., 1999. Some remarks on the evolution of sedimentary basins along the Eastern Brazilian continental margin. Episodes, vol. 22, n. 3, p. 206 – 216.

Chang, H. K., Kowsmann, R.O., Figueiredo, A.M.F. and Bender, A., 1992. Tectonics and stratigraphy of the East Brazil Rift system: an overview. Tectonophysics, v. 213, p. 97 - 138.

Demercian, L.S., Szatmari, P., and Cobbold, P.R., 1993. Style and pattern of salt diapirs due to thin-skinned gravitational gliding, Campos and Santos basins, offshore Brazil. Tectonophysics, v. 228, p. 393 - 433.

Dias, J.L., 1993. Evolução da fase rift e a transição rift / drift nas bacias das margens leste e sudeste do Brasil. 3rd International Congress of the Brazilian Geophysical Society, Rio de Janeiro, Expanded Abstracts, vol. 2, p. 1328 - 1332.

Fonck, J.M., Cramez, C. and Jackson, M.P.A., 1998.

Role of subaerial volcanic rocks and major unconformities in the creation of South Atlantic margins. In: M. R. Mello and P.O. Yilmaz (eds.), Extended Abstract Volume, 1998 AAPG International Conference and Exhibition, Rio Janeiro, Brazil, p. 38-39.

Gladczenko, T.P., Hinz, K., Eldholm, O., Meyer, H., Neben, S., and Skogseid, J., 1997. South Atlantic volcanic margins. Journal of the Geological Society of London, vol. 154, p. 465 - 470.

Jackson, M.P.A., Cramez, C., and Mohriak, W.U., 1998. Salt tectonics provinces across the continental – oceanic boundary in the Lower Congo and Campos Basins on the South Atlantic Margins. AAPG Bull., v. 82, p. 1926. In: M. R. Mello and P.O. Yilmaz (eds.), Extended Abstract Volume, 1998 AAPG International Conference and Exhibition, Rio Janeiro, Brazil, p. 40-41.

Jackson, M.P.A., Cramez, C., and Fonck, J.M., 2000. Role of subaerial volcanic rocks and mantle plumes in creation of South Atlantic margins: implications for salt tectonics and source rocks. Marine and Petroleum Geology, v. 17, p. 477 – 498.

Manighetti, I., Tapponnier, P., Gillot, P.Y., Jacques, E., Courtillot, V., Armijo, R., Ruegg, J.C., and King, G., 1998. Propagation of rifting along the Arabia – Somalia plate boundary: into Afar. Journal of Geophysical Research, vol. 103, no. B3, p. 4947-4974.

Macedo, J.M., 1990. . Evolução tectônica da Bacia de Santos e áreas continentais adjacentes. In: G.P.R. Gabaglia and E.J. Milani, Origem e evolução de bacias sedimentares. Petrobrás, Rio de Janeiro, p. 361-376.

Marton, L.G., Tari, G.C., and Lehmann, C.T., 2000. Evolution of the Angolan passive margin, West Africa, with emphasis on post-salt structural styles. In: W. U. Mohriak and M. Talwani (eds.), Atlantic rifts and continental margins, AGU Geophysical Monograph 115, p. 129-149.

Mohriak, W.U., 2000. Arquitetura crustal e geometria do rift no Atlântico Sul: implicações para a interpretação de sistemas petrolíferos na margem leste brasileira e oeste africana. VII Simpósio de Geofísica da Petrobras, Salvador – BA.

Mohriak, W.U., Jackson, M.P.A., and Cramez, C., 1999. Salt tectonics provinces across the continental-oceanic boundary in the Brazilian and West African margins, 6th International Congress of the Brazilian Geophysical Society, CD with Abstracts, SBGf 191.

Mohriak, W.U., Gomes, P.O., e Oliveira, J.A.B., 2000. Análise regional da arquitetura do rifte da Bacia de Santos. Relatório Interno Petrobras –E&P – GEREX/GEDOC – Rio de Janeiro, 41 p. + figs.

Reston, T.J., Ranero, C.R., and Belykh, I., 1999. The structure of Cretaceous oceanic crust of the NW Pacific: constraints on processes at fast spreading centers. Journal of Geophysical Research, vol. 104, n. B1, p. 629-644.

Schobbenhaus, C., Campos, D.A., Derze, G.R., and Asmus, H.E., 1984. Geologia do Brasil. MME / DNPM, Brasilia, 501 p.

Souza, K. G., Fontana, R.L., Mascle, J., Macedo, J.M., Mohriak, W.U. and Hinz, K., 1993. The southern Brazilian margin: an example of a South Atlantic volcanic margin. Third International Congress of the Brazilian Geophysical Society, Rio de Janeiro, RJ, November 7 - 11th, 1993, vol. 2, p. 1336 - 1341.

**Acknowledgments**

I would like to thank PETROBRAS for permission to publish this work. Several explorationists at Petrobras E&P and at Petrobras Research Center are thanked for enlightening discussions, particularly P. O. Gomes, J.A.B. Oliveira, P. Szatmari, O. Paula, and M. Bassetto.

**South Atlantic Ocean**

FIG.1


*Modified from Dias, 1993.*

FIG.2

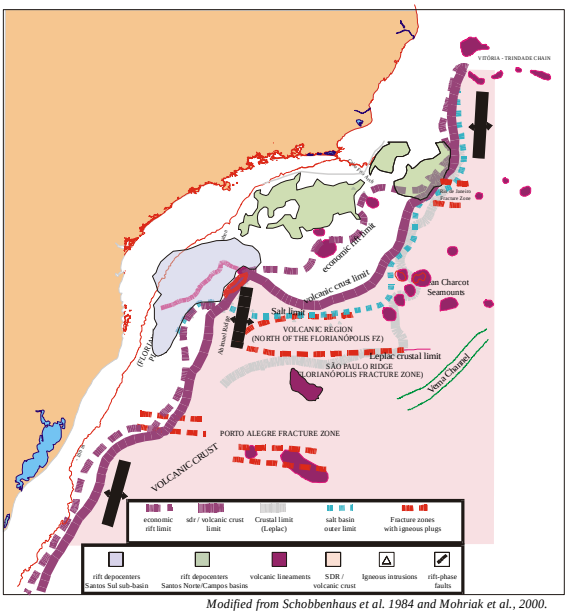


*Modified from Schobbenhaus et al. 1984 and Mohriak et al., 2000.*

FIG.3

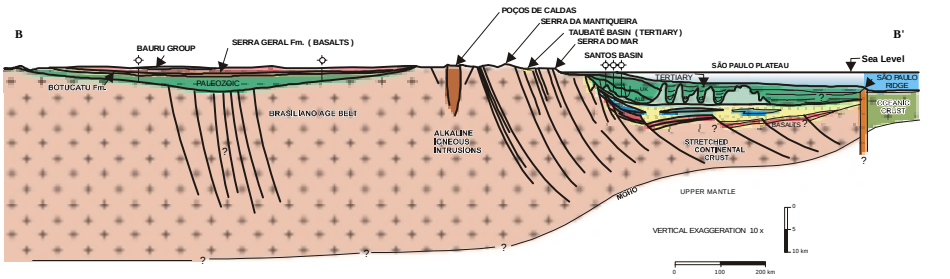


Modified from Macedo, 1990.

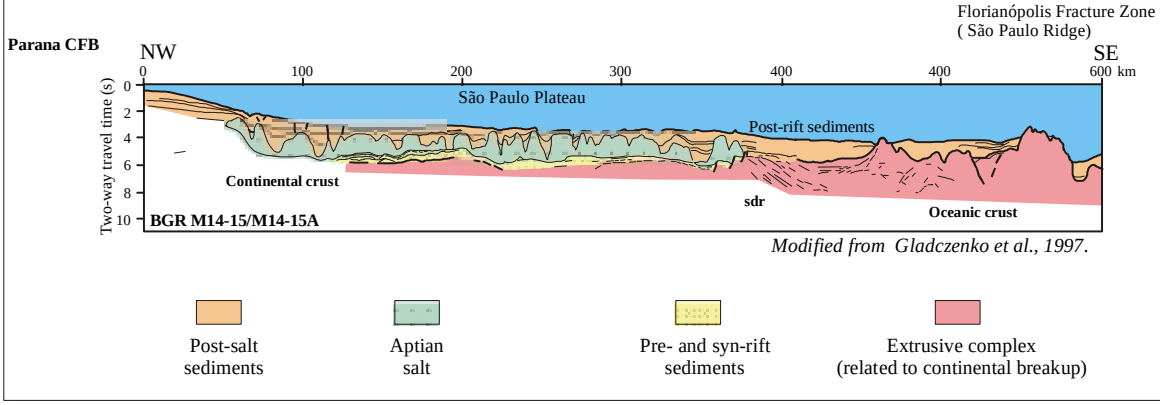


*Modified from Gladczenko et al., 1997.*

web4213

# Seabed Potential Hazards on the Ilha Grande Bay, Rio de Janeiro, Brazil

*Wellington Ceccopieri* [1], *LAGEMAR-UFF*, Brazil; *Gilberto T.M. Dias* [2], *LAGEMAR-UFF*, Brazil; *Marcelo Sperle* [3], *LOG – UERJ*, Brazil; wceccopieri@netscape.net [1]; gilberto@igeo.uff.br [2] ; msperle@gbl.com.br [3]

**Abstract**

Based on a quali-quantitative evaluation of high resolution seismic records, bottom samples and a digital bathymetric map, studies of the seabed on the Ilha Grande Bay were carried out in order to investigate the regional seabed potential hazards to the operational oil and gas industry activities. These hazards were divided into two general environmental risk attributes: structural and sedimentary. In these studies, we observed a juxtaposition of environmental risk attributes at three sites: the area of Estrelas sound, the area between Itapinhocanga and Conceição de Jacareí sounds and the central channel. Close to Estrelas sound evidences of fractures (or faulting) were observed, besides bottom texture transitions and sediments with high porosity, susceptible to great packing at superficial level. Between Itapinhocanga and Conceição de Jacareí sounds, sites of strong topographic slope (greater than 30º) were observed, combined to mobile seabed (subjected to bottom flows around 50 cm/s). The coastal depression between the land and Ilha Grande (central channel), showed large basement outcrops. They reach depths of 23 m, in places where depths are around 40 m. These integrated studies revealed a structurally heterogeneous seabed associated to bottom texture transitions and mobile seabed sedimentary sites.

**Introduction**

Qualitative estimatives of submarine potential risks can be appraised by integrating geophysical, oceanographic and geological information of the seabed (e.g. Baraza *et al.*, 1999). These information are currently used in to geo-technical calculations for submarine structures establishment, and in offshore engineering projects (Lee & Baraza, 1999).
The identification of potential risk sites in high environmental sensibility areas such as Ilha Grande Bay is important to the efficient development of oil and gas sector activities. Particularly, this bay is close to a prospective brazilian sedimentary basin (Santos Basin). Further, there is an oil terminal facility (TEBIG) located in this region, where the inner shelf bottom geomorphology allows large oil tankers approach to the coastal line. These turn the bay into a strategic area for the oil industry. In the study area, the risks were qualitatively defined in two basic attribute types: the structural ones and the sedimentary ones. These attributes were verified based on high-resolution seismic records (sub-bottom profiler 7.0 kHz and side scan sonar 100 kHz), besides bottom samples collected with van-Veen grab sampler. A digital bathymetric map, and the results obtained in previous studies of ecofacies and the observed bedforms (Ceccopieri, *in prep.*) where also used. Moreover, some physical properties of the sediments were investigated, as an additional sedimentary risk attribute.

**Potential Risk Attributes**

**Structural**
Structural risk is related to several features of the seabed: basement outcrops, islands, old marine terraces, the coastal depression between the land and Ilha Grande (central channel). Besides, there are the troughs of paleo-channels and dredged channels, on the eastward side of the bay, that are used to access TEBIG (the oil terminal) and the Sepetiba Port. All of these features define strong topographic slopes (greater than 30º). They are real obstacles to the establishment of submarine structures, and also may represent unstable areas of the sedimentary layer prone to mass movements. Further, the seismic record analysis showed several rocky outcrops, combined to alignments of possible faults and fractures of the area, associated to depressed and uplifted blocks. The alignments and fractures are predominantly oriented in the NE-SW direction (N50-70E) and, secondarily, in the NW-SE direction. According to Natrontec (1998), since the Jurassic the region has been subjected to tectonic events, due to old fault zones reactivation and the installation of new ones. This neotectonism has been observed mainly in the Monsuaba´s area. Then, the structural characteristic of the bay can be observed by the orientation of the islands and the rivers of the Ilha Grande, and by the submerged paleo-channels. They are related to a past drainage of this region during sea level low-stands (Mahiques, 1987).

**Sedimentary**
Previous studies concerning to the Ilha Grande Bay ecofacies and bedforms (Ceccopieri, *in prep.*) identified two sedimentary risk attributes: bottom texture transitions and mobile sea-bottom. Evidences of modern sediment transitions from facies dominated by higher energy agents (waves) to facies dominated by lower energy agents (tides, bottom currents) were observed. They were related to the complex subma-

rine topography and to the coast line orientation. The analysis of bedform parameters suggested that the combined effects of currents and waves exist in these areas. Among the bedforms observed, mega ripples were dominant in depths around 15 to 17 m, mainly close to Conceição de Jacareí sound. In this site, occurs a westward-to-eastward transition from fine ecofacies to the thick ones. Based on these features, bottom flows were estimated and a gradation in the magnitude of the same ones was observed. The flows close to the bottom might vary between 35 to 60 cm/s, randomly reaching 80 cm/s, turning the bottom mobile. These transition areas reflected sites of variable energy. The mobile bottom can cause erosion, displacements and burials of the structures, implying in loads not forecasted. Even so, certain sediment properties that compose the different bottom types, can attenuate or increase these undesirable situations. Then, these properties should be considered to access the sedimentary risk potential in the study area.

Sediment Physical Properties

This study of the superficial sediments (~10 cm) was based on the analyses of five bottom samples, considering their bulk density, water content and porosity. These properties were obtained by the difference among humid and dry weights of these samples. These samples were selected in addition to 153 ones that were collected in a previous study by Mahiques (1987). Sample 1 is a terrigenous sandy mud. Samples 2 and 5 are a terrigenous mud. Samples 3 and 4 are, respectively, a sandy mud (rich on bio-clastics content) and a muddy sand.

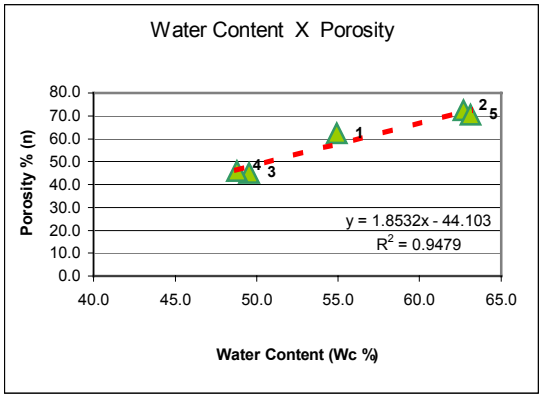


Figure 1 - Linear correlation between porosity and water content of the Ilha Grande Bay bottom samples.

Sediments with high porosities (~60%), are susceptible to great packing capacity. They represent a potential risk to the submarine structure installation that may sink in the porous bottom, associated to the high values of water content. These attributes also generate buoyancy problems, by causing the structure to be unstable over the substratum. In these analyzed bottom samples, the water content, the bulk density and the porosity showed a normal behavior. Porosity and water content had a direct linear correlation (fig.1), and an inverse relation with bulk density (fig.2). Therefore, sites 1, 2 and 5 would be unstable, at least in a superficial level of the bottom. The samples with relative larger bio-debris and sand content (samples 3 and 4) showed the smallest porosities. It is related to the relative poorly sorting of its sedimentary matrix. This characteristic also define a relatively larger density for these bottom types and a smaller packing capacity in these sites, in a superficial level of the seabed.

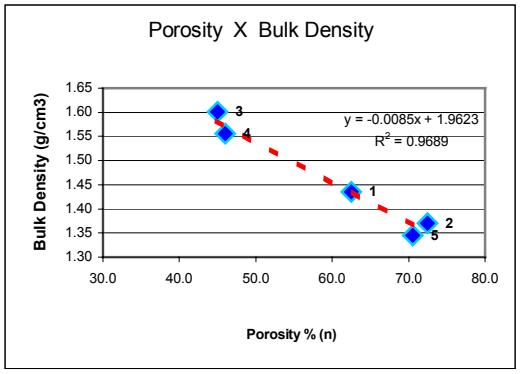


Figure 2 - Linear correlation between porosity and the bulk density of the Ilha Grande Bay bottom samples.

## Conclusions

As a result of the accomplished studies, it can be traced at least three sites in the study area that deserve attention, in case the area comes to be used for pipelining, and even for engineering works. It was observed some sites where a juxtaposition of some risk attributes occurred. It can be observed that there are basement outcrop alignments, transitional bottom textures and highly porous sediment in the surroundings of Estrelas sound. Between Itapinhocanga and Conceição de Jacareí sounds, it was observed mobile seabed combined to transitional textures. In the central channel the rocky outcrops and the greater slopes

are prominent obstacles. This approach recognized important bottom features of the seabed. It was a contribution to studies of environmental impact and risk analyses, aiding the environmental and territorial management of Ilha Grande Bay.

## References


Baraza, J.; Ercilla, G. & Nelson, C.H. (1999) "Po tential geological hazards on the eastern Gulf of Cadiz slope, SW Spain" *Marine Geology.*, 155, 191-215 pp.

Ceccopieri, W. (*in prep.*) "Estudos integrados do fundo marinho da Baía da Ilha Grande, RJ" **MSc thesis**. Laboratório de Geologia Marinha, LAGE-MAR, Universidade Federal Fluminense.

Lee, H. & Baraza, J. (1999) "Geotechnical character istics and slope stability in the Gulf of Cadiz" *Marine Geology.*, 155, 173-190 pp.

Mahiques, M.M. (1987) "Considerações sobre os sedimentos de superfície de fundo da Baía da Ilha Grande, Estado do Rio de Janeiro" **MSc thesis**. Instituto Oceanográfico da Universidade de São Paulo, vol 1 e 2.

Natrontec - estudos de engenharia de processos ltda. (1998). Relatório de Impacto Ambiental (RIMA) da Usina de Angra II - relatório técnico. 379 p.


## Acknowledgments


We would like to thank the National Petroleum Agency (ANP) Program of Human Resources (PRH-ANP/MME/MCT) for financial support. Also we are grateful to Marine Geology Laboratory (LAGEMAR – UFF) and to Geological Oceanography Laboratory (LOG – UERJ) for material support. We are also grateful to the colleagues Cleverson Guizan Silva, Arthur Ayres Neto, José Antônio Baptista Neto and Sidney Luiz de Matos Mello for useful discussions during the course of this work.


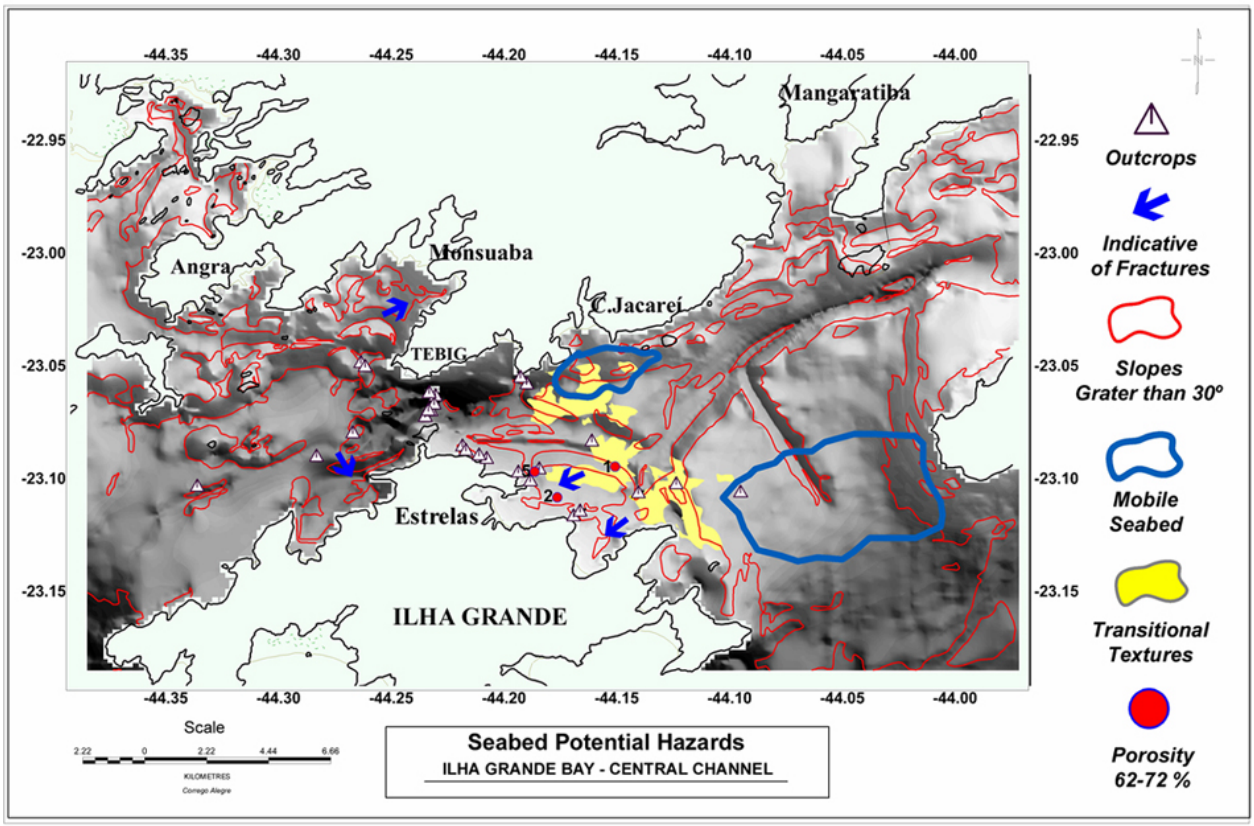


Figure 3 - Potential Risks Attributes of the Ilha Grande Bay seabed, Rio de Janeiro, Brazil.

# Sonar Characterization of Modern Subaqueous Mass-Movement Deposits Bordering the Brazilian Continental Slope.

*Luis Claudio Ribeiro Machado, PETROBRAS S/A, Brazil*

## 1- Introduction

Diamicts are very badly sorted siliciclastic sediments or rocks (Flint, 1961) and are the main product of mass movements, especially debris flow. Diamicts, which are deposited by debris flow, form tongue-shaped bodies. In the marine realm beyond 200m deep, particularly at the continental slope, the predominant sediment is mud. This mud is the source sediment for mass movement deposits that cover the sea bottom of the Brazilian offshore margin at the foot of the continental slope, roughly between 2000m and 2500m of water depth (Fig.1-A). This study of mass movement deposits is based on a very comprehensive geological and geophysical database of the Campos Basin at these water depths. Its philosophy is being successfully extended to the Brazilian offshore basins which have a steeper upper continental slope.

Because of the nature of the source rock (slope mud) these diamicts are muddy: a matrix of disintegrated mud involving mud clasts (Fig. 1-B) which vary in size from pebble to coarse slab (megagravel).

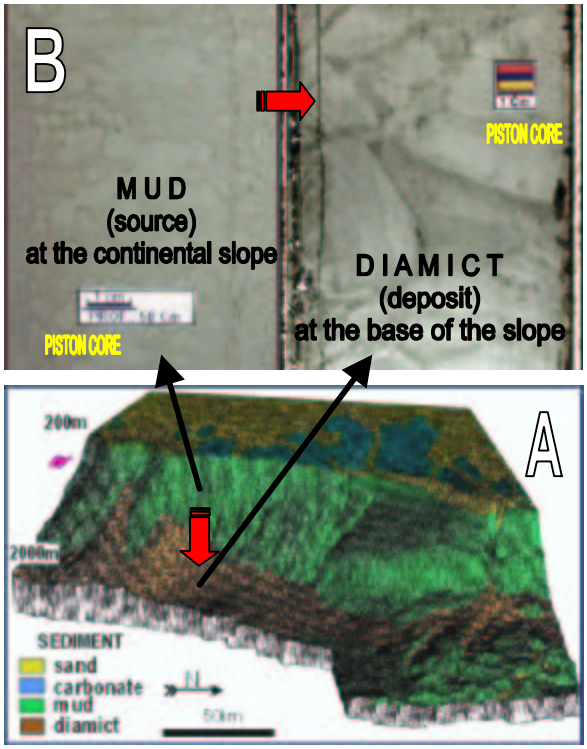


***FIGURE 1 - A- Continental shelf, slope and São Paulo Plateau. Mud (green) falls along slope originating debris flows that deposit diamicts (brown) at the foot of the slope. B- Samples (piston cores) from Magalhães et al. (2000).***

Diamict tongues are now widely recognized at the sea bottom due to regional surveys using side-scan sonar and swath bathymetry, Sub-Bottom Profiler (2D seismic of 3,5 kHz) and piston cores. Regional side-scan sonar surveys both in the USA East Coast (USGS' EEZ Survey) and in the Campos Basin in Brazil (Petrobras' Procap-2000) have displayed the pervasiveness of the giant offshore mass movement deposits bordering the continental slope of these Western Atlantic continental margins.

In the Campos Basin the presence of a carbonatic outer continental shelf since the Paleocene is indicative of an earlier existence of the physiography of steep continental slope. It is believed that the eodiagenetically cemented carbonate bioherms (coral and red algae) at the outer continental shelf builds a stiff wall that keeps the steepness of the continental slope. A muddy steep upper slope is the main reason for the existence of mass movement deposits at its base. The presence of a widespread debris apron bordering almost the entire Brazilian continental slope northward of the 24° latitude seems irrefutable now.

## 2- Sonar Record and Diamicts

Side-scan sonar is an acoustic geophysical tool which provides a cheap regional big picture of the area. Sonar intensity of the backscatter provides soil grain size information and reveals subtle depositional features and sedimentary geometries. Soil grain size is key in side-scan sonar interpretation. Backscatter is proportional to the soil roughness and acoustic impedance contrast between water and soil. Smooth surface like fine sand normally reflects forward and absorbs almost all the signal and nearly nothing comes back to the fish to be recorded. Irregular soil reflects backwards considerable fraction of the sound waves, producing intense sonar records.

The main type of mass movement at the foot of the slope is debris flow. Debris flows are dominated by jellified behavior of the matrix, have a basal shear zone, mainly responsible for the movement, and the top usually is a rigid plug, which travels at the piggy-back of the flow (Middleton & Hampton, 1973). During the flow evolution, the biggest clasts are expelled towards the top of the flow by grain collision, hindered settling and dispersive pressure, producing a rough inverse grading. The top of the resultant deposit is a diamict populated by a miryad of large

protudent clasts. In a subaereal mass movement deposit it is possible to see the protudent clasts (figure 2), mainly in the boulder/cobble granulometric class.

Clast size is key in mass movement sonar identification. The gravel (granule/pebble/boulder/cobble) granulometric class showed in Fig. 2 is one of the roughest soils that can be found in marine basins and usually produces the highest soil backscatter of the entire sonar survey. This high backscatter is due to the high roughness, providing the clast size is inferior to the pixel of the sonar.

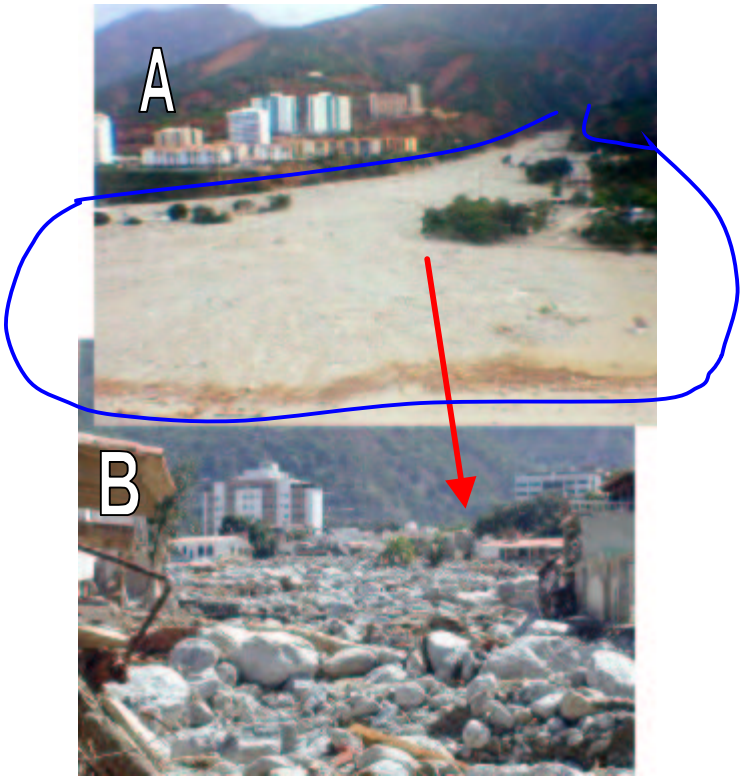


*FIGURE 2 - Mass Movements occurred in December of 1999 in La Guaira (near Caracas, Venezuela). A- The blue line sketches the shape of the diamict tongue. Flow lines are noticeable. B- Protudent clasts of gravel size. Photos' author unknown.*

Each pixel is a unique mean value of the roughness and acoustic impedance contrast of all the soil contented in its limits.

The pixel size of most sonar records used by the marine geology team at Petrobras is around 5m x 5m (precisely 6.5x6.5m). The granulometric class of gravel (grain size from 0.002 up to 4.1m - Blair & McPherson, 1999) is smaller than this pixel size. Gravel is a very common coarse grained sediment while megagravel (grain size from 4.1m up to 1075km) is not. Examining these numbers, we see that megagravel generally is bigger than the size of the pixel of the sonar which means that this tool is capable of resolving individual grains. The resultant sonar texture over a megagravel deposit is variegated, with patches and spots, like a leopard skin.

Diamict tongues of gravel size are interpreted as deposits of highly-disintegrative debris flows (Fig.4) while of megagravel size are considered of the less-disintegrative ones (Fig 6.).

### 3- Diamict Tongues

The diamict tongues typically display the elliptical contour of a tongue, whose length generally doubles the size of its width. Most of them have giant dimensions, some 10 x 20 km, eventually reaching 15 x 30 km or more (Fig. 3).

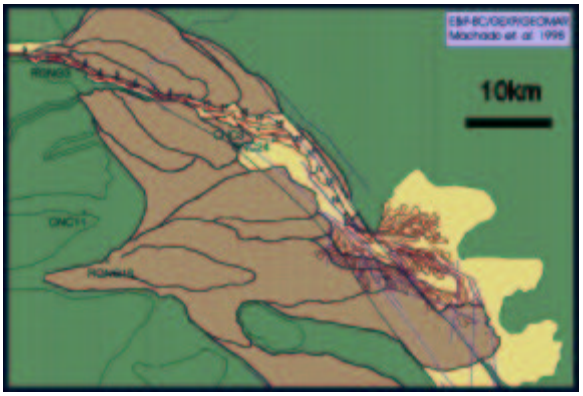


*FIGURE 3 - Continental slope-related diamict tongues (in brown) with giant dimensions. Their overlapping forms the debris apron shown in Fig. 1. The slope and its canyons are to the left, in green.*

The tongues stack up with enough lateral superposition to produce a unique, big, stripe of debris apron around the slope, as shown in Fig. 1.

In deepwater areas like the São Paulo Plateau, it is common to find abrupt elevations around 150m in height. These elevations, generally salt tectonic driven, have also debris aprons at their foot. In this case the size of the debris apron is proportional to the contrast in relief: they are not more than 1km in length (in the downslope direction).

### 4- Highly-Disintegrative Debris Flows Deposits

The main signature of these tongues is the overall homogeneous surficial texture, of very high backscatter intensity. Once the diamict tongue is a giant feature, its side-scan signature is characterized as giant areas of high backscatter intensity. Generally it is the highest value of all the survey. It is just the roughest soil that is contained into this pixel size.

This typical texture is showed in the non-painted area at the bottom of figure 6-B (painted at Fig. 4C).

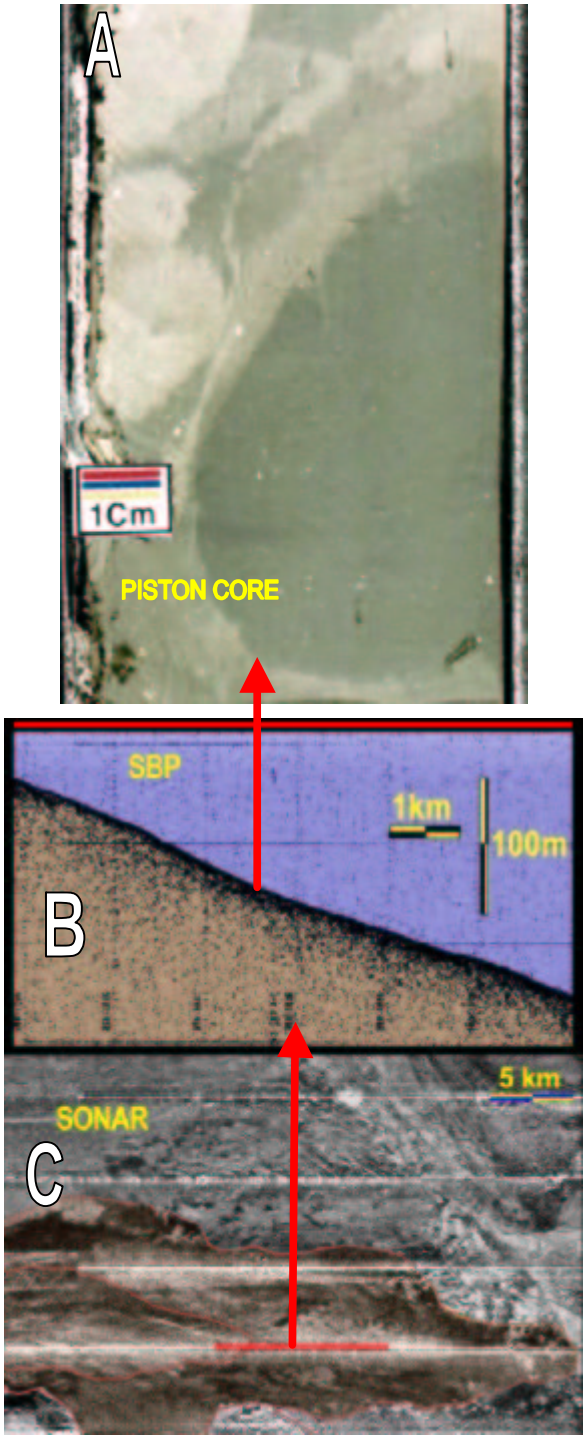


*FIGURE 4 - Highly-Disintegrative Debris Flow Deposits.*

In the areal geometry aspect, the elliptical-like typical tongue outline is outstanding, usually with very well defined and smooth-traced borders and with strong backscatter contrast to the surrounding environment. Sometimes transversal pressure ridges near the outer edge are evident. Often lines of the radial spreading of the flow are present. Sometimes these lines are straight and very long (Fig. 5). They are thought to be furrows produced by the ploughing of big outrunner clasts, which slide over the entire tongue in different velocity or timming.

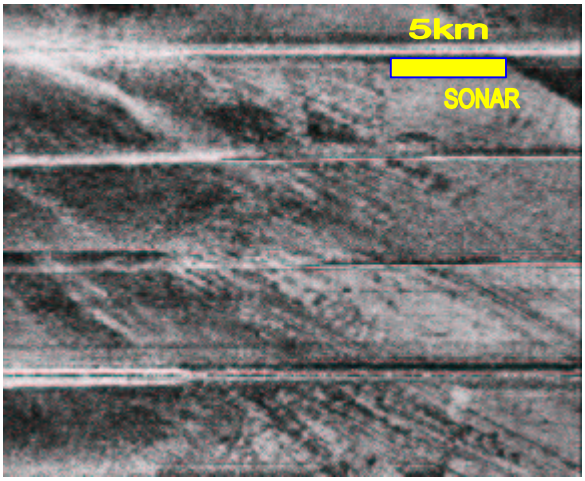


*FIGURE 5 - Furrows produced by outrunner clasts over a diamict tongue.*

In a quick processing with incorrect radiometric (intensity) compensation, this strongest signal decays intensely and steadily towards the nadir of the fish, producing a feature that resembles a negative photograph of a steel-tube (bottom of Fig. 6-B and upper left of Fig. 5). The artifact allows the immediate identification of muddy diamicts resulting from highly-disintegrative debris flows.

### 5-Less-Disintegrative Debris Flow Deposits

The soil of the slope, which collapses to give origin to the debris flows, is stratified: stratified mud and eventually some diagenetically hardened carbonate of the outer shelf. During the disintegration process of the debris flow (comminuition) these sediments are bound to produce oblate clasts, respecting the anisotropy of the stratified material. During the debris flow these oblate clasts, particularly the big ones, tend to travel in a horizontal position like a surfboard. That is also the position they are prone to rest at the top of the diamict in the end of the process. It is a slab of the slope which was transported to deep water. Once the pixel size (~5m) is smaller than the clast, many pixels would rest over the horizontal surface of the oblate horizontal clast, giving the backscatter of the horizontal mud, and the clast will be easily individualized by the sonar, creating the mentioned big patches at the record.

Megagravel horizontal oblate clasts often appear equidimensional in areal view, and somehow they are roughly equally distributed over the top of the mass movement, covering the entire tongue of diamict. This gives a sonar signature which is like a leopard skin (Fig. 6D). Many of these clasts reach diameters as big as 300m (olistostromes).

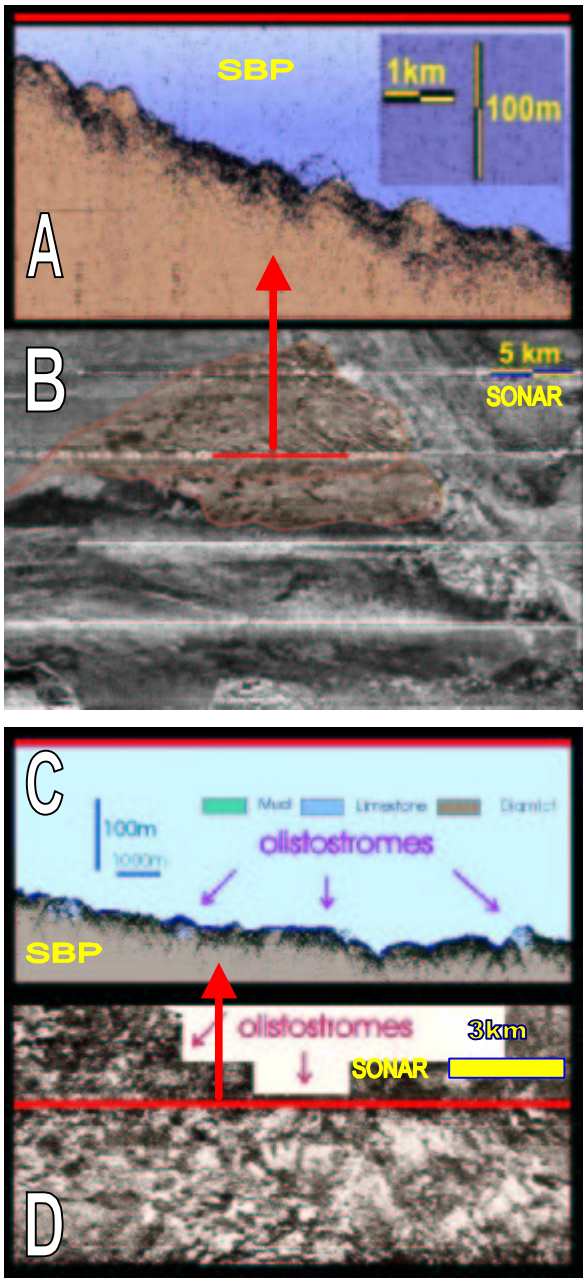


***FIGURE 6 - Less Disintegrative Debris Flow Deposits. Both in Sonar and SBP the huge protudent clasts (megagravel - olistostromes) are evident.***

Considering the abundance of carbonates in the outer shelf near the shelfbreak, it would not surprising to find that many of the megagravel clasts found over some tongues in water depths around 2500m could be olistostromes or olistolists, of carbonate composition. The eodiagenetic early cementation of the carbonates could help to explain why such big clasts travel such large distances (over 50km) without disintegrating. However, these features, which are abundant on sonar and SBP records, are yet to be sampled to test this hypothesis.

## 6- Conclusions

The East Brazilian continental margin is frequently dominated by carbonate-rich outer shelves and a siliciclastic muddy slopes. Since the outer shelf is partially cemented it holds the topography and the continental slope is steep. This steep muddy slope is a fabric of mass movements, producing an extensive debris apron at its foot. The debris apron is composed of stacked and overlapped huge muddy diamict tongues with dimensions around 10x20km.

Two types of debris flow deposits (diamict tongues) are recognized: highly-disintegrative and less-disintegrative. Sonar signature of the less-disintegrative debris flow deposits is variegated, like a leopard skin. The pixel of the sonar record, some 5 x 5m, is smaller than the megagravel clasts at the top of the diamict tongue. Some clasts are more than 300m in diameter, and could be olistostromes.

Smooth and very strong backscatter signature of the highly disintegrative debris flow deposits is produced when clast size (gravel) is smaller than the pixel of the sonar record. Many clasts are contained into a unique pixel. In this case the soil is the roughest one for the sonar sensor and consequently produces strong intensity of sonar recorded. This strong backscatter easily identifies this diamict from the other sediments of the basin.

## 7- References

BLAIR, T.C. & McPHERSON, J.C. - 1999 - Grain-size and textural classification of coarse sedimentary particles. Tulsa, **Journal of Sedimentary Research, 69 (1):** 6-19.

FLINT, - 1961 - Diamictite, a substitutive term for Symmictite. Tulsa, **Am. Assoc. Petrol. Geol. Bull.**

MAGALHÃES, J.L.C.; ANDRADE, S.B.; VOELCKER, H.E. - 2000 - **Piston Cores Descriptions.** Macaé, PETROBRAS/E&P-BC/GEXP/GELAB (Diverse Internal Reports).

MIDDLETON, G.V. & HAMPTON, M. - 1973 - Sediment gravity flows: mechanics of flow and deposition. In: MIDDLETON, G.V. & BOUMA, A.H. - **Turbidites and Deep-Water Sedimentation.** Anaheim, CA, Pacific Section of SEPM Short Course, p.1-38.

# Surface geological mapping using 3D seismic attributes as an aid to subsurface geology understanding: An example

*Fernando Barbosa da Silva, Petrobras/UN-Rio/Atex/Abig-PL, fernandobs@petrobras.com.br*
*José Joaquim Gonçalves Rodrigues , Petrobras/UN-Rio/Atex/Abig-PL, josejoaquim@petrobras.com.br*

**Abstract**

This article is an example on how to approach a new marine seismic 3d dataset and get a fast understanding of the surface geological behavior, which leads to an easier process of building a subsurface geological interpretation.

**. Introduction**

Present days deep water 3d are being collected as a normal procedure in the petroleum exploration routine. The surface geology can be easily understood highlighting the subsurface interpretation model by performing some easy to do tasks on the sea bottom reflection. This is the modern equivalent of surface geological mapping and is possible to be done under water tables of more than 1000 meters. The simple mapping of the time horizon plus the maximum amplitude and dip attribute extraction will give the interpreter a welcome insight of the geological framework. The joint analysis of these maps linked to seismic data inspection will be normally enough to build this interpretation.

**. Example**

The following maps were obtained from a recently acquired deepwater Brazilian offshore data. It has almost 50 km in the transverse direction and less than 3000 $km^2$. Figure 1 is the time topographic map, figure 2 is the dip attribute map and figure 3 the maximum positive amplitude map. All 3 maps are from the sea bottom. Figure 4 is a seismic section obtained at the position shown by a yellow line at figure 2. A quick look at the figures will pop up the geological picture of the sea bottom.

The first feature we want to emphasize is the exact locations were faults outcrop at the sea bottom. It is not easily detected on the sections as can be seen at figure 4, but are well shown at the dip attribute map, as weak amplitudes. They also appear as weak amplitude trends on the amplitude map. The small circles that appear on both amplitude and dip attribute maps are collapse structures. Figure 4 shows a sequence of interpreted features. From left to right : 1-Local fault expression; 2-Slope edge line; 3-Collapse structure; 4-Collapse structure associated to a deep normal fault. Also remarkable are the 3 fault complex trends: A northwestern aligned, on the SW corner of the map; a NE trend at the right and a transverse direction fault system related to the slope edge, around T6600. The first and second fault systems are salt related structures. Their sea bottom expression is an indication of the importance of salt tectonics on present days. The amplitude map can be used to lithology prediction. Stronger amplitudes are usually related to carbonate bottoms and weak amplitudes to shaly sediments. Sand filled sediments will show an intermediate amplitude behavior. In this case amplitudes don't change very much and are probably associated to a shaly bottom. They also show acquisition and processing footprints: In the L (line) direction the observed variations are probably related to source energy changes and cable feathering. The 12 T (trace) direction regular spaced amplitude marked lines are probably related to artifacts derived from the blocked seismic data migration. Stronger amplitudes regions can be also related to concave surfaces which are known to focus the energy at the recording surface.

**. Conclusions**

There are still other attributes that can be extracted from this data, including the pre-stack (AVO) related ones. There is still a lot of information not mentioned here that can be enounced. The point is the way this kind of procedure may help the interpretation of a given area. One must keep in mind that this will only be feasible on good seismic data quality areas.

**. Acknowledgements**

We thanks Luiz Antônio Pierantoni Gambôa for previous discussions on the methodology and Petrobras to allow this presentation.

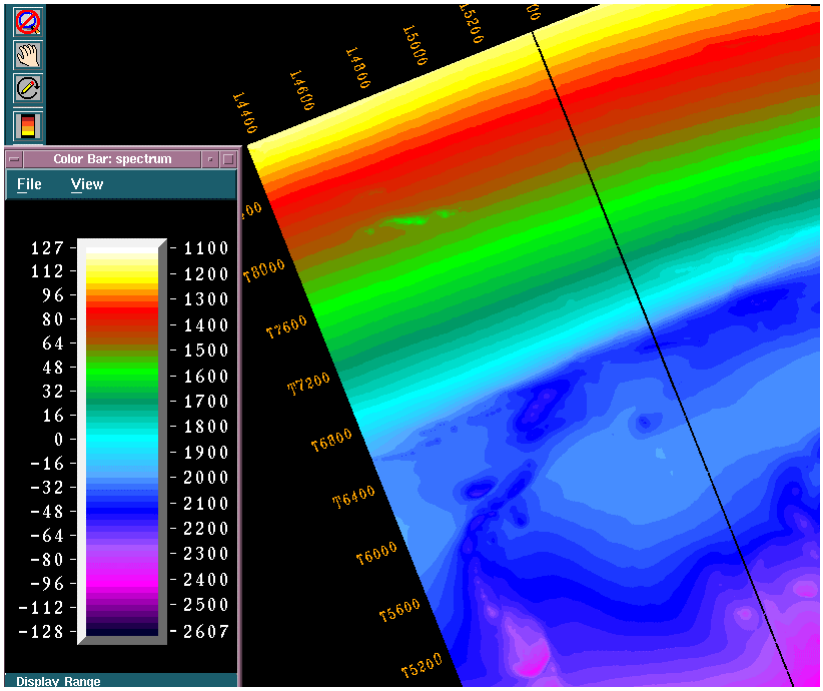


Figure 1- Topographic map (2 way traveltime, milliseconds)

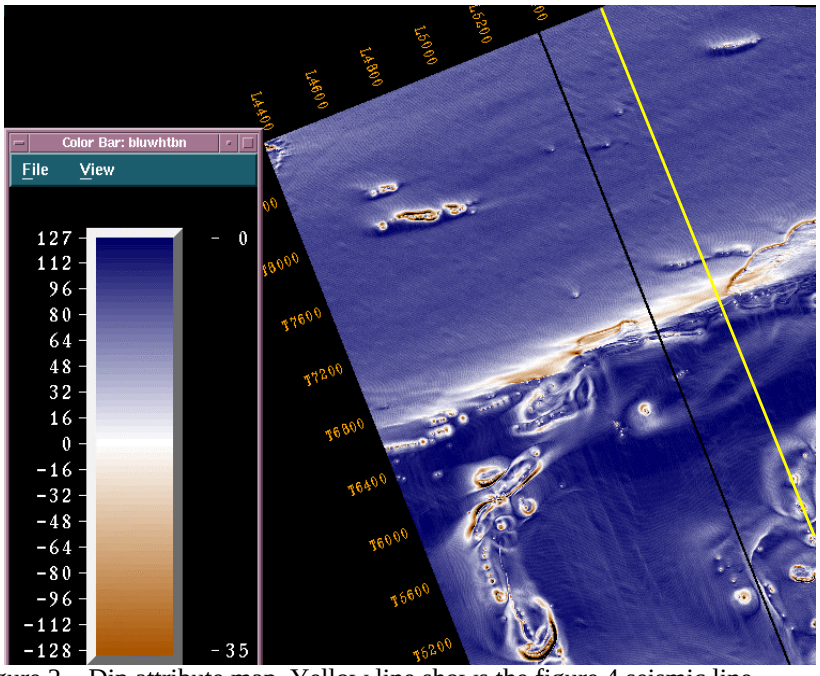


Figure 2 – Dip attribute map. Yellow line shows the figure 4 seismic line

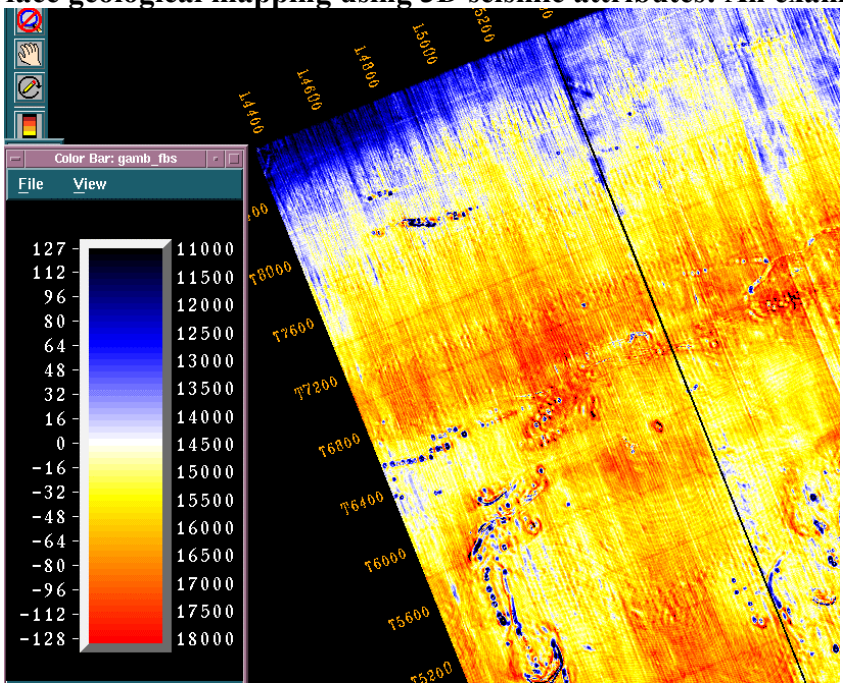


Figure 3 – Amplitude map

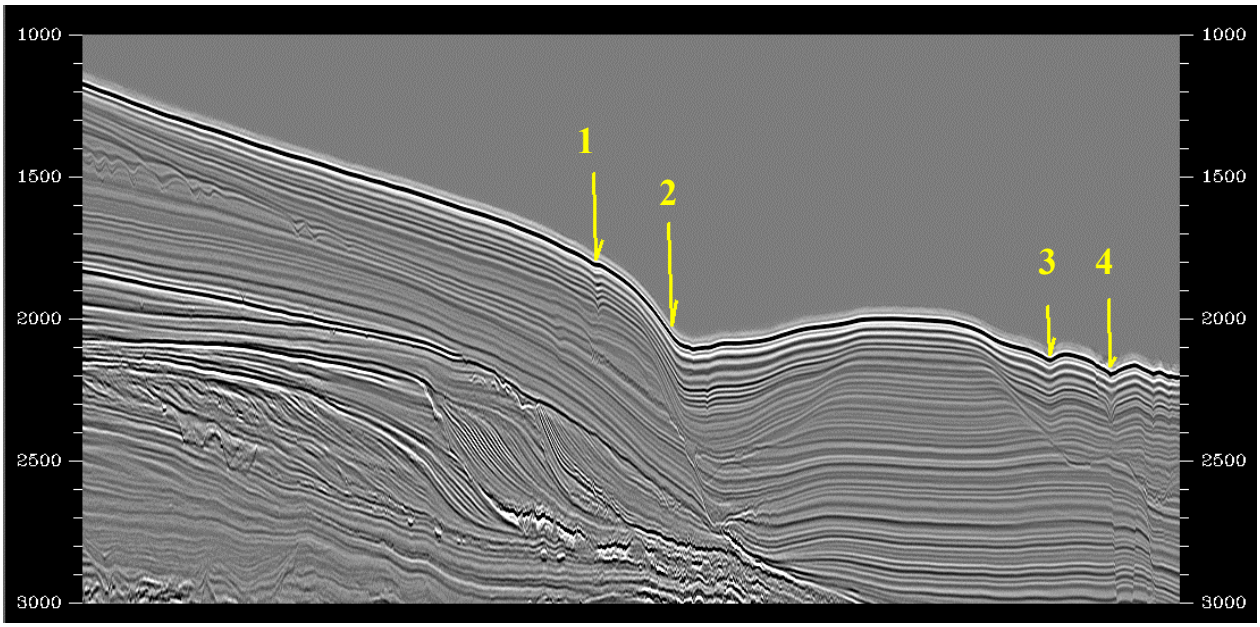


Figure 4 – Seismic section

# Synthesis on the Tectonics and Geochemistry of the St. Paul Transform Fault, Equatorial Atlantic

*[1]SICHEL, S.E.; [2]MAIA, M; [3]ESPERANÇA, S; [4]HEKINIAN, R.; [2]JUTEAU , T.; [1]CARNEIRO, LM.; and [1]ALVES, E. C*
*[1]Dept.Geologia, UFF, Niterói, Brazil, susanna@igeo.uff.br [2]CNRS/UMR 6538, marcia@univ-brest.fr, Plouzané, France, [3]Dept. of Geology, U. of Maryland, College Park, MD 20742, USA; [4]IFREMER, Centre de Brest, 29280, Plouzané, France*

**Abstract**

The tectonic evolution through time of the Saint Paul's Fracture Zone System (SPFZ) was determined based on the analyses of free air anomalies, predicted bathymetry, magnetic isochrons, as well as data from 13 deep submersible dives. The SPFZ is located at 1°N on the MAR and represents one of the largest discontinuities, which offsets the MAR axis roughly 600 km. The relative age difference between the opposite sides of the transform fault is about 36 Ma.

The evolution through time show that in the inactive segment of SPFZ changes its configuration from a triple FZ in the transform fault to a double FZ and can be traced up to the continental shelf break in Brazil. A fossil spreading segment is observed at 33°W. Towards the west (37°50W, 60Ma), the SPFZ is cut by a N25°W structure, and at 40°W (80Ma) by the North Brazilian Ridge (NBR).

Evidence from analysis of the ridge axis morphology, petrology of both basalts and uplifted abyssal peridotites, high ultramafic/volcanic ratio, osmium isotope composition, plate kinematics, and mantle tomography suggest that the mantle surrounding the SPFZ is cooler than other areas in the Atlantic Ocean. Re-depleted model ages ranging from 0.56 to 1.1 Ga for peridotites samples indicate that the lithosphere entrained in this part of the oceanic mantle could have formed in the Pan-African-Brazilian orogeny. Chemical and physical tools support the hypothesis that parts of the mantle in the Equatorial Atlantic preserve an older, subducted slab formed in a collision event period prior to 460 Ma.

**Introduction**

Several studies (e.g., Gorini, 1977, Bonatti et. al 1993, Bonatti, 1990; Bonatti, and Honnorez, 1976; Schilling et al 1995) allowed to characterize different tectonic and magmatic aspect on the Atlantic Equatorial region. More recently submersible dives (Hekinian et al, 2000; Sichel at al, 2000), Os isotopic analysis (Esperança et al., 1999), mantle tomography and plate kinematics (Maia et al., 2001) provide arguments on the origin of the mantle underlying this region. This paper syntheses all information of a multiyear project CAPES/COFECUB (LAGEMAR – UBO and IFREMER).

**Results**

The Equatorial Atlantic contains the highest concentration of closely spaced fracture zones recognized in the world's oceans. One of these major structural discontinuities is the St-Paul's Fracture Zone (SPFZ) located between 1°N-30°20'W and 0°30'N-24°W. The distribution of Free–air gravity altimetric data shows that the SPFZ cuts the entire Atlantic Ocean, from the Amazon basin in Brazil through the coast of Liberia in Africa (Haxby, 1987; Sandwell and Smith, 1997) (Figure 1a). The SPFZ is a multiple fracture zone system (Gorini, 1977). The St.Paul transform fault is a triple fracture zone interrupted by four Intra-Transform Ridges (ITR) spreading centers (Figure 1b). The northern portion of the SPFZ has two inter ridge segments. The St. Peter-St. Paul massif (SPSPM) was a small ridge segment discontinuity where spreading ceased during mantle uplift. The ITR display rift valleys showing recent volcanic and tectonic activities at depths of 4700m. These rift valleys are less than 2 km wide and about 20km long, and exhibit a general N-S strike orientation. Five dives took place in the southernmost inter ridge segment and their adjacent walls. In the East wall, there is evidence of recent volcanic (e.g., glassy flow surfaces) and tectonic activity is observed from the N-S oriented fissures. There is abundant cover of pelagic sediment in the ITR. A complete geological section from 4500m to 1850m was done based on submersibles dives (Hekinian et al., 2000) (Figure 1c). Several dikes that are 2-4m thick cut the section. Peridotites associated with basalt flows and dikes were also observed near the 3970-4000m depth.

Significant tectonic movement allowed the exposure of abundant abyssal peridotites; some of them exposed in the islets of St. Peter and St. Paul. The SPSPM massif consists of a sigmoid ridge divided by an E-W trending fault into two domains: A) N Ridge - strongly tectonized fault scarps composed of foliated mylonitized peridotite with sporadic gabbroic intrusions at depths of 3900 - 2500m, with several thin outcrops of basalt (2700 - 1700m); B) S Ridge – undeformed spinel lherzolite (2000 - 1400m). The active E-W fault that divides the two ridges consists of basalts and dolerites (Figure

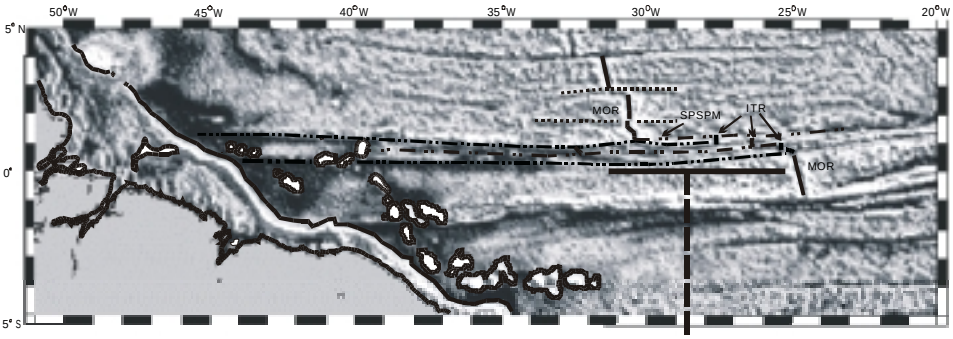


1a. Free - Air Gravity anomaly map showing the St. Paul Fracture Zone System.

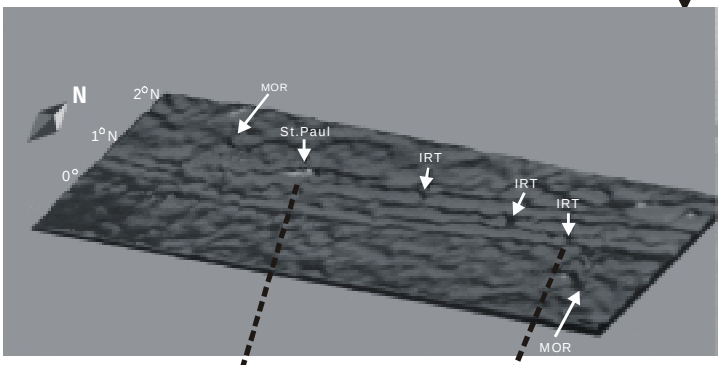


1b. Close up of St. Paul Transform. Note three inter-ridge transform and the St. Peter St. Paul Massive.

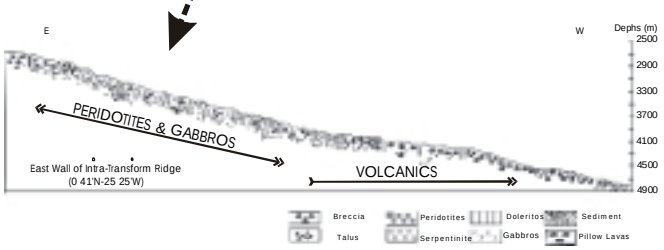


1c. Eastern wall of their transform accretion zone. Geological section based on two submerrsible dives.

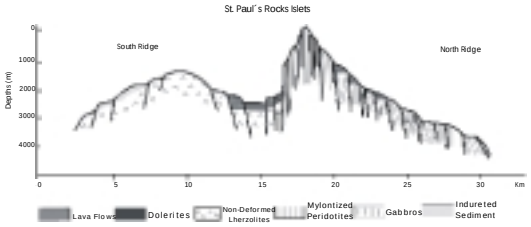


1d. Geological section from St. Peter St. Paul Massive, inferred from seven deep dives (NAUTILE)

1d). These informations are inferred from observations of seven deep dives (NAUTILE)

Immediately out of the transform section, the SPFZ changes from a triple to a double FZ. A fossil inter ridge spreading segment is observed at longitude 33°W. Towards the west, at 37°50W (60 Ma), the SPFZ is cut by a N25°W structure, and at 40°W (80 Ma) it is cut again by the North Brazilian Ridge (NBR) Carneiro, 2000) (Figure 1a). Detailed work on the SPFZ structure near the Brazilian continental margin is shown in this volume (Perales et. al., 2001in this Volume).

The existence of cold, depleted upper mantle beneath the equatorial Mid-Atlantic Ridge (MAR) was inferred from the ridge axis morphology, petrology of both basalts and uplifted abyssal peridotites, Re and Os concentrations, and Os isotopic compositions. Preliminary results suggest a Re-depletion Os model age of 560 Ma to 1.1Ga for some subchondritic samples (Esperança et al., 1999). These data show a good correlation between $^{187}Os/^{188}Os$ and Pt/Os that is consistent with a mantle source that preserved chemical characteristics of an older depletion event.

Global upper mantle tomographic models and the Os model ages are both consistent with the presence of "cold", depleted mantle in this region. It is speculated that perhaps a fossil detached subducted slab is present in the equatorial region (Maia et al, 2001). The existence of a fossil subduction in the Equatorial Atlantic is corroborated by paleo-reconstructions for the period between 460 and 300 Ma. This old subduction zone remained active until around 300 Ma. The Os model ages for the mantle material are consistent with a fossil subducted slab model that is at least that old, and it could also have been created in another divergent period prior to 460 Ma**.**

**Conclusions**

***1.*** *Physical aspects of the ITRs of the SPFZ:*

**a**- The SPFZ is the only fracture zone in the Equatorial Atlantic to present intra-transform ridges.

**b**- These ridges do not show a sigmoid shape like the Fracture Zones in the Pacific that is attributed to the relatively cooler thermal state of the mantle in the SPFZ region.

**c-** The ridge axes show some sparse volcanic activity (i.e., pillow lavas, diabase dikes) but marked tectonic activity (i.e., normal faults).

**d**- Serpentinized peridotites are observed in the flanks of the axial valley. These are cut by diabase dikes and pockets of gabbro.

**2**- *The St. Peter and St. Paul's Rocks Massif:*

**a**- The N flank is composed of mylonitized peridotites, plastically deformed at high temperature. A thin basaltic cover is seen in some of the deformed blocks.

**b**- The S flank is composed of serpentinized peridotites that are not mylonitized. They are covered by endurated carbonate sediments.

**c**- A E-W tectonic graben covered by basalts is found in the junction of the two flanks.

***3****. Behavior of the SPFZ System from the MAR to the Brazilian Coast:*

**a.** The transform portion of the SPFZ can be defined as a triple FZ. Out of the active portion towards the west the SPFZ changes its configuration to a double FZ.

***4.*** *The Re-Os isotope composition of the SPFZ abyssal peridotites:*

**a**. The range of $^{187}Os/^{188}Os$ of the abyssal peridotites sampled in the area is large (0.1211-0.148). A number of the samples have chondritic to sub-chondritic compositions.

**b**. The range of Os isotopic composition of these peridotites is similar to that of other oceanic peridotites.

**c.** The samples with sub-chondritic Os isotopic compositions have a petrogenetic history that suggests parts of the oceanic mantle in the region was depleted in the late Proterozoic to early Phanerozoic (i.e., they were not formed only by recent depletion of asthenospheric mantle during MORB formation).

It is proposed that the physical and chemical evidence support the hypothesis that parts of the underlying oceanic mantle in the Equatorial Atlantic preserve an older, detached subducted slab formed in a previous collisional event, and can represent a cold spot region.

**Acknowledgements**

We thank to Ms. Giselle Agostinho for her help with the figures, to CAPES/COFECUB (project#220/97) and IFREMER for their financial support, to Dr. Richard Walker and Mary Horan for the isotopic analises and to Dr. Sidney Mello for his useful comments.

**References:**

Bonatti, E., 1990. Subcontinental mantle exposed in the Atlantic Ocean on St. Peter –St. Paul islets. Nature, 345, 800-802.

Bonatti, E., 1993, A cold suboceanic mantle belt at the Earth's Equator. Science, 261, 315-350.

Bonatti, E. and J. Honnorez. 1976. Sections of the Earth's crust in the equatorial Atlantic, J. Geophys. Res., 81, 4104-4116.

Carneiro,M.L 2000. Comportamento Temporal da Zona de Fratura de São Paulo-Atlântico Equatorial. Monografia, UFF, 37p.

Esperança, S.; Sichel, S.E.; Walker, R.J. Horan, M.F, Juteau, T. and Hekinian, R. 1999 Some Abyssal Peridotites From Cold Oceanic Lithosphere are Old (abstract). 9th Annual V.M. Goldschmidt Conference, USA. LPI Contribution no.971, pg 81.

Gorini, M.A.1977 Tectonic Fabric of the Equatorial Atlantic and Adjoining Continental Margins: Gulf of Guinea to Northeastern Brazil. Ph.D Thesis, Columbia University, USA.

Haxby, W.F. 1987. Gravity field of the wold´s oceans. Published for the Office of Naval Research by the National Geophysical Data center, NOAA.

Hekinian, R.; Juteau, T; Gracia, E; Sichler, B, Sichel, S; Udintsev, G; Apprioual, R. and. Ligi M. (2000). Submersible observation of Equatorial Atlantic mantle: The St. Paul Fracture Zone region. Region. Marine Geophy. Resch. 21, 529-560.

Maia, M;. Sichel, S.E; Esperança, S. and J. Thirot 2001. The Equatorial Atlantic "cold spot": Constraints from osmium isotope composition, plate kinematics and tomography. EUG XI – Marine Geology and Geophysics, 516.

Sandwell, P.T. and Smith, W., 1997 - Marine Gravity anomaly from Geosat and ERS-1 Satellite Altimetry, J. Geophys. Res. - 102, 10039 - 10054.

Schilling,J-G, Ruppel,C, Davis A.N., Mccully, B. Tighe,S.A., Kingsley, R.H. and Lin, J. 1995. Thermal structure of the mantel beneath the equatorial Mid-Atlantic Ridge: Inferences from the spatial variation of dredged basalt glass compositions. J.Geophys. Res. 100, 10057-10076.

Sichel, S.E.**,** Esperança, S., Walker, R.J., Horan,M.F, Juteau,T., Hekinian,R., Udintsev, G., Garcia, E., Sichler, B. and Apprioual, R 2000 Tectonics and Isotopic Composition of Saint Paul Transform Fault. 31st International Geological Congress , Rio de Janeiro, Brazil (CD ROOM).

# The South Atlantic Ridge Segmentation between the Ascension and Bode Verde Fracture Zones

*Sidney L. M. Mello, Depto. de Geologia/LAGEMAR - UFF, smello@igeo.uff.br*
*Jorge J. C. Palma, Depto. de Geologia/LAGEMAR - UFF, jorge@igeo.uff.br*

**Abstract**

Analysis of bathymetry and gravity data reveals the morphostructure and the mantle Bouguer anomaly (MBA) variation along the ridge axis between the Ascension and Bode Verde Fracture Zones. These fracture zones are first order ridge discontinuities, which are superimposed by four second order discontinuities and at least two main third order discontinuities. Such discontinuities bound seven individualised ridge segments with distinct morphotectonic styles. Despite of this segmented structural framework, two tectonic domains encompass the lower order discontinuities. To the south of the Ascension Fracture Zone and north of the Bode Verde Fracture Zone the ridge axis shows a deep median valley (> 3000 m), suggesting a domain controlled by extensional processes. On the other hand, the median valley is generally absent midway between the two fracture zones. Instead, there occurs a topographically high volcanic edifice shallower than 2000 m associated with several off-axis seamounts to the east. The existence of such topographic anomaly along the ridge crest should reflect a domain controlled by intense magmatism and probably less faulting. The MBA variation within the whole first order segment agrees with this interpretation. The crustal thickening associated to the anomalous topographic high at segment centre is not necessarily an indicative of a hotspot influence at ridge axis.

## Introduction

The large scale segmentation of the South Atlantic Ridge apparently outlines long-lived tectonic corridors with wavelengths between $10^2$ to $10^3$ km [*Kane and Hayes*, 1992]. Superimposed on these long wavelength segments are smaller scales of segmentation dividing the ridge into progressively smaller and short-lived segments [*Macdonald et al.*, 1988]. The overall segmentation is generally defined by large to small offset fractures.

The Ascension (AFZ) [*Van Andel et al.*, 1973; *Palma et al.*, 1984] and Bode Verde Fracture Zones (BVFZ) [*Gorini et al.*, 1984], bound a ridge segment with no major transform offsets and unusual tectonics [**Figure 1**]. The region displays several off ridge axis volcanic edifices, including the Ascension Island at 7°50´S and 14°20´W. Particularly, between 8°30´S and 10°S, a high crestal topography lacking axial valley and earthquake epicentres contrasts with the typical relief of the Mid-Atlantic Ridge [e.g., *Brozena*, 1986; *Mello*, 1993; *Palma*, 1998]. Rock samples dredged along and off ridge axis show isotopic spikes in the La/Sm, Nd/Zn and Sr/Nd ratios [e.g., *Schilling et al.*, 1985; *Fontignie and Schilling*, 1996].

According to *Schilling et al.* [1985], *Brozena* [1986] and *Brozena and White* [1990], the ridge segment, between the AFZ and the BVFZ is influenced by a hotspot near or at the ridge axis. This hotspot influence explains the high crestal topography and the enriched basalt geochemistry along the ridge axis. *Schilling et al.* [1985] proposed that the Circe hotspot, located about 450 km east of the ridge axis at 8°10´S, is responsible for an aesthenospheric flow which is being channelled from it toward the ridge axis. *Brozena* [1986] suggested that the hotspot is, in fact, beneath the high crestal topography at 9°50´S and 13°20´W. Ridge jumps and propagating rift at about 8°30´S on the ridge axis are interpreted as a consequence of such hotspot [*Brozena and White*, 1990]. Alternatively, *Mello* [1993, 1994] suggested that the elevated topography and enriched basalt along the ridge axis might result from a tectonic and magmatic segmentation that varies in time and space. An increase in crustal thickness and/or mantle temperatures was modelled at the centre of the segment around 9°10´S [*Palma*, 1998; *Minshull et al.*, 1998]. However, *Minshull et al.* [1998] proposed that the thermal anomaly in the region is relatively small ~50°C and not compatible with a mantle plume. They suggested that the ridge tectonics around the Ascension area could be explained either by a weak and episodic plume or by melting of small mantle heterogeneities.

Here we investigate the ridge segmentation, between the AFZ and the BVFZ from multibeam bathymetry and shipborne gravity. Detailed analysis of both data allows the correlation of structure and gravity anomalies, providing further discussion on the previous ideas about the South Atlantic Ridge around the Ascension area.

## Data set

The predicted bathymetry derived from a combination of satellite gravity and shipborne bathymetric data [*Smith and Sandwell*, 1997] provides an overview of the regional topography [**Figure 1]**. For local scale analysis, we used multibeam bathymetry, single beam 12 kHz

bathymetry and shipborne gravity. A total of 9 cruises and 11 legs surveyed the ridge axis between the AFZ and the BVFZ.

The multibeam bathymetry grid was gathered from the Ridge Multibeam Synthesis Project (*http:// imager.ldeo.columbia.edu/*). Contoured maps of these data allowed detailed interpretation of the ridge axis morphostructure. The single beam bathymetry and gravity data were obtained from the GEODAS/NGDC Data Base (CD-ROM V3.0). An overall crossover error analysis of these data checked their reliability, especially considering that they were collected by several cruises at different times. We performed the levelling of these data applying methods by *Wessel* [1989] and *Prince and Forsyth* [1984]. This analysis assumes that the effect of whatever the source of error is constant over the length of straight-line segments. The corrected data were used to compute the MBA.

## Analysis and Interpretation

The topographic maps [**Figures 1 and 2**] and the MBA map [**Figure 3**] show that the morphostructure of the ridge crest in the region is formed by seven segments named from A to G. Immediately to the south of the AFZ, Segment A depicts a rugged crestal relief with a rift valley (> 3000 m) in the ridge axis. The rift valley floor shows axial volcanic ridges (15-30 km long, 3-6 km wide and 100-200 m high) that are associated with a crustal thickening as indicated by a MBA low. Apparently, Segment B is a transition zone between Segments A and C further to the south. Segment B is short and bounded by two second order discontinuities, showing no significant MBA variation (less focused magmatic activity) within de median valley. The southern second order discontinuity outlines a V-shape structure and corresponds to an abrupt limit, marked by a steep topography and MBA gradients between Segment C and B. The inside corner highs edging both second order discontinuities are associated with MBA highs and so crustal thinning/denser lower crust. Segment C shows two terrains with no apparent discontinuity. To the north, there is a smoother crestal relief associated with an incipient median valley, which presently appears filled in by axial volcanic ridges not related to notable MBA signature. To the south there exists a shallow (~2700 m) median valley flanked by elevated rift mountains (< 2000 m) and a significant MBA low (-60 mGal) ~20 km to the east of the median valley. This feature is consistent with the existence of several off-axis volcanisms in the region (seamounts). Segment D displays a volcanic high (< 1500 m) at the ridge axis. Such high correlates well with the location of the lowest MBA (-70 mGal) along the ridge, marking the site of maximum crustal thickening and intense magma upwelling. To the north of the BVFZ, Segments E, F and G show a rift valley within the axial zone.

## Conclusions

The ridge segment between the AFZ and the BVFZ is formed by four second order discontinuities and two main third order discontinuities. Such discontinuities limit individualised ridge segments with distinct morphotectonic styles. Two tectonic domains control the region and are superimposed by the second and third order discontinuities. Segments C and D show morphotectonic styles related to intense magmatic activity as indicated by the morphology and the MBA signature, while Segments A, B, E, F and G seem to be less magmaticaly controlled. The existence of a V-shape discontinuity pointing north may reflect a recent preferential northward magma flow along the ridge axis, but it may change in time and space as the accretion process progresses. In fact, ridge discontinuities of lower order are seen as variable features that may migrate along the ridge strike.

The maximum MBA low observed along Segment D can be explained by a crustal thickening of ~3 km, which is about the same amount observed along ridge segments in the North Atlantic away from hotspot influence [*Sempéré et al*., 1993; *Detrick et al*., 1995]. *Minshull et al.* [1998] also showed that if there is a hotspot there, it is only 50°C hotter than normal mantle. Therefore, the existence of a plume in the region requires further constrain.

## References

Brozena, J. M. Temporal and spatial variability of seafloor spreading processes in the Northern South Atlantic. *J. Geophys. Res.*, **91**: 497-510, 1986.

Brozena, J. M. and White, R. S., Ridge jumps and propagations in the South Atlantic Ocean. *Nature*, **348**: 149-152, 1990.

Detrick, R.; Needham, H. D.; Renard, V. Gravity anomalies and crustal thickness variations along the Mid-Atlantic Ridge between 33°N and 40°N. *J. Geophys. Res.*, **100**: 3767-3787, 1995.

Fontignie, D. and Schilling, J.-G, Mantle heterogeneities beneath the South Atlantic Ridge. *Geophys. J. Ast. Soc.*, **20**: 271-284, 1996.

Gorini, M. A.; Fleming, H. S.; Carvalho, J. C.; Brozena, J.; Griep, G. H.; Cherckis, N. S.; Mello, S. L. M. Características morfotectônicas da zona de fratura dupla Bode Verde e o seu traçado em direção aos montes submarinos da Bahia. *In: Anais do XXXIII Cong. Bras. Geol.*, Rio de Janeiro, RJ, SBG, **4**: 1615-1628, 1984.

Kane, K. A. and Hayes, D. E. Tectonic corridors in the South Atlantic: evidence for long-lived Mid-Ocean Ridge segmentation. *J. Geophys. Res.*, **97**: 17317-17330, 1992.

Macdonald, K. C.; Fox, P. J.; Perram, L. J.; Eisen, M. F.; Haymon, R. M.; Miller, S. P.; Carbotte, S. M.; Cormier, M.-H.; Shor, A. N. A new view of the mid-ocean ridge from the behaviour of ridge axis discontinuities. *Nature*, **335**: 217-225, 1988.

Mello,S.L.M., Marine Geology and Geophysics of the Mid Atlantic Ridge Between Ascension and Sta. Helena Islands, *Master Dissertation*, *Universidade Federal do Rio de Janeiro/IG-Depto de Geologia*, RJ, 90 pp, 1993.

Mello,S.L.M., Morfologia e Tectônica da Cordilheira Mesoceânica ao sul da Ilha de Ascensão, in: *An. XXXVIII Congresso Brasileiro de Geologia Camboriú, SC,* **2**:.30-31, 1994.

Minshull, T. A.; Bruguier, N. J.; Brozena, J. M. Ridge-plume interactions or mantle heterogeneity near Ascension Island? *Geology*, **26**: 115-118, 1998.

Palma, J. J. C.; Brozena, J.; Mello, S. L. M.; Carvalho, J. C. Mapeamento morfoestrutural preliminar da Zona de Fratura de Ascensão até a margem continental nordeste brasileira. *In: Anais do XXXIII Cong. Bras. Geol.*, Rio de Janeiro, RJ, SBG, **4**: 1643-1654, 1984.

Palma, J. J.C., Morfotectônica e Gravimetria da Falha Transformante de Ascensão e Crista da Cordilheira Mesoatlântica de 6°20´S a 10°05´S, *Tese de Doutorado, Instituto Astrônomico Geofísico (IAG) da Universidade de São Paulo*, pp. 105, 1998.

Prince, R. A. and Forsyth, D. W. A simple objective method for minimizing crossover errors in marine gravity data. *Geophysics*, **44**: 1079-1083, 1984.

Schilling, J.-G.; Thompson, G.; Kingsley, R.; Humphris, S. Hotspot-migating ridge interaction in the South Atlantic, *Nature*, **313**:187:191, 1985.

Sempéré, J-. C.; Lin, J.; Brown, H. S.; Schouten, H.; Purdy, G. M. Segmentation and morphotectonic variations along a slow spreading centre: the Mid-Atlantic Ridge (24°N-30°40'N), *Mar. Geophys. Res.*, **15**: 153-200, 1993.

Smith, W. H. F. and Sandwell, D. T. Measured and Estimated Seafloor Topography (v 4.2), World Data Center A for Marine Geology and Geophysics research publication RP-1, 1997.

Van Andel, T. H., Rea, D. K., Von Herzen, R. P., Hoskins, H. Ascension Fracture Zone, Ascension Island, and the Mid-Atlantic Ridge. *Geol. Soc. America Bull.*, **84**: 1527-1546, 1973.

Wessel, P. XOVER: A cross-over error detector for track data. *Comput. Geosci.*, **15**: 333-346, 1989.

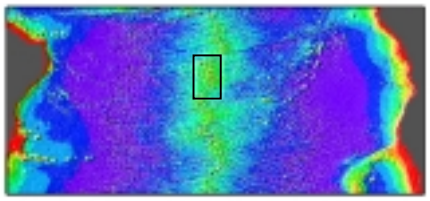

Study area

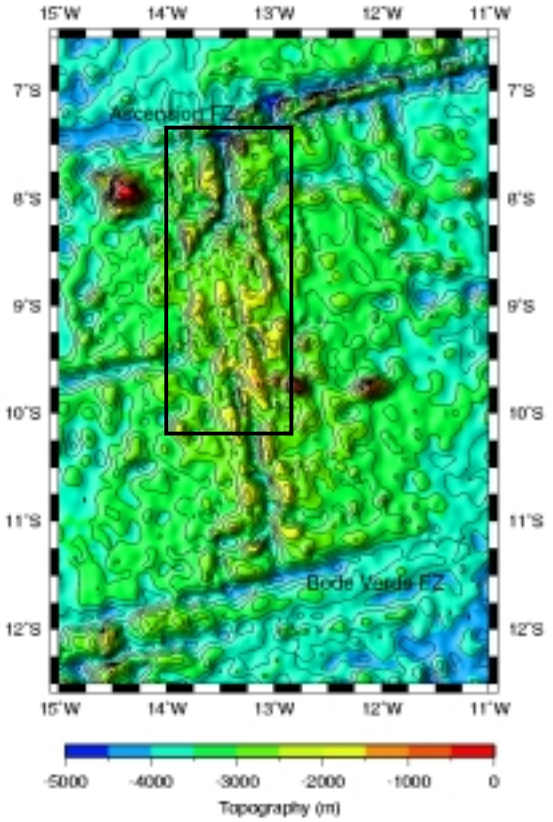


Figure 1 – Predicted topography map. The black box corresponds to the area covered by scientific surveys.

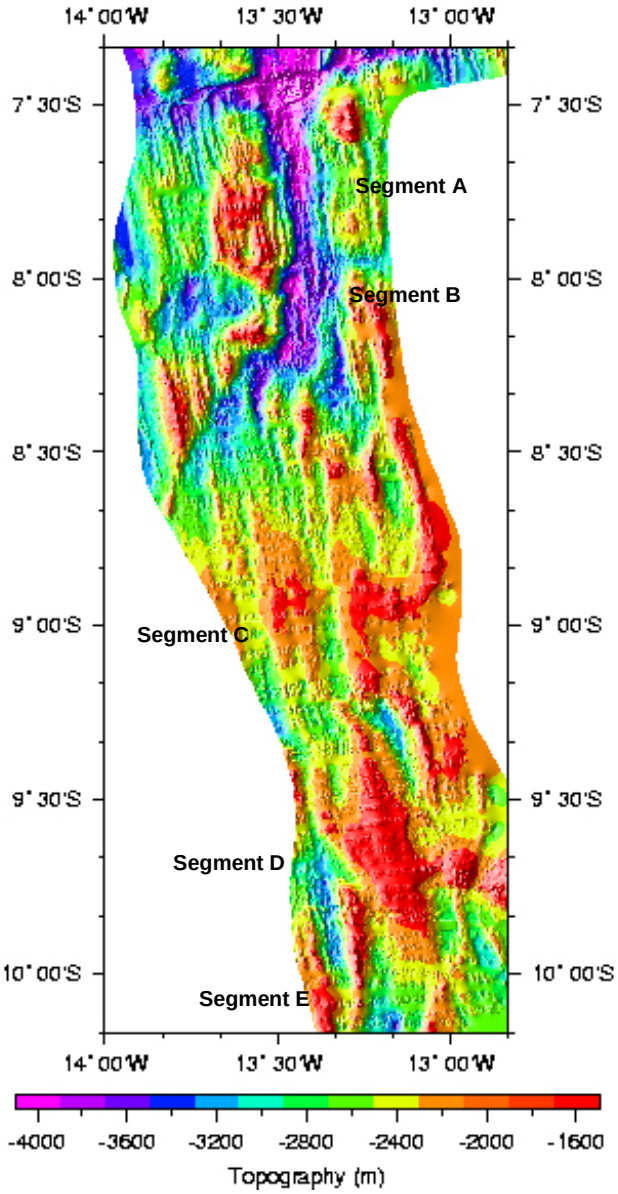


Figure 2 – Topographic map from multibeam bathymetry (Conrad cruises C2601 and C2602) displaying the ridge structure formed by 5 segments.

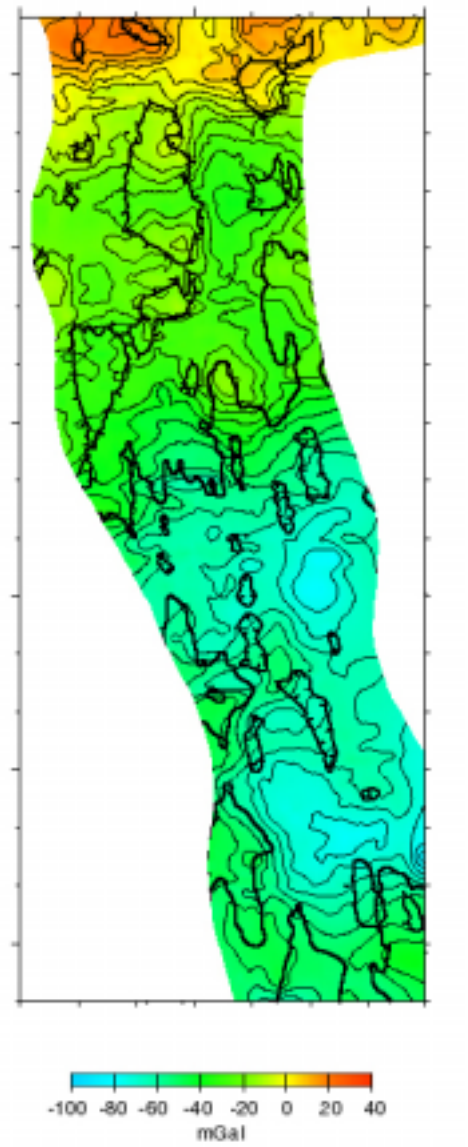


Figure 3 – Mantle Bouguer Anomaly variation along the ridge axis. The black contour lines correspond to the isobath of 2500 m.

**Acknowlegments.** We thank S. Quental for helping in the final edition of this abstract. In different phases of this work, we used the Generic Mapping Tools – GMT (version 3.3.4). For reference, see Wessel, P. and Smith, W. H. F. New, Improved Version of Generic Mapping Tools Released, *EOS Trans.*, AGU, **79** (47): 579, 1998.